This article was downloaded by:
On: *21 January 2011*
Access details: *Access Details: Free Access*
Publisher *Taylor & Francis*
Informa Ltd Registered in England and Wales Registered Number: 1072954 Registered office: Mortimer House, 37-41 Mortimer Street, London W1T 3JH, UK

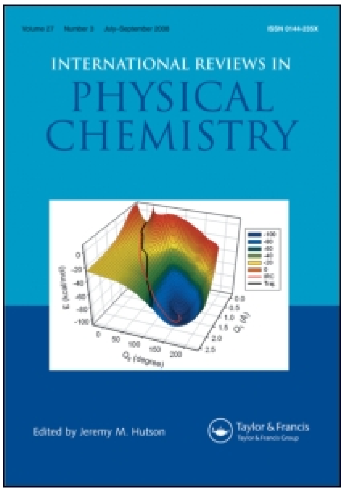

International Reviews in Physical Chemistry

Publication details, including instructions for authors and subscription information:
http://www.informaworld.com/smpp/title~content=t713724383

Adsorption and dissociation of diatomic molecules on transition-metal surfaces

C. A. Taft; T. C. Guimaraes; A. C. Pavao; W. A. Lester JR

Online publication date: 26 November 2010

To cite this Article Taft, C. A. , Guimaraes, T. C. , Pavao, A. C. and Lester JR, W. A.(1999) 'Adsorption and dissociation of diatomic molecules on transition-metal surfaces', International Reviews in Physical Chemistry, 18: 2, 163 — 233
To link to this Article: DOI: 10.1080/014423599229947
URL: http://dx.doi.org/10.1080/014423599229947

PLEASE SCROLL DOWN FOR ARTICLE

Full terms and conditions of use: http://www.informaworld.com/terms-and-conditions-of-access.pdf

This article may be used for research, teaching and private study purposes. Any substantial or systematic reproduction, re-distribution, re-selling, loan or sub-licensing, systematic supply or distribution in any form to anyone is expressly forbidden.

The publisher does not give any warranty express or implied or make any representation that the contents will be complete or accurate or up to date. The accuracy of any instructions, formulae and drug doses should be independently verified with primary sources. The publisher shall not be liable for any loss, actions, claims, proceedings, demand or costs or damages whatsoever or howsoever caused arising directly or indirectly in connection with or arising out of the use of this material.

INTERNATIONAL REVIEWS IN PHYSICAL CHEMISTRY, 1999, VOL. 18, NO. 2, 163–233

Adsorption and dissociation of diatomic molecules on transition-metal surfaces

C. A. TAFT, T. C. GUIMARÃES
Centro Brasileiro de Pesquisas Fìsicas, Rua Dr Xavier Sigaud 150, Urca,
22290-180, Rio de Janeiro, RJ, Brazil

A. C. PAVÃO
Departamento de Quìmica Fundamental, Universidade Federal de Pernambuco
50.960-540, Recife, PE, Brazil

and W. A. LESTER, JR
Chemical Sciences Division, Lawrence Berkeley National Laboratory, and
Department of Chemistry, University of California, Berkeley, California
94720-1460, USA

The interaction between transition-metal surfaces and simple diatomic molecules (CO, NO, H_2, N_2 and O_2) may lead to the breaking and making of chemical bonds and trigger important surface-catalysed reactions. We discuss the most common surface interaction and orientation models and consider the electronic structure of the transition metal, and the influence of structure, bonding and coordination of the diatomic molecule. We emphasize the importance of the tilted precursor in the dissociation of diatomic molecules on transition-metal surfaces.

1. Introduction

Surface chemistry has a long and distinguished history. Benjamin Franklin studied the spontaneous spreading of oil on water. Dobereiner discovered the platinum-surface-catalysed reaction of H_2 and O_2 in 1823 and used this reaction in his lighter. Today, heterogeneous catalysis serves as the basis for most petroleum and chemical technologies with substantial importance for the life sciences as well as environmental protection and has been intensively investigated with the increasingly available tools of physics, quantum chemistry and surface science [1–12]. A particularly interesting and important area of catalysis and surface science is the interaction of diatomic molecules (CO, N_2, NO, H_2 and O_2) with transition-metal (TM) surfaces which can lead to the breaking and making of chemical bonds and trigger important surface-catalysed reactions.

The development of modern surface science has made possible the investigation of catalysts on the atomic scale, leading to understanding at the molecular level of how catalysts function. The goal of surface scientists is to develop a predictive understanding of electronic properties, elementary dynamical processes and surface structure, laying the groundwork for improved control of numerous technologically important phenomena. The enormous economic significance of surface-related technologies, from semiconductor devices to catalytic surface chemistry, from stability and friction to materials growth, wear and lubrication, explains the continued financial support and vitality for surface science research. Despite these impressive objectives, during the first two decades of surface science research, efforts were mostly

International Reviews in Physical Chemistry ISSN 0144–235X print/ISSN 1366–591X online
http://www.tandf.co.uk/JNLS/rpc.htm http://www.taylorandfrancis.com/JNLS/rpc.htm

devoted to developing tools for preparing and characterizing samples and obtaining useful information from acquired data with little hope of analysing trends, verifying theories or improving technology.

In the early 1960s a catalyst was viewed as a ‘black box’ that mysteriously converted entering reactant molecules to desirable products. From the late 1960s to the early 1980s, the focus was on developing crystallography of single-crystal surfaces and investigating the elements of surface electronic and vibrational behaviour. By the mid-1980s, the surface structure problem had largely been solved through the development of a host of experimental techniques and many surface structures became well known. For theorists, the availability of a meaningful information base meant that computational methods for predicting surface behaviour could be tested and improved. In the 1990s, catalyst design, based in part on the understanding obtained from a host of experimental techniques as well as quantum-chemical computational methods, is the norm rather than the exception [1–28].

The control of the rate and direction of chemical reactions has held the imagination of scientists and technologists for many centuries. Today, the benefits of catalytic reactions are well represented by the datum that about 85% of all chemical products are made with the use of catalysts which make possible the large-scale production of numerous products for daily use. These include, for example, gasoline and other fuels, fertilizer, plastics, detergent, pharmaceuticals and certain foods. If the catalyst can be used in solid form, there are additional advantages for the chemical process because various separation stages are eliminated, corrosion of equipment is minimized, and the prospect of environmental pollution is lessened. In addition, solid catalysts have more thermal stability that facilitates higher temperatures and allows more frequent regeneration [1–9].

The success of many commercial catalytic processes involving chemistry on TM particles and surfaces for designing active selective poisons, surface ensembles and promoters is based on knowledge of the fundamental principles of TM surface chemistry and theoretical methods. Because of limitations in raw computer (central processing unit (CPU)) requirements and the accuracy of available computational methods, rigorous descriptions and high-energy predictions for each elementary reaction step of an entire catalytic cycle from first-principles theoretical methods is still unattainable. However, progress in computational resources and quantum-chemical methods have advanced the theoretical treatment of adsorbate–surface interaction and, in many cases, reliable quantitative predictions of energetics and structure can be made.

Owing to the multisite nature of a catalyst and the array of competing elementary surface steps, understanding the kinetics of heterogeneous catalytic systems is complex. The chemical make-up of a particular catalytic site, which can change as the surface becomes covered with reaction intermediates, is an important factor for selectivity and activity. Molecular adsorption, dissociation, recombination and molecular desorption are the basic elementary steps of a catalytic reaction cycle. Dissociation and/or molecular desorption are the slow reaction steps that control catalytic activity whereas surface composition and competition between the dissociation rate and the recombination rate of coadsorbates can control selectivity. Prediction of the overall selectivity and activity of a catalytic reaction can strongly depend on the elucidation of each of the steps comprising the reaction mechanism. These factors can be estimated using a range of semiempirical to first-principles quantum-chemical methods. The latter techniques provide a good means of probing the effects of altering the surface TM, manipulating the nature of the active site, changing the active particle size ensemble and gaining understanding of the structural and electronic features that govern the kinetics, which are the first steps towards catalyst design.

The absorbate–surface interaction governs the stability of reactive surface intermediates and controls whether these intermediates diffuse, react or desorb. One can analyse the occupation of antibonding and bonding surface–adsorbate orbitals to obtain insight into adsorbate reactivity and adsorbate–surface bond strength. Many analyses rely on concepts from frontier molecular orbital (MO) theory for which the lowest unoccupied molecular orbital (LUMO) and highest occupied molecular orbital (HOMO) are important parameters for understanding the adsorbate–surface interaction. Further, the concepts of electron donation and back donation can provide a satisfying description of the attractive part of the interaction potential. For TM surfaces, differences in reactivity are often controlled by the interaction of the adsorbate with the d valence electrons. In addition, bonding properties provide insight on the relative stability of adatoms or admolecules at geometrically different surface sites [9].

The quantitative accuracy of a quantum-chemical calculation for the prediction of surface–adsorbate reactivity and binding can be highly dependent upon the method used as well as the size and configuration of the cluster. For the present discussion, it is convenient to classify the methods employed to study diverse aspects of catalysis and chemisorption on a TM surface into the following areas: empirical, semiempirical, *ab initio* MO theory, formal theory (analytic solutions) and density functional theory (DFT).

The formal theory of chemisorption (a theoretical approximation that provides a parameter-dependent model of chemisorption) involves analytical representation of the surface–adsorbate interaction. One approach treats the covalent bonding aspect of the surface-chemical bond in a formalism in which electron–electron interactions are only implicity considered through one- and two-centre electron repulsion integrals. Solutions of the chemisorption problem are sought for the semi-infinite surface as a function of valence-electron-band occupation, overlap between surface and adsorbate orbitals, and delocalization of surface electrons [10]. In another approach, the jellium model, in which electrons are treated as free, a continuous positive background replaces discrete attractive due to positive nuclei and the density is chosen so that the electron–nuclear attraction exactly cancels the electron–electron repulsion. A popular semiempirical method, the effective-medium theory, is a combination of the tight-binding MO appoach and the jellium model [10]. Intermediate between the DFT and the effective-medium theory is the scattered X_α theory, which approximates a solid by spheres of constant potential and describes a metal solid or a molecule by equations of motion of a free electron scattered by the spheres and their corresponding potentials representing the atoms; potentials and sphere radii are adjustable parameters in this formalism [11].

The bond order conservation (BOC)–Morse potential (MP) is an empirical treatment of reaction energetics and surface adsorption [12]. For non-directed bonding, BOC–MP yields analytical expressions relating atom–atom bond strength to the strength and the number of nearest-neighbour interactions. The tight-binding or Hückel method is an example of a semiempirical method also used for clusters. However, Pauli repulsion effects, which are important for absorbate–substrate interactions, require the explicit accounting of the non-orthogonality of the atomic orbitals that comprise the basis set for MOs. This requirement is absent in the simple Hückel method. The atomic superposition and delocalization MO method (atomic superposition of electron densities (ASED)) is an extension of the extended Hückel method where the repulsive part of the bond is determined by the superposition of fragment electron densities with a correction for the delocalization of electron density [13]. The modified neglect of atomic overlap (MNDO) and its variants the Austin method 1 (AM1), parametric method 3 (PM3) and semi-*ab-initio* model 1 (SAM1) are more advanced and widely used semiempirical methods in which electron–electron interaction effects are explicitly taken into account [14]. However, some of these methods are inapplicable to the treatment of catalytic surface problems owing to the current absence of parameterizations for TM systems. The well parametrized Zerner intermediate neglect of differential overlap (ZINDO) [15] package has been used in a number of interesting catalytic studies.

The first-principles models, namely the *ab initio* MO method and the DFT, have provided new insights into the high-energy and electronic properties of TM systems [16]. *Ab initio* approaches were historically severely limited to small systems. However, current computational quantum chemistry has reached a level of sophistication where much larger and scientifically meaningful calculations are routinely made for reliable quantitative predictions of electronic properties, geometric structures and interaction energies for metallic systems. The *ab initio* approach was used by the present authors to investigate catalysis on metallic oxides, TMs as well as alloys [9]. The Hartree–Fock self-consistent field (SCF) method is the most basic *ab initio* MO approach. By expanding the many-electron state function into a linear combination of Slater determinants the electron correlation can be incorporated, yielding a more complete representation of the active configurational space. Such a full configuration interaction (CI) expansion is computationally intractable for larger systems. An excellent alternative is many-body perturbation theory coupled cluster approach which includes single, double and perturbation inclusion of triple excitations (CCSD(T)). Size consistent treatments include the coupled pair functional method and the modified coupled pair functional method [16, 17]. Other methods vary the initial one-electron functions and expand the many-electron wavefunction in a linear combination of Slater determinants to incorporate a more complete representation of the active configurational space, such as the complete-active-space self-consistent field (CASSCF) or multiconfiguration self-consistent field (MCSCF) methods. Other methods such as pseudopotentials are also used to reduce the computational expenditures involved in treating larger TM systems [18].

An alternative first-principles approach, pioneered by Hohenberg and Kohn, is the DFT method in which the energy is a unique functional of the density. The electron density is computed by solving a set of Kohn–Sham equations in a self-consistent manner. Electron interactions and CIs are treated explicitly as a functional of the density. DFT algorithm specifics include the choice of exchange–correlation functional, non-local gradient corrections, basis set functions, degree of grid accuracy, gradient and second-derivative solutions [19]. Extended two- and three-dimensional slab or surface algorithms are now offered by both DFT and *ab initio* methods as well as molecular dynamic simulations based on interactions described by hybrid quantum–classical methods [20].

The quantum Monte Carlo (QMC) method is a stochastic approach for sampling the exact wavefunction [27]. The parameters in a trial wavefunction are optimized typically by minimizing the variance of the energy. The QMC method yields energies and other properties in excellent agreement with exact values. QMC methods offer considerable advantages over other techniques for treating electron correlation owing to the capability of including functions explicitly dependent on interparticle distances in the trial wavefunction. Among the other advantages of QMC are the comparatively mild scaling of the CPU time with the number of electrons, the inherent parallelism of the computations, and the weak dependence of the results on the basis set used in constructing the trial wavefunction used to guide the random walk. The QMC method has been demonstrated to scale better with CPU time than the CCSD(T) method does.

The use of pseudopotentials or effective core potentials (ECPs) has made possible the application of *ab initio* methods to large systems that would be otherwise inaccessible. ECPs have been found to yield energies of accuracy comparable with that of all-electron calculations, multireference CI and coupled cluster calculations. For this reason, ECPs are routinely used for treating valence correlations in TM systems and at present make possible the application of post Hartree–Fock methods for which large basis sets are currently impractical owing to high computational demands and poor scaling [9, 27]. ECPs are essential to the application of the QMC method to systems containing more than ten electrons.

Chemisorption, in contrast with physisorption, means that the substrate–adsorbate interactions leads to bonding comparable in strength with that found in molecules. The resulting species resemble chemical moieties with structure and reactivities that can be explained by consideration of the local structure around an active surface site with the help of an appropriate electron count. A chemical approach to understanding these problems is based on the assumption that phenomena are local which in its most naive sense means that a metal–adsorbate property, such as vibrational frequency, bond distance or bond dissociation energy remains the same regardless of the electronic environment. This is sometimes found to hold, justifying the use of the most elementary description for the surface. The electronic distribution on a reactive site could also influence bonding properties. Notwithstanding the approximations involved, finite cluster models implemented following first-principles-based methods are often applied to the treatment of reactive surfaces because of their less demanding computational requirements [20].

Three approaches have been used mainly to restrict the molecule–surface system to manageable size. In some respects the most elegant is the embedding method in which the aim is to solve as accurately as possible a system consisting of a small number of atoms around the adsorbate while taking the rest of the system into account through some form of embedding potential that serves as an additional boundary condition on the system. While potentially very powerful, this method is at an early stage of development compared with the methods outlined below. The second approach is to model the substrate as a finite cluster. This approach is similar to the embedding method, except that no account is taken of the part of the substrate that is neglected. The third technique involves the use of a supercell geometry, which has become popular largely because of its computational simplicity and efficiency. The semi-infinite substrate is replaced by a periodic array of extended two-dimensional slabs and the single adsorbate is also replaced by a periodic array.

Some other models involve rigorous optimization of the local interactions between a small cluster of surface or bulk atoms and an adsorbate. The resulting system is then embedded into a larger cluster to model the interactions due to the bulk. Other models use frozen-core d valence electron or pseudopotential methodology to treat the electronic structure of the local adsorption complex which enables the calculation of larger clusters. Yet other proposals involve the redistribution of electrons in the cluster so as to populate the strongly interacting orbitals that are empty in the small cluster but become occupied on the surface [20, 21]. Some workers, however, have indicated that there should be changes in the local surface orbitals available for binding change according to cluster size and proposed the bond preparation scheme in which the occupied surface molecular orbital either is partially filled and available to accept an adsorbate electron easily or is completely filled. An electron must first be promoted to the LUMO before adsorption. In order to reduce the large energy cost, owing to substantial HOMO–LUMO gaps, the bond preparation scheme manipulates the electronic state of the bare cluster so as to mimic the electronic state of the bulk making the cluster more favourable for adsorbate binding.

The MO cluster model for surface chemistry and surface phenomena is a simple and yet valuable way to investigate the chemisorption bond and surface processes. Many properties of the adsorbate–substrate system are relatively local and the MO cluster model wavefunctions can reproduce these properties well [22]. Some features of the interaction such as binding energies of the adsorbate may depend on the cluster size or on the electronic state of the cluster. What conditions should a cluster model fulfil in order to represent correctly a wide range of surface properties? Upton and Goddard [23] indicated that the cluster model should have a ground-state wavefunction in which the HOMOs, which represent the surface conduction band, have

(*a*) significant amplitude at the adsorption site,
(*b*) a large number of HOMOs in a small range of energy constituting a high density of the conduction-band state,
(*c*) a highly polarizable cluster model wavefunction and
(*d*) an ionization potential close to the work function.

Bagus and co-workers [24] in their study of N_2 and CO adsorbed on Cu and Ni surfaces used very small clusters to represent the key features of the substrate adsorbate chemical bond and showed that excited states of clusters which contained the adsorbate plus a single atom could be successfully used to interpret core level photoemission spectra. Hermann *et al.* [25] argued that the chemical bond with an adsorbate depends on the size of the cluster model chosen to represent the substrate. The present authors [9] also used small clusters to represent the key features of the substrate adsorbate chemical bond for the 3d MTs [31]. Analysis of these interactions using the constrained-space orbital variation method [24] indicated that all the cluster models studied interact with CO through the same mechanism. Except for the initial Pauli repulsion and cluster polarization, the different contribution to the chemisorption bond did not strongly depend on the cluster size. In order to have net bonding, the cluster must have the conduction-band π levels near the Fermi level. This orbital structure results in a larger π back donation. The orbital symmetry of the HOMOs appears to play a key role.

Panas *et al.* [26] using a 'bond preparation method' concluded that the density of conduction-band states and the cluster polarizability are not properties which significantly affect the calculated chemisorption bond energies. Panas *et al.* have stated a proposition referred to as the Stockholm rule, which encompasses the work of Hermann *et al.* [25] for guiding cluster modelling of chemisorption. The Stockholm rule essentially states that, in order for a cluster to be a reasonable model of the surface in a chemisorption calculation, the electronic state of the cluster must be a 'properly prepared' bonding state. On the other hand, one of the important features and advantages of the *ab initio* cluster model approach used by many workers to determine the leading physical interaction mechanism with an *ab initio* quantum-mechanical formulation is the requirement, as input, of only the cluster geometry and the level of cluster wavefunction. Following Bauschlicher, electron correlation can also be included [24] in order to further the description of the absorbate absorbant system in the cluster model approach.

In working with molecules interacting with metals, it is quite useful to make a connection with a molecular treatment in order that chemical knowledge and experience with orbitals, bonds, and charge transfer can be used as tools for analysing molecule–surface interactions. Comparing orbital interactions in isolated molecules with those of a molecule on a surface, one discovers that in the latter case it is possible to assume that a small set of frontier orbitals dominates. In a one-electron picture, for both the molecule and the surface, the controlling interactions are likely to be the two-orbital two-electron stabilizing interactions. Depending on the relative energies of the orbitals and the magnitude of the overlap, each of these interactions will involve charge transfer from one system to another. *Ab initio* unrestricted Hartree–Fock (UHF) studies by Bagus *et al.* [24] and the authors [9, 30–35] on TM monocarbonyls supports these views, that is mainly that the bonding of CO to metal carbonyls is one of σ forward donation and π back donation and is reflected in the classical Dewar–Chatt–Duncanson bonding model in an organometallic molecule or CO bonding to a surface in the Blyholder [28] model. These primary interactions are the fundamental electronic origins of the cluster–surface analogy and a remarkably useful construction of a structural, spectroscopic and thermodynamic link between organometallic chemistry and surface science. One can then use the available tools of theoretical chemistry with special emphasis on charge transfer, which can be reasonably well determined quantitatively using modern *ab initio* Hartree–Fock computer programs.

The representation of a TM surface in terms of an individual atom or a small group of atoms is based on the supposition that the surface atoms retain much of their atomic character, the adsorption properties are strongly influenced by local site effects, and band effects are secondary. Consider a molecule, described by occupied and unoccupied electronic levels, approaching a surface. After initial long-range attraction, repulsion sets in as the molecule approaches the surface more closely. When, however, a bonding combination of wavefunctions of the absorbate and absorbant overlaps significantly, the interaction becomes attractive. The simplest model would be the interaction of two isolated atoms, one representing the metal and the other the gas particle. As the number of surface atoms is increased to improve the representation of the molecule–surface interaction, it also becomes of interest to ascertain the effect of the defect morphology on the structure of adsorbed molecules and to investigate whether the richer stereochemistry and differing electronic structure of high-Miller-index surfaces can give rise to unique chemisorption complexes whose reactivity might significantly differ from that exhibited by species adsorbed on close-packed ideal planes.

Two mechanisms are used, in general, namely the direct and precursor states models, to describe the dissociation of molecule on a surface. In direct dissociative chemisorption, the incident molecule dissociates into adsorbed fragments immediately upon collision with the surface. In dissociative chemisorption through a precursor state, the molecule is adsorbed intact before dissociating. The precursor state arises as a result of the loss of incident kinetic energy of the molecule to the surface upon collision. The molecule remains in this state until enough energy is received from the solid to reorient it into an energetically favourable configuration for dissociation or diffusion or, alternatively, until sufficient energy is supplied from the solid for it to desorb without dissociating.

The mechanism for dissociation is dictated by the potential energy hypersurface of the interaction. As a molecule approaches a surface, its long-range attractive van der Waals interaction with the surface gives way to a short-range repulsive interaction. However, the repulsion does not continue to grow at increasingly shorter distances. Instead, because of electrons from the surface filling antibonding orbitals of the approaching molecule, the interaction becomes less repulsive and then turns attractive. The orientation of the incident molecule on the surface can determine the likelihood of direct dissociation or molecular adsorption because there are typically few orientations of the incident molecule and few surface sites that are energetically favourable for direct dissociation.

A handful of recent studies investigating the dynamics of molecular chemisorption have suggested that two similar mechanisms govern non-dissociative chemisorption. In the precursor mechanism for molecular chemisorption (trapping-mediated chemisorption) the impinging molecule dissipates its kinetic energy in the collision with the surface and physically adsorbs or traps. Once the molecule is trapped, there is a kinetic competition between desorption and chemisorption on the surface that is governed by surface temperature. In the case of a direct dissociative mechanism, chemisorption occurs upon impact with the surface provided that the molecule has sufficient translational and vibrational energy to overcome the barrier to dissociation. A similar direct mechanism for molecular chemisorption in which the final product remains an intact molecule is also possible.

Many of the ideas about how a molecule traps and locates a site for chemisorption originate from experimental studies of adsorption kinetic [1–7]. Simple Langmuir kinetics results in an adsorption probability that is linearly dependent on the number of empty sites. The most common deviation from this mechanism arises near the point of saturation coverage where independence of the adsorption probability on coverage is attributed to the existence of precursor molecules, initially adsorbed above filled sites, that migrate to empty sites where adsorption can take place. The precursor molecules above the empty and filled sites have come to be known as intrinsic and extrinsic precursor molecules respectively. The precursor molecule is capable of diffusion over empty sites and over and around filled sites until a favourable configuration or site for adsorption is attained. The independence of the adsorption probability on coverage provides evidence for the existence of the extrinsic precursor molecule. Kinetic measurements and the corresponding models are often suggestive of the important role of a precursor molecule in the adsorption and dissociation processes. The kinetic energy may also assist in surmounting barriers to molecularly chemisorbed surface states, which then serve as precursors to dissociation. A number of experimental features have been invoked to distinguish between direct dissociation and direct molecular chemisorption mechanisms. These include surface temperature effects, dependence of saturation coverage on incident kinetic energy, and energy–angle scaling; the latter is a data characterization which is dependent on the initial adsorption probability at various incident angles.

TM systems and molecular interactions with TM 3d surfaces, in particular, pose a considerable challenge to both experimentalists and theoreticians. The reason is because TM surfaces with adsorbed molecules have complex spectra arising mainly owing to the proximity of low-lying states (s, p, d), of similar spatial extent and energy, and to many spin multiplicities. From an experimental viewpoint, this complexity is frequently exacerbated by different isotopes with large nuclear spins and magnetic moments. Despite these difficulties, new and refined experimental techniques [9] have facilitated the acquisition of an immense data base of molecule–metal binding, structure and reactivity information. Molecular-beam techniques permit the collision energy and the direction of the incoming adsorbate to be varied over a wide range. Experimental arrangements that couple molecular-beam techniques with electron spectroscopies, especially those with vibrational resolution provide sensitive detection of chemisorption by identifying the adsorbate and quantitatively measuring its coverage. By applying field (or laser) pulses with variable repetition rates, one can evaluate kinetic data of the surface processes. Among the various spectroscopic techniques, ultraviolet photoelectron spectroscopy (UPS) and X-ray photoelectron spectroscopy (XPS) are certainly powerful tools for studying the nature of adsorbed molecules on solid surfaces. Comparison of the relative spacing and intensities of the photoelectron spectra between adsorbed and free molecules enables one to gain insight into bonding geometry, bond strength and details of the electronic properties of adsorbed molecules.

Well characterized (usually single-crystal) surfaces under low-pressure conditions are nowadays generally accepted as suitable model systems for studying the elementary processes underlying chemical reactions at surfaces which are of considerable practical relevance for phenomena such as heterogeneous catalysis and oxidation. Although the surface science approach indicated substantial progress via the arsenal of tools from surface physics previously indicated, it was Langmuir who introduced the concept of chemical interactions at well defined surfaces without being able to conduct the appropriate experimental studies as well as the idea of the chequerboard on to which chemisorption of particles from the gas phase may take place. With the tools of present-day technology, the macroscopic rates and outcomes of many important processes including those occurring during heterogeneous catalysis, the manufacture of semiconductor devices, and the modification of materials depend ultimately on the interactions between individual atoms and molecules and the nature of specific sites on solid surfaces.

One of the first key findings of low-pressure surface science studies was the importance of surface irregularities (kinks and steps) in breaking and rearranging chemical bonds of adsorbates [5]. Catalyst additives, or so-called promotors, have frequently been deposited from the vapour phase on metal model single-crystal catalysts to study their effects as structure or bonding modifiers. Alkali metals, halogens and oxide or sulphide islands are deposited on TM surfaces with variable surface concentrations to build complex catalyst systems on single-crystal surfaces or on thin films of the catalyst. There is a higher reaction rate and stronger bonding at defects and on rough surfaces. Not only are the latter catalytically more active, but also they are more active in breaking chemical bonds.

Chemisorption-induced restructuring can be viewed as the initial phase of a solid-state reaction whose kinetics are controlled by atom transport (diffusion) [5]. When adsorbate-induced restructuring creates crystal faces that are beneficial to catalytic activity, these adsorbates are called ‘structure modifiers’ or structural promoters. If the reaction rate is decreased owing to adsorbate-induced restructuring, the adsorbate is called a catalyst poison. Restructuring occurs in order to maximize bonding and stability of the adsorbate–substrate complex. It is driven by thermodynamic forces and is most likely to occur when the stronger adsorbate–substrate bonds compensate for the weakening of bonds between the substrate atoms (which is the result of the chemisorption-induced restructuring process). Substrate restructuring also occurs during chemisorption of molecules. Metal surface atoms that are relaxed by moving inwards on a clean surface move outwards during the formation of a chemisorption bond. Structure modifers are often introduced as important additives when formulating the complex catalyst systems.

Structural promoters can change surface structure which is often the key to catalyst selectivity. Alloy components may not participate in reaction chemistry but modify structure and site distribution on the catalyst surface. Site blocking can improve selectivity as has been proven for many working catalyst systems. S and Si and other strongly adsorbed atoms that seek out certain active sites can block undesirable side reactions. The activation energy for surface diffusion of chemisorbed species is low compared with their heats of desorption; therefore, these atoms and molecules migrate along the surface, visiting various adsorption sites during their surface residence time. It is likely that the adsorption of reactants on a strongly chemisorbed overlayer-covered surface occurs by laterally displacing the overlayer, thereby creating a reaction site. As long as the activation energy for surface diffusion of the deposit is small, this process can always create new sites for adsorption and reaction.

The heat of chemisorption per atom or per molecule declines with increasing coverage for most chemisorption systems [5]. Not only does increasing coverage of chemisorbed species lead to sequential filling of binding sites, but also it can weaken adsorbate–substrate bonds markedly. This effect of coverage influences surface residence times of adsorbates and subsequently their behaviour during chemisorption and surface chemical reactions. Under high pressures and high surface coverages of adsorbed reactants and reaction intermediates, the heat of desorption is low compared with the situation at low coverages. In most surface science studies, adsorbates are investigated at low coverages because their stability under these conditions makes their study easier and because of the low-pressure conditions necessary to utilize many surface science techniques.

The coadsorption of two different species can lead to repulsive or attractive adsorbate–adsorbate interactions [5]. The ordering of one adsorbate by the coadsorption of another through donor–acceptor interaction is commonly observed. Repulsive interactions between two donor or two acceptor coadsorbed molecules leads to separation of the adsorbates by island formation or disorder in the adsorbed layer. Strong attractive interaction among adsorbates can lead to dissociation of the molecular species. Alkali metals are often used as additives during catalytic reactions. They are 'bonding modifiers' since they influence the bonding and therefore the reactivity of the coadsorbed molecules. Halogen species can also be important bonding modifiers because they are powerful electron acceptors and are used as promoters in several catalytic processes. Oxide–metal interfaces can exhibit very high activity compared with the metal alone whether the metal is laced on the oxide or the oxide on the metal. The phenomenon of 'strong metal support interaction' emphasizes the unique high catalytic activity due to oxide–metal interfaces. The typical activation treatment for catalysts of this type involves reduction in hydrogen, during which the oxide encapsulates the metal, resulting in much reduced CO or H_2 chemisorption activity followed by an oxygen heat treatment that activates the catalysts during which the oxide forms small islands in such a way as to maximize the oxide–metal periphery area. The chemically active surface undergoes adsorbate-induced restructuring that is often local (short range) and can also be diffusion controlled (long range). Structural rearrangements occur with the absorbates as well as on the substrate side of the chemical bond. One of the challenges for the surface science of catalysts is the development of selective catalysts for the stereoscopic synthesis of drugs and fine chemicals for the human body. Biological catalysis provides us with many examples of processes that occur with 100% selectivity in making a product. Therefore, we should extend our understanding of the causes of selective catalytic surface chemistry in the production of small molecules as well including diatomic molecules—the focus in this review.

Macroscopic rates and outcomes of heterogeneous catalytic events depend on the dynamics and microscopic kinematics of the interactions on the atomic scale. The interaction of molecules with surfaces is dependent on molecular orientation, molecule–surface separation, lateral position of the molecule within the surface unit cell, and molecular velocity, angular momentum, electronic and vibrational states as well as the effects of steps and defects of the surface. In addition, one must also consider substrate degrees of freedom including phonons, plasmons and electron–hole pairs [36]. Since a full theoretical description that includes all degrees of freedom is a prohibitive task, one approach is to choose a model system for which the influence of certain degrees of freedom is minimized or to investigate the influence of those degrees of freedom over which one can exert considerable control. Since one cannot follow continuously the changes in positions and velocities of the nuclei in the electronic state of the system, one can at best hope to infer the detailed dynamics of the interaction from a series of 'snapshots' of the system before, during and after the interaction.

Molecules are adsorbed on surfaces with preferential orientations that reflect the response of the molecule to the orientation dependence of the potential energy surface (PES) describing the interaction. This cannot be taken, however, as evidence that the dynamics of gas–surface interactions are governed by the initial molecular orientation in the gas phase. At very low energies the molecule may achieve adiabatically its energetically preferred orientation during its approach to the surface, independent of its initial orientation, or the oriented chemisorption state on the surface may be reached by first trapping into a precursor state in which the tilted state may play an important role. Experimental studies have given indirect evidence for the possible importance of steric effects and orientation on adsorption [36].

In seeking to understand the role of molecular orientation in the molecule–surface interaction, we must focus on identifying the connection between the orientation of the molecule as it approaches (or leaves) the surface and the orientation of the molecule in the adsorbed state. We note, for example, that molecular dynamics simulations indicate that the process of ion desorption is accompanied by significant rotational excitation, so the initial orientational order on the surface is lost. The overall shape of the angular distribution is governed by the electrostatic image potential experienced by the charged ion as it leaves the surface. On the other hand, the yield of desorbed ions depends very significantly on the initial orientation of the molecule on the surface. These findings suggest that molecular orientation can be an important factor in surface dynamics.

Beyond the physisorption regime, charge transfer dominates the interaction of a slow molecule with the surface of a metal. It often leads to the making of bonds between the atoms of the molecule and the surface and to the breaking of bonds within the molecule.

Summarizing this section, understanding the mechanism of adsorption and dissociation is related to molecular-level knowledge of various factors including the reactions of adsorption and desorption, the structure of the catalytic surface, and the bonding and coordination of the reaction intermediates to the surface. Consequently, detailed studies of gas–solid heterogeneous catalysis retain considerable theoretical and experimental interest and make heterogeneous catalysis a multidisciplinary research field requiring the collaboration of scientists and technicians from many areas. The development of modern surface science has provided the opportunity to investigate catalysts on the atomic scale and to understand the molecular ingredients that make them function. Evaluating quantitatively the energy of interaction between a gas molecule and a surface is a computationally demanding task and presents many difficulties, making it desirable to find empirical, phenomenological and, where tractable, *ab initio* methods that can describe experimental results more precisely and the gas molecule–TM surface interactions more generally for many kinds of metals and surfaces. Calculations of molecular properties containing TM atoms have proven to be more difficult than those for first- and second-row atoms although recent advances in methodology and high-speed computers have now made it possible to also obtain quantitative information of many molecular systems containing TMs.

The development and refinement of new experimental techniques have also made possible the acquisition of an immense data base for the chemical identity of the adsorbate, its binding site, structure and reactivity. Questions are now being asked not only about the structure and stability of adsorbates but also about their dynamics and mechanisms. There is better understanding of the dominant features of the molecule–surface potential energy hypersurface and how they govern the dynamics and mechanism of both dissociative and molecular chemisorption. Despite considerable progress in both theory and experiment, however, many questions remain unanswered regarding chemisorption, dissociation, precursor states, back donation and other interesting effects such as the influence of the choice of metal plane, surface structure, geometric and electronic configuration, defects, impurities, steps, kinks, terraces and doping, some of which will be reviewed below for selected diatomic molecules in their interaction with TM surfaces.

In this review we discuss the interaction of simple diatomic molecules (CO, NO, H_2, O_2 and N_2) involved in important catalytic processes and may lead to breaking of bonds on TM surfaces. We begin with CO and N_2 adsorption and dissociation on TM surfaces since these interactions can in general be used as models for chemisorption and dissociation on metallic surfaces via donation and back-donation primary interactions and in some configurations via a tilted precursor state proposed by the present authors and co-workers [9, 30–35].

2. Adsorption and dissociation of CO on transition-metal surfaces

For many systems the TM–CO adsorption geometry has the C end lying directly above a surface metal atom. This geometrical arrangement permits many features of chemisorption to be determined by considering the interaction of CO ligands with metal atoms in complexes. This rather simple conceptual picture of metal–CO bonding remains applicable for many cases of molecular CO adsorption. In the early 1960s, Cotton and Kraihanzel [37] investigated CO–TM bonds and showed that in substituted carbonyls a linear metal–C–O system can have CO stretching frequencies strongly reduced from gas-phase values. In 1964, Blyholder [28] indicated that the bonding in isolated CO can be regarded as resulting from an sp_z hybrid orbital of C combining with the p_z orbital of O to produce a σ bond, whereas the p_x and p_y orbitals of the C and O atoms combine to produce two π bonds. This leaves a lone pair of electrons on the O 2s orbital and a lone pair on a C sp_z hybrid orbital which can form a coordinate bond in a complex with suitable acceptor orbitals such as a d orbital on a metal atom. This leads to a σ bond between C and the metal atom. Since the formation of this σ bond puts a formal negative charge on the central metal atom, it is usually stated that back donation from a metal d orbital to the antibonding π MO on the CO ligand occurs to remove this excess negative charge and to stabilize the bond. This statement about π bonding between the metal and the ligand seems slightly misleading because, at first glance, it implies the placement of electrons in a high antibonding orbital. However, these MOs are lower in energy than the metal d orbitals.

Sung and Hoffman [29] in 1985 summarized the main ideas at the time supporting the early pioneering work of Blyholder [28]. From theory the MOs of isolated CO are well known. The HOMO is mainly a C lone pair whose energy is lower than the d states of TMs. In the generally accepted end-on CO chemisorption configuration the 5σ is pushed down by surface states relative to other CO levels. The lowest unoccupied MO set, the free CO 2π, consists of two antibonding orbitals with large coefficients on C. During adsorption the 2π-derived orbitals are partially populated and the CO bond weakened. The 5σ loses electron density in going from the free molecule to the chemisorbed system. The states that are pushed up above the Fermi level and which originated from d_{z^2} are in reality an antibonding mixture of d_{z^2} and 5σ orbitals. A similar mechanism can explain surface bonding with N_2. In this case the MOs that participate predominantly in bonding to the surface are the donating $3\sigma_g$ and $2\sigma_u$ orbitals which are essentially non-bonding with respect to the molecular bond (the N_2 $3\sigma_g$ orbital is weakly bonding and the N_2 $1\pi_g$ orbital is strongly antibonding). Strong metal–absorbate σ bonding implies little regarding the C–O and N–N bonds whereas metal-to-adsorbate back donation will lead to substantial weakening of the molecular bond [31–35].

In the Blyholder [5] molecular view of chemisorbed CO, the molecule is adsorbed in a linear metal–C–O structure, with electron donation from the CO 5σ orbital into d orbitals, and back donation from the surface 3d orbitals into the CO 2π orbitals. The metal atoms generally have various degrees of coordination with other metal atoms on the supported surface, the lower-frequency bands arising from CO bonded to metal atoms having less than the maximum number of neighbours. Within the HOMO–LUMO description of chemical bonding, the interaction of two fragments is described in terms of virtual excitations between occupied and unoccupied fragment orbitals. The donating interaction populates unoccupied metal surface orbitals by excitation of an electron from occupied adsorbate orbitals, whereas the back-donating interaction populates unoccupied MOs with electrons from the occupied metal surface orbitals. The donating and back-donating interactions between occupied and unoccupied orbitals on the respective fragments result in attractive interactions. The Hückel MO theory suggests that the bond energy decreases when antibonding orbital fragments become occupied. High coordination sites are favoured when electrons populate bonding orbital fragments. Electron occupation of antibonding orbital fragments favours low-coordination sites [3].

Adsorbate–metal fragment interactions control adsorption geometry. Both donation and back donation contribute to the total bond energy of the adsorbate–surface complex. Adsorbed molecules will interact with d as well as s and p valence electrons of a TM surface. For diatomic molecules such as CO, NO or O_2, the energy difference between bonding and antibonding orbitals is relatively small. This implies that the back donation arising from the interaction between occupied metal valence electrons and unoccupied adsorbate MOs must be considered. CO binds perpendicular to the metal surface through C to help to optimize both donating and back-donating interactions. This is due to the lower electron affinity of C. Donating interactions between an adsorbate and a surface behave oppositely to those of back-donating interactions. For example, a low work function, which acts to increase back-donating attraction, actually decreases the attractive donating interaction.

In spite of the success of the Blyholder model in describing the CO interaction with TMs, this model does not consider the existence of tilted states. During the period when Blyholder developed his model, there was no evidence that inferred postulation of tilted states. Only recently have tilted states been observed at unusually low CO stretching frequencies around 1100–1330 cm^{-1} for Fe(100), Fe(111) and Cr(110) [38–44]. Tilted precursor states and low N_2 stretching frequencies were also observed for Cr(110) [45–47]. Coordination of a diatomic molecule can also occur parallel to the metal surface. Overlap between the molecular $2\pi^*$ orbital and TM surface orbitals could be optimum when the diatomic molecule is adsorbed parallel to the surface. The antibonding character of the CO $2\pi^*$ orbital weakens the C–O bond, resulting in an elongation of the bond length and a lowering of the CO stretching frequency.

Much effort has been devoted to understanding the specific behaviour of each TM and the influence of its surface structure on the dissociation of diatomic molecules. Depending on the choice of TM and experimental conditions, the molecule can undergo either dissociation or molecular adsorption. The trends across the TM series indicated by Broden *et al.* [48(a)] two decades ago still hold, namely firstly that, for a given TM series, the further to the left a metal lies in the periodic table, the greater the tendency for dissociation, and secondly that the approximate boundary for dissociative or molecular adsorption moves to the left as one proceeds down the periodic table from 3d- to 4d- to 5d-electron-containing metals.

In order to understand better the approximate boundary for dissociative or molecular adsorption, one must also take into consideration the unoccupied d levels and the differences in energy among the 3d-electron-containing TMs arising from the relative separation of atomic states. The $d^n s^2, d^{n+1} s^1$ energy separation varies significantly across the 3d transition row. As the 3d orbital becomes more stable relative to the 4s orbital with increasing nuclear charge, there is, in general, a decrease in the $3d^n 4s^2 \rightarrow 3d^{n+1} 4s^1$ and $3d^n 4s^2 \rightarrow 3d^{n+2}$ excitation energies from left to right of a row. Since the d^n orbital contracts more rapidly than the d^{n+1} orbital with increasing nuclear charge, the propensity for s–d hybridization decreases across a row. There is also little net 4s–4s bonding at the optimal 3d–3d bond length. Andreoni and Varma [48(b)] analysed systematically the trend across a TM row of molecular against dissociative adsorption and noted that the dominant mechanism is hybridization of the 2π orbital with the TM surface density of states. The trends in charge transfer and in binding energy are determined by gross parameters of the metal, that is the position of the centre of gravity of the d band with respect to the atomic level and, to a lesser extent, the d bandwidth. The main features of chemisorbed CO on TM surfaces are strikingly similar to those of a carbonyl complex with a small number of TM atoms. The basic properties of the chemisorptive bond and the driving mechanism for the dissociation of the molecule are both essentially determined by the gross features of the TM substrate.

Now a question arises: is the tilted state the precursor molecular site of the dissociation of diatomic molecules on 3d metal surfaces? The existence of the bent geometry of diatomic ligands in TM complexes was a first indication implying tilted states on TM 3d surfaces. Also a bent geometry was proposed for several carbonyl haemoglobin compounds [49]. The present authors and co-authors [30–35] proposed a resonating valence bond mechanism of CO and N_2 dissociation on metal 3d surfaces that when combined with *ab initio* Hartree–Fock calculations predicts the occurrence of tilted states and dissociation on TM 3d surfaces.

The mechanism for the dissociation of a diatomic molecule (AB) on a TM 3d surface can also be viewed as a charge-transfer process with bonds resonating among the metal, and atoms A and B of the diatomic molecule. The theory is applicable since the surface–AB interaction is dominated by charge transfer [30–35]. Pauling's [50] resonating-valence-bond theory describes charge transfer in metals as transferring a bond from one atom to the next, accompanied by the creation of M^+, M^- and M^0 states. Synchronized resonance leads to charge separation and in fact describes an insulator state. Unsynchronized resonance, however, requires that the atom receiving a bond (M or M^+) has an orbital available for its reception (occupied in M^-). It is the existence of such an orbital (the lowest unoccupied $2\pi^*$ MO of CO or $1\pi_g$ of N_2) that permits the interaction of the adsorbed molecule as a Lewis π acid with the metal surface. Schematically, one has

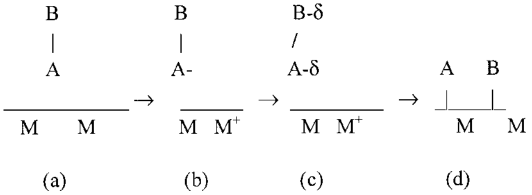

Following the approach of the diatomic molecule AB to the surface (with surface atoms M, step (a)), the first electron-transfer (b) leads to incipient bond formation between the surface (which acquires a positive charge represented by M^+) and A atom (the C atom of CO or the N atom of N_2). In step (c), the A–B bond is transferred to the metal surface. Dissociation occurs when the electron returns to the surface, step (d), restoring electrical neutrality as must occur in a catalytic process. The electron traverses a closed loop in the dissociation of AB. In the intermediate step of electron transfer from the A–B bond to the surface, the molecule becomes inclined to the surface. This mechanism predicts a tilted precursor state of dissociation of diatomic molecules on TM surfaces.

During the sequence of reactions of CO promoted by TM catalysts, the metal attacks C since the unoccupied $2\pi^*$ molecular orbital is mainly localized on it. The extent of $3d \rightarrow 2\pi^*$ back donation is directly correlated to the strength of the M–CO bond. The CO $5\sigma \rightarrow$ metal 3d donation contributes to reduce the excess negative charge on CO; however, there is very little CO 5σ-to-metal $3d\sigma$ donation if the $3d\sigma$ shell is also filled. By occupying the antibonding $2\pi^*$ MO, the C–O bond is weakened. The charge-transfer process leads to a build-up of negative charge mainly on C, although a significant portion delocalizes on to O as well. This charge-transfer model is supported by the results of our previous UHF SCF calculations [30–35].

The dissociation of diatomic molecules such as CO and N_2 holds high interest for understanding heterogeneous catalysis and much effort has been devoted to the comprehension of the specific behaviour of each TM and the influence of the metal surface structure on the interaction with the diatomic molecule. The molecule CO, in particular, is partly dissociated at relatively low temperatures on some TM surfaces whereas higher temperatures are required for other surfaces and yet on other surfaces only molecular adsorption is observed. The surface structure also has significant influence. On most densely packed surfaces, dissociated CO could not be detected even at relatively high temperatures while CO dissociation was reported on various stepped TM surfaces. It is found generally that, in going from left to right in the periodic table and from TMs containing 3d to 5d electrons, dissociative adsorption is suppressed. We note that to the left of the periodic table, one finds dissociation of CO on the TMs Fe, Cr, V, Ti, Nb, Ta, W, Re and Ru. To the right of the periodic table, one finds molecular adsorption on the TMs Cu, Co, Ni, Rh, Pd, Ag, Au, Pt and Ir. CO adsorbs in an end-on orientation with the C end towards the surface for the metals on the right side of the transition series, for example Ni, Pt, Pd and Cu. Weak CO chemisorption was observed on Cu(100), Cu(111) and Cu(110) and strong chemisorption on Ru(001), Pd(100) and Pt(111).

Under certain experimental conditions, we can also find dissociation on some of the metals on the right side of the periodic table. On densely packed surfaces of Co, Ni and Rh, for example, dissociated CO was not detected even at high *T*, while CO dissociation was reported on stepped surfaces of these metals. Special step and bridge sites, small crystallites with special surface sites with a low coordination number occurring in high concentration on small metal particles, low-index faces, films and rough surfaces, with surface defects such as steps and kinks can facilitate CO dissociation on TMs including those to the right of the periodic table. In addition, K and Li can also promote dissociation on some TMs to the right of the table, including Cu(100), Ag(001) and Ni(100).

The effects of an alkali-metal promoter can be important. We note that, on clean Ru(001), CO is found to lie on the surface and, when K coverage exceeds $\frac{1}{3}$ ML where ML indicates monolayer, CO is found to stand perpendicularly to the surface even on Ru(001). Proceeding further left in the transition series one expects that side-on bonded CO will be more stable than end-on bonded CO even on an unpromoted surface. This behaviour has been confirmed in studies of CO and N_2 adsorbed on Cr(110) surfaces. Remarkably, most of the data on CO and N_2 chemisorption on TM systems can be unified and understood in terms of the simple conceptual Blyholder metal–CO bonding model as modified by the present authors and co-workers [9, 39–35] with the introduction of the tilted precursor state.

There are four interesting and even unusual findings arising from experimental results of chemisorption and dissociation of CO on TM 3d surfaces. First, why does the adsorption of CO on first-row TM surfaces Sc to Fe tend to dissociate CO whereas from Co to Cu the CO tends to remain adsorbed on the surface. Second, what is the origin of the unusually low observed CO stretching frequencies at 200–1260 cm^{-1} for Fe(100) and 1150–1330 cm^{-1} for Cr(110)? Third, what is the precursor state for CO dissociation on TM surfaces? Fourth, how do modified catalytic 3d surfaces, such as those formed by doping with alkali atoms, lead to more efficient chemisorption and dissociation?

The interaction of CO with clean Fe surfaces has been investigated by various techniques owing to the important role the CO–iron interaction plays in Fischer–Tropsch synthesis [51–56]. These studies showed that CO is molecularly adsorbed at low temperatures, but that it is decomposed at higher temperatures (above about 300 K). CO adsorption takes place via a weakly bound precursor state. The dissociated C and O recombine and desorb as CO molecules around 800 K for the low-Miller-index Fe crystal surfaces. Three molecular adsorption sites, two 'hollow' sites and one 'on-top' site for Fe(111), have been reported [55]. CO molecules adsorb on-top sites of Fe(110) at 120 K. A clean well characterized Fe(100) surface yielded three low-temperature desorption peaks at high CO coverages labelled α_1, α_2 and α_3. An unusually low band at 1200 cm^{-1} is the C–O stretching frequency associated with the α_3 precursor to a dissociative state. The broad peak with the higher frequency at 2100 cm^{-1} is the C–O stretching frequency associated with the α_1 and α_2 molecular species [53]; the free-molecule CO stretching frequency is 2143 cm^{-1}. The α_3 state indicates a tilt angle of about 45° for CO in the fourfold hollow site on the Fe(100) surface and provides direct experimental evidence that CO (α_3) is the precursor to CO dissociation on an Fe(100) surface.

Our previous [32] *ab initio* calculations of Mulliken populations, bond index and Fermi levels of FeCO indicated that, as CO is tilted, there is increased Fe → CO charge transfer as well as a corresponding decrease in the C–O bond order as the Fermi level moves to more negative values. In order to improve our description of the interaction between CO and an Fe surface, we considered an Fe_5CO cluster model for the CO–Fe(100) surface. Calculations were carried out for five CO configurations: end on with CO at 90° with respect to the surface, and at 0° and 45° with respect to the surface with the CO placed both diagonally and parallel to the Fe_4 plane.

Our earlier effective-core potential (ECP) and multiple-scattering (MS) X_α calculations indicated that two mechanisms are mainly responsible for this C–O bond weakening [32]. First, as Fe–CO bends, the Fe–C bond changes character from sp to sp^2 hybridization with loss of the triple-bond structure of CO. Second, as Fe → CO charge transfer increases, the population in O antibonding orbitals increases, weakening the CO bond. This increase in charge transfer arises from the new overlap of the 3d orbitals of Fe with the CO sp^2 and p orbitals in a bent structure. Charge transfer from the metal dπ orbitals also contributes to CO bond weakening. In cases where molecular symmetry is lowered from C_{4v} to C_s, the system has only one symmetry element, the x–z plane, which makes possible mixing of the $2p_x$ and p_z orbitals from the C and O atoms while the p_y orbital retains its symmetry. Although this lowering of molecular symmetry smears the distinction between σ and π charge transfer, it is now possible to have both charge transfer into and out of the CO sp^2 hybrid orbitals. The same holds true for the CO p_y orbital. These results indicate that metal back donation is considerably larger than CO → metal donation. The monocarbonyl complex, in which the surface is represented by only one Fe atom as well as the larger Fe_5CO cluster, obtained using *ab initio* MS X_α and ECP methods, indicate the same finding, that is that back donation is the dominant mechanism. More negative values of the Fermi level facilitate Fe → CO charge transfer and, for the bent 45° pre-dissociative state, its Fermi level is found to be the lowest of all the configurations considered. The vibrational frequency of the adsorbed molecule can be taken proportional to the inverse of the back donation. The ratio of the calculated Fe_5CO MS X_α back donation for the perpendicular and the bent (45°) CO configurations is 0.5 in reasonable agreement with the value obtained by comparing the corresponding two observed frequencies, $1260/2070 \approx 0.6$. This suggests that the α_3 state is effectively the tilted state of CO on the Fe(100) surface and the α_1 and α_2 states may be associated with perpendicular adsorption. Analysis of the spread of back-donation values with CO inclination indicates that the changes in stretching frequencies can be correlated with variation in Fe → CO back donation using a cluster model representation of the molecule–surface interaction.

CO chemisorption on a Cr(110) surface indicated that two molecular binding modes are sequentially populated [57]. The first of these, α_1(CO), is bound with its axis nearly parallel to the Cr(110) surface. The C–O has a stretching frequency of 1150–1130 cm^{-1} and is π bonded at twofold symmetric surface hollow sites—precursor states to dissociation. At higher CO coverages, an α_2(CO) binding mode is observed at 1865 cm^{-1} and at 1975 cm^{-1}, indicative of terminally bound molecules adsorbed atop and at bridge sites and aligned approximately perpendicular to the surface.

Our [34] *ab initio* calculations of the CrCO and $\mathrm{Cr_2CO}$ model systems indicated charge transfer and 3d orbitals to CO as well as weakening on the CO bond as it is tilted. The net surface $\rightarrow$ CO charge transfer is typically larger when CO is tilted. The additional charge transfer for the tilted states contributes to the population increase in CO antibonding orbitals. For all sites and for all fixed Cr–Cr and surface–CO distances, the CO bond order decreases as CO is inclined towards the surface. We also observed that differences in CO bond order are typically smaller between the onefold and twofold sites than the difference between the perpendicular and parallel configurations which suggests that the important effect is inclination as opposed to site adsorption. We infer that the CO vibrational frequencies around 1975 cm^{-1} reflect differences in site adsorption, whereas frequencies around 1330 cm^{-1} correspond to inclined CO at these same sites. Preferential inclination occurs in the direction of the closest Cr atom. As expected, an increase in the Cr(1)–Cr(2) distance results in reduction in charge transfer. Further, reduction in the surface–CO distance results in increased charge transfer whereas an increase in the CO bond distance results in a reduction in CO bond order. Comparison of the calculated ratios of back donation for the perpendicular and parallel CO configurations suggests that there should be increased back donation, CO bond weakening and subsequent reduction in stretching frequencies in the tilted state, supporting experimental results which indicate that the binding mode at 1360 cm^{-1} is due to twofold symmetric surface hollow sites with the intramolecular axis nearly parallel to the Cr(110) surface. The binding mode at 1975 cm^{-1} is indicative of terminally bound molecules adsorbed and aligned approximately perpendicular to the surface.

The present authors and a co-worker [31] used *ab initio* calculations of MCO systems (M ranges from Sc to Cu) in order to describe general trends of CO adsorption on TM 3d surfaces. In general, the metal $\rightarrow$ CO charge transfers for the $3d^{n+1}4s^1$ metal configuration are higher than those corresponding to the $3d^n 4s^2$ configuration. The $3d^{n+1}4s^1$ configuration has an additional 3d electron which further increases charge transfer. As expected for a given TM, the occupation of 3dπ orbitals leads to higher back donation. The electronic configuration is an important factor in determining the extent of TM $\rightarrow$ CO charge transfer and therefore the occurrence of dissociation. For Co, Ni and Cu, the calculated ground-state configuration of the MCO system has smaller back donation which suggests that there are surface configurations of these metals that do not have a tendency to dissociate CO, as observed experimentally. There are, however, some excited configurations that have back donation and could lead to dissociation.

Turning now to other TM surfaces [31], we consider as a simple illustrative case the Sc surface in which each of the two 3d orbitals has typically one electron. The electronic configuration of the Sc surface, represented here by the electronic state of linear ScCO is interesting to analyse because with it one can study the behaviour of the $3d_{xz}$(π) and $3d_{zy}$(π) orbitals in tilted states. The inclination of CO at 30° relative to the surface increases the net SC $\rightarrow$ CO charge transfer by almost 50% (from 0.42e to

0.59e). The major contribution to this increase in charge transfer with CO inclination comes from 3d orbitals. There is also a small −0.01e increase in CO→ Sc charge transfer to the $3d_{xy}$ and 4p orbitals as CO inclines. The ScCO electronic configuration changes from $(3d\pi)^2(4s)^1$ to $(3d\pi)^1(\mathrm{CO}\ 2\pi^*)^1(4s)^1$, illustrating the important role of Sc (3dπ)→ CO (2π*) charge transfer. The symmetry of the $3d_{xz}$ and the $3d_{yz}$ orbitals is broken with inclination. The Mulliken population of the $3d_{xz}$ orbital increases slightly, but the metal→ CO charge transfer remains large. On the other hand, charge transfer via the $3d_{yz}$ orbital increases significantly, by about 0.5e (the $3d_{yz}$ Mulliken atomic population drops from 0.70e to 0.23e). Analysis of bond order for different tilt angles of CO on TM surfaces indicates that, for all the dissociative surfaces studied, inclination leads to increased charge transfer and reduction in CO bond strength as it inclines.

Cu, which is to the right of Fe in the periodic table, tends to be non-dissociative for CO chemisorption. If we compare CuCO with FeCO in excited states without back donation, we find that for inclined CO there is only a small increase in charge transfer for CuCO compared with FeCO even though CuCO has more d electrons available to participate in back donation to 2π* orbitals [9].

The CO interaction with TM surfaces has been investigated using a wide range of experimental techniques. For example, CO adsorption on the Ni(100) surface has been studied experimentally by low-energy electron diffraction (LEED), near-edge X-ray absorption fine structure (NEXAFS), normal photoelectron diffraction, Fourier transform infrared (IR) adsorption reflection spectroscopy, thermal desorption spectroscopy (TDS), electron-energy-loss spectroscopy (EELS), high-resolution electron-energy-loss spectroscopy (HREELS), IR reflection absorption spectroscopy, angle-resolved X-ray photoemission spectroscopy and IR spectroscopy [58–69]. On the flat closed-packed surface of Ni(111), surface adsorption of CO is both non-dissociative and unactivated [70–72]; the activation energy for desorption has been measured to be 1.3 eV. For a wide range of incident translation energies, approximately 50% of an incident beam of CO will stick to a Ni(111) surface [70–73]. The adsorption of CO on Ni(111) is an example of multiple CO coordination possibilities to surface Ni atoms, in which continuous conversion from threefold to twofold CO bridge bonding has been observed with increasing coverage [74]. In addition, spectroscopic measurements showed that the interaction among CO molecules at high coverages is strongly repulsive. At saturation coverage, a strong repulsive interaction for CO on Ni(110) was suggested to force a tilt of 21° in the [100] direction to lower the total energy of the system [75]. CO molecules are also expected to interact strongly at high coverages on Ni(111). The CO stretching band was observed to shift from 1815 cm^{-1} at the lowest coverage to up to 1915 cm^{-1} upon saturation. This behaviour was attributed to increased CO bond strength at higher coverages caused by reduced back donation into the 2π* antibonding CO orbital [76]. The latter was attributed to indirect chemical and electrostatic interactions between adsorbed molecules and, at the highest coverages, to strong intermolecular repulsive forces, which arise because of the closeness of adjacent CO molecules.

The interaction of CO with Ni surfaces has also been investigated theoretically by numerous techniques, such as ASED–MO [77], model Hamitonian self-consistent field [78], generalized valence bond (GVB) [79], CASSCF [80], X_α [81], Hartree–Fock–Slater [82] and the linear combination of Gaussian type orbitals (LCGTO)–local spin-density method [83]. In addition to the Blyholder model, other approaches place importance on the interaction of the CO 2π orbital with the metal p_π rather than d_σ orbitals. The orbital energies of the bare cluster indicate few levels with appreciable s character and a d band with a high density of states around the Fermi level. The 2π* orbital, possessing mainly C 2p character, lies above the Fermi level of the bare cluster system. Upon CO adsorption the Fermi level lowers relative to the bare cluster. When CO approaches a Ni surface, charge transfer occurs from the surface to CO. The increase in charge on C is due to the increase in 2p contributions arising from the partial occupation of the CO 2π* orbital.

It is well known that both electronegative (e.g. O, Cl and C) and electropositive (e.g. Na, Cs and K) atoms exert strong influence on catalytic performance [84–87]. Pre-adsorbed K increases the rate of dissociative adsorption of CO often by orders of magnitude. This behaviour has been related to increased binding of the molecularly adsorbed species in the neighbourhood of K atoms. The increase in dissociation rate is then simply interpreted as a decrease in the desorption probability relative to the dissociation probability. Further, it has been found that pre-adsorbed S, Cl, P and C act as poisons for CO adsorption by destabilizing the molecularly adsorbed species. S, O and C adlayers all reduce the binding energy of CO to a surface and inhibit CO dissociation. K was observed to enhance CO bond strength to a surface and to increase the amount of CO dissociation relative to a clean surface. CO chemistry on an Fe surface, for example, is markedly influenced by pre-adsorbed atomic species whereas S, O and C adlayers all reduce the CO binding energy and inhibit CO dissociation [21].

Interesting studies of the effects of CO coadsorbed with alkali metals on TM surfaces have been carried out. An example is the determination of vibrational shifts of CO on Cu(100) which is of considerable experimental [88–92] and theoretical interest [93–96]. It is well known that the alkali atoms influence the electronic structure of CO and lead to significant changes in chemisorption properties. One of the most dramatic changes induced by coadsorbed alkali atoms is the decrease in CO vibrational frequency, which in some cases can be as low as 1200–1400 $\mathrm{cm^{-1}}$ [97] compared with the free CO stretching frequency of 2143 $\mathrm{cm^{-1}}$. Several mechanisms have been suggested to explain this decrease and the enhanced catalytic activity of CO coadsorbed on TM surfaces in the presence of promoters.

The mechanisms that induce lowering the CO vibrational frequency [88–103] can be roughly classified into five groups. One is a through-metal effect [98] that assumes that electron donation occurs from the alkali atom to the surface resulting in a upward shift of the Fermi level and increased capability of the metal to back donate charge into the 2π* MO of CO, resulting in bond weakening and reduction in vibrational frequency. Another mechanism suggests that there is sp^2 rehybridization of the metal–CO bond with reduction of the triple-bond character of C–O [99]. Recently, a third mechanism has been proposed that emphasizes direct interaction between the outermost s orbital of the alkali metal and the 2π* MO of CO [100, 101]. In this picture, direct charge transfer from K to CO, for example, leads to the formation of K^+–CO^- surface complexes and to dramatic vibrational shifts. The electrostatic interaction between the electric field created by the positively charged alkali-metal ions and the dipole moment of adsorbed CO may also be an important path. It has been shown that this purely electrostatic effect may induce a substantial red shift of the CO vibrational frequency [94, 102]. Geometric effects have also been suggested to play a role [103].

Pacchioni and Bagus [88] indicated that the activation of coadsorbed CO, and hence the dramatic lowering of the CO vibrational frequency, arises from a combination of various mechanisms with differing relative importances. Two of the dominant mechanisms are electrostatic interaction prevailing at long range and enhanced back donation from polarized Cu electrons prevailing at short range. For K–CO, no direct charge transfer was found. Bauschlicher [24] also studied theoretically CO/Cu(100), including electron correlation at the modified coupled-pair functional level, using a large basis set for Cu atom at the adsorption site and for CO. Electron correlation is found to increase the binding energy by about 1 eV, which is in very good agreement, as is the geometry, with experiment for the largest Cu cluster considered. Unlike binding energies, the CO vibrational frequency shift relative to free CO is found to be independent of cluster size and the inclusion of electron correlation. Pacchioni and Bagus [104] also investigated CO chemisorption on the bridge site of the Pd(100) represented by Pd_2 and Pd_8 clusters using *ab initio* relativistic and nonrelativistic Hartree–Fock and MCSCF calculations. The interaction energy was decomposed into contributions arising from intraunit polarization and interunit effects including charge transfer and covalent bonding. Besides classical π back bonding found for other TM surfaces, CO σ donation to the partially occupied 4dσ–5sp metal hybrid orbitals significantly contributes to the chemisorption energy.

Some more recent work indicates the new trends. The surfaces of bimetallic systems are being intensively studied because of their unique properties and indicate marked effects when the constituents differ considerably. When the two metals are neighbours in the periodic system, often a rich variety of interesting phenomena is observed. For example, Pt grows epitaxially on Ni(111) and, owing to the large atomic-radii misfit, departure from the compressed ideal Pt structure can be anticipated [105, 106]. For CO on the (111) face of PtNi alloys a reduction in chemisorption heat has been reported. A tight-binding model study [107] of CO adsorption on a Pt/Ni(111) surface yielded a chemisorption energy lower than on pure Pt(111), most probably owing to overlayer compression.

NEXAFS spectroscopy absorption features indicate that, for simple diatomic molecules such as CO, two pronounced resonances, labelled π and σ, are observed. Lower in energy, the sharp π resonance is associated with the excitation of a core electron into the lowest unfilled antibonding MO of π symmetry. At higher photon energies, the broader σ resonance can appear, which is explained either by a transition into an unfilled antibonding σ MO or by MS of the excited electron in the molecular potential, resulting in the first intramolecular extended X-ray absorption fine-structure wiggle [108].

In order to elucidate the dynamics of surface-chemical reactions, it is important to measure the internal (vibrational and rotational) energy and the translational energy of product molecules desorbed from catalyst surfaces [109–111]. The oxidation of CO on Pt and Pd surfaces are the prototype reactions for dynamics studies and the source of information on the translational and internal energy states of CO_2 produced by catalytic reaction. The vibrational and rotational states of product CO_2 are sensitive to surface structure, that is the transition state of CO oxidation is strongly affected by the structure of the reaction sites. Vibrational dynamics on surfaces are an elementary class of gas–surface energy transfer problems whose description is a step towards full understanding of crystal growth and chemical reactivity at surfaces. Beyond measuring time scales and delineating whether such energy transfer is vibrational or electronic, the central problem is understanding the relationship between the observed dynamics and features of the chemical interactions between adsorbate and surface. In recent years there has been important experimental progress in unambiguously characterizing the vibrational relaxation of adsorbates on metals for which the most intensively studied systems to date are CO/Cu(100) and CO/Pt(111) [112–114].

The oxidation of CO on CO/O_2/Pt(111) has been attributed to O released from dissociation of O_2 and to excited O_2. The rate of CO_2 production is consistent with dissociation of O_2 prior to the oxidation of CO. If CO oxidizes by an atomic pathway, then the capture of O by CO is highly efficient; if CO oxidizes by a molecular pathway, then the O atoms in the CO_3^* transition state are inequivalent [115]. The rates and pathways by which adsorbates at surfaces are energized or de-energized play an integral role in dynamical processes such as adsorption, surface diffusion, chemical reaction and desorption [116].

Consider coadsorption of CO and CH_3O on Ni surfaces. The adsorption of methoxy (CH_3O) on TM surfaces has received a great deal of attention because of its role in catalytic oxidation and combustion reactions. Furthermore, CH_3O is a commonly occurring fragment in the O–H bond scission decomposition of methanol on most metal surfaces. On Ni(100), methoxy decomposes a surface-bound CO and H_2 for which a quasistable COH or HCO intermediate has been proposed. Similarly, methoxy decomposes to CO and H on Ni(110) and Ni(111) at room temperature. In all cases, the C–O bond is retained along the decomposition pathway [117].

Several mechanisms have been proposed to rationalize the observed intraligand vibrational frequency shifts induced by an electric field [118–122]. One mechanism assumes that the degree of coverage changes with the electric potential and that the shifts originate from the coupling of oscillating C–O dipoles. Another explanation assumes that the external electric field changes the amount of charge back donated from the metal to the $2\pi^*$ antibonding MO of CO, thereby modifying the CO stretching frequency. A third explanation is based on an electrostatic argument according to which the shifts are determined by physical effects and, in particular, the interaction between the adsorbate dipole and the external field. It has also been argued that a combination of chemical and physical effects is required to explain the potential-induced shifts of CO on Pt electrodes [122]. The theoretical analysis by Bagus and Pacchioni [118] of the vibrational shifts of CO chemisorbed on Pd(100) indicated that the Stark turning rate is not altered significantly by the electronic rearrangement induced by the field. They argue that the shifts arise primarily from the field–dipole electrostatic interaction and that chemical effects are small. Although the consequence of electronic rearrangements, which are caused by the applied field, are small for the change in shifts observed, these chemical effects lead to large changes in the intensity of the IR transition. The chemical changes may be within the CO unit and may not involve changes in charge transfer or dative bonding between the TM and CO.

A great deal of recent attention has focused on the physics and chemistry of Pd thin films on several metal single-crystal surfaces owing to significant differences in the structural, electronic and chemical properties between these films and bulk Pd. The former are also of particular interest because the observed changes in CO chemisorption properties are greater than those found with Ni and Pt films. For example, a comparison of CO desorption from Ni, Pd and Pt monolayer films supported on W(110) with that from bulk Ni(111), Pd(111) and Pt(111) samples shows that the CO desorption temperature decreases by 50 K for Ni and by 60 K for Pt monolayer films, but a surprising 180–195 K for a Pd monolayer. The electronic structure of Pd monolayers on different substrates has also been observed to differ considerably from that of bulk Pd, showing a low density of states at the Fermi level characteristic of the group 1B (Cu, Ag and Au) metals. This alteration of the electronic structure is not strongly dependent on substrate, with similar changes seen for Pd thin films on Ta(110), Nb(110), W(110), Cu(111), Ag(111), Au(111) and Al(111). This is most striking in view of the reasons proposed for these alterations including lowered Pd–Pd overlap (suggested for the highly strained Pd–Nb system, but inapplicable to the almost unstrained Pd–Ag and Pd–Au systems), d-state covalent interactions between the substrate and adsorbate (also proposed for Pd–Nb), and charge transfer [123–126].

The transition from a molecular to a metallic adsorbate system is also of recent interest. For extended metallic systems a detailed understanding of electron correlation, charge transfer, screening response upon ionization, electron excitation and decay dynamics is not easily achieved owing to the large number of electronic levels involved; nevertheless, cluster calculations and band-structure models have been rather successful. An important step towards a more complete understanding of the adsorption bond was taken by introducing complexes consisting of molecules bonded to only a few metal atoms as intermediates [127]. For CO, the prototype absorbate, experimental data on carbonyls were found to exhibit many features similar to the CO methyl case. Two alternative methods were used to monitor experimentally the development of a CO adsorption system that gradually changes from molecular to metallic: first, CO was deposited under ultrahigh-vacuum (UHV) conditions and adsorbed on Pd islands of increasing size and, second, Pd was deposited in a CO atmosphere leading to the growth of Pd carbonyl-like species. For CO adsorbed on UHV-deposited islands, the electronic properties of the CO–Pd complex is strongly dependent on the island size and CO coverage: large amounts of CO result in reduced screening ability, and small effects characteristic of molecular systems can be detected even for islands containing about 100 Pd atoms [127].

The reaction site identification and its modifications are requisite for designing catalyst surfaces with new functions as well as for understanding the reaction dynamics of surface elementary processes. The angular and the velocity distributions of desorbing products provide structural information on the reaction sites. Identification and switch-over of reaction sites in CO oxidation of Pt(113) and Pt(112) are indicated by heating the co-adlayer of CO and by five O_2 peaks in the range 160–420 K sharply collimated along either the (111) terrace of the (001) step normal [128]. A fundamental property of any model for the geometrical structure of an adsorption system is the specification of which of the available sites on the surface is occupied by the adsorbate and how surface site occupation changes with adsorbate coverage. A method with the potential of providing such information in a rather straightforward manner is high-resolution core-level photoemission applied to the core levels of the adsorbate and the substrate. Such studies were used to investigate adsorption sites at low temperatures of CO on a Rh(111) surface as a function of CO coverage. At coverages up to 0.5 ML, the majority of the molecules are found to adsorb in on-top sites and, at higher coverages, threefold sites become increasingly populated [129].

The study of CO adsorption and oxidation on Pt electrodes is of both fundamental and applied importance in electrochemistry. Comparisons between the vacuum and the electrochemical environments will facilitate the understanding of CO behaviour in electrochemical environments. Incomplete oxidation of small organic molecules results in the formation of adsorbed CO which poisons electro-oxidation reactions [130]. Extensive studies of catalytic oxidation of CO over the past couple of decades have lead to the development of a general mechanism that applies to a wide variety of TM-based catalysts. In this mechanism the CO and O_2 adsorption steps, which are believed to be molecular and dissociative, respectively, are followed by recombination between CO and O on the surface (via a Langmuir–Hinshelwood step) and fast desorption of the resulting CO_2. Although the kinetics of this reaction have been investigated in some detail, owing to its complexity, questions remain.

Rate dependence on surface coverages for isothermal studies of the kinetics of CO oxidation on Pt(111) have indicated that the reaction rates depend not only on reactant coverage but also on surface preparation. While the presence of O on the surface helps the production of CO_2, increasing CO coverages increase the activation barrier for this reaction [131]. Recent advances in *in-situ* measurements have brought about greatly improved characterization of electrode surfaces and fundamental knowledge about the interaction of molecules, solvents and solutes with a well defined metal surface. This information is important for understanding the physics and chemistry at a solid–solution interface. Coadsorption of CO with water on Pt(111) has shown strong interaction with overlayer water molecules and retarded the oxidation of CO to CO_2 [132].

In discussion to this point, adsorbed molecules and atoms on metal surfaces are in registry with the substrate lattice so that adsorption-induced reconstruction can be explained by assuming local movement of substrate atoms. In contrast with this image, the metal surface often brings about a kind of chemical reaction during catalysis and adsorption. In these cases, metal atoms react with adsorbed molecules or atoms to yield low-dimensional quasicompounds which undergo self-assembly on the surface [133]. Ordered alloy surfaces, which are known to have a stable, well defined structure, provide the possibility of relating surface properties to microscopic data. An example is Cu[110]c(2× 2)–Pd which is usually obtained by depositing 0.5 ML of Pd on to a clean Cu(001) surface. On this surface, CO is bonded only at on-top positions of Pd atoms and the CO stretching vibration is independent of CO coverage. For Ni[001]c(2× 2)–Al, CO is bound at the on-top position of Ni atoms and also fourfold bridge positions between two Al and two Ni atoms. Increasing the CO exposure leads to a shift of the two C—O bond stretching vibrations. The d electrons that back donate into the $2\pi^*$ antibonding orbital of CO come from the Ni atoms both in the first and in the second layer [134]. For CO adsorption on Cu(100) there are two known adlayer structures. At very low coverages, the adlayer is disordered but, at 0.45 ML, some ordering occurs; at higher coverages, there is uniaxial compression. Vibrational energy transfer processes that are known to have considerable influence on the chemistry and physics of surface processes including adsorption, reaction and diffusion are important in this system in which dipole–dipole coupling results in C—O frequency shifts [35].

The development of powerful experimental techniques has helped us to understand the bonding of molecules to metal surfaces and to reveal the basic mechanisms of heterogeneous catalysis. Theoretical studies, however, have generally focused on equilibrium geometries, vibrational frequencies and bonding mechanisms [136], but little is known about the potential energy surfaces for bonding of diatomic molecules to TM surfaces. For CO/Pt(111) the bonding mechanism can be described by the Blyholder model for which reactants smoothly reach the chemisorbed state by a process explained in terms of a single PES. This mechanism differs from other work [137] which indicated that π back donation does not contribute to the interaction of CO with Pt(111).

The surface chemistry of metal oxides holds considerable importance in catalysis. A large fraction of industrial catalytic processes involves reactions occurring at TM oxide surfaces. One of the most promising techniques proposed for non-destructive analysis of an oxide catalyst surface makes use of CO. The CO IR frequency is measured at various temperatures and degrees of coverage. The vibrational frequency shift of adsorbed CO relative to the gas-phase value provides an indirect measure of formal charge, coordination and number of cation sites on the catalyst surface. The great advantage of this technique is that it can be used for powders and other non-single crystal surfaces. Bagus and co-workers [24] have reported interesting findings on bonding and vibrations for CO chemisorption on oxide surfaces.

The molecular adsorption of CO on Pd(110) revealed a fascinating sequence of reconstruction and de-reconstruction of the metal surface induced by changes in adsorbate coverage. The theoretical dissociation energy barrier of CO on a Ni(111) surface is much smaller than that on a Pt(111) surface, in agreement with experimental results. The adsorption sites for CO on a Rh(111) single crystal surface indicates that, at low coverages, the majority of the molecules are found to adsorb at on-top sites whereas, at higher coverages, threefold hollow sites are increasing populated. The lateral interactions between CO molecules chemisorbed on the Rh(110), Rh(100) and Rh(111) surfaces have weakly repulsive and attractive interactions on all three surfaces whereas non-monotonic interactions between chemisorbed CO molecules are rather common on low-index surfaces [138–140].

Theoretical studies of the bonding mechanism of CO to Pt(111) and its effect on the vibrational frequency of chemisorbed CO indicates that the bond is found to be dominated by σ donation and π back donation, whereas the major contribution to the experimentally observed vibrational shift is explained by the π back donation mechanism. The effects of coverage on IR frequency shifts of CO adsorbed on Ni(111) surface was recently attributed to lateral interactions between the adsorbed molecules and the adsorption of CO on different fcc and hcp threefold hollow adsorption sites. The site-occupancy pair correlation function for CO adsorbed on Pt(111) indicated that, at low coverages a diffuse superstructure involving only on-top sites appears while, on increasing the coverage, more and more bridge sites are occupied and a superstructure grows progressively. The adsorption dynamics for precursor adsorption in the systems N_2/W(100), CO/(Fe–Si(100)) and O_2/Ni(111) indicate that there is no discernible influence of rotational state on the sticking coefficient for intrinsic or extrinsic precursors. Apparently the molecule can rotate more or less freely and the rotational energy can be accommodated subsequently leading to trapping. Some very interesting work has also appeared recently on CO chemisorption over metal surfaces and overlayers [141], surface electronic structure and reactivity of transition and noble metals [142], a comparison of N_2 and CO adsorption on Ru(001) [143], structure sensitivity in adsorption for CO interaction with stepped and reconstructed Pt surfaces [144], and the theory of adsorption and surface reactions [145].

Temperature dependence (90–440 K) of the vibrational spectra of CO adsorbed on a disordered Pt(111) substrate has been studied by sum-frequency generation. At low temperatures a centre-frequency of 2091 ± 4 cm^{-1} was determined which is characteristic of the stretching vibration of top-bound CO at Pt terrace sites. At a temperature of 360 K, a centre frequency of 2074 ± 5 cm^{-1} was obtained which is characteristic of the stretching vibration of CO bound on step sites of the disordered Pt(111) substrate [146]. Recently, the coadsorption of CO and Cs and Ru(0001) has been investigated and provided detailed information on atom location and vibrational properties. Starting from a pre-covered surface, coadsorption of CO leads to improved ordering and the formation of a mixed Cs +CO overlayer. Cs atoms remain in on-top positions while CO changes its adsorption site from on top, as found on a clean surface, to the threefold hollow site in the mixed Cs +CO overlayer [147]. This site change was ascribed to a purely electronic effect. CO molecules can utilize the enhanced charge density at the surface due to the Cs overlayer by a substrate-mediated charge transfer into the CO $2\pi^*$ MO. Since back donation is more efficient in highly coordinated sites than in on-top positions, CO changes its adsorption site.

The adsorption behaviour of the K/CO coadsorbate system was studied at an adsorption temperature of 95 K on the Cu(332) surface [148]. Thermal desorption spectroscopy experiments show that K adatoms influence the electrostatic potential induced by the steps of the surface, with the result that COs adsorbed on step sites are the first to be influenced by coadsorbed alkali. With K present on the surface a strong K–CO interaction is evidenced by the stabilization of the adlayer up to temperatures greater than 599 K. Work-function change measurements reveal a change in CO bonding towards the pre-covered surface, that is the results cannot be readily interpreted in terms of direct interaction of K with the CO 1π orbital. The existence of this direct interaction gives rise to absence of the $(1\pi + 5\sigma)$ degeneration in CO-induced states in the ultraviolet photoelectron spectra.

The adsorption of CO on Pd(111) and Pd(100) surfaces has been extensively documented experimentally [149]. On Pd(111), CO is adsorbed on a threefold hollow site at low coverages and on a bridge site at higher coverages. On Pd(100) a bridge site has been detected. Only a few data exist concerning the adsorption of CO on Mn. It seems that CO adsorbs in both the dissociative and the molecular forms. The study of CO adsorption on Pd_3Mn alloys indicates a decrease in the binding energy on the alloy surfaces compared with pure metal surfaces. The local chemical properties of bimetallic surfaces are often drastically different from those of each of the components. Using CO adsorption as a probe, it was shown [150] for two model systems, Au/Pd(111) and Pt/Ru(001), that their chemical properties depend critically on local surface structure and that the correct interpretation of area integrating spectroscopic and kinetic data obtained from these surfaces requires detailed knowledge of their (defect) structure and the distribution of different components in the surface layer. In addition, information on the local chemical properties of specific structural elements such as monolayer islands and monolayer island edges, and specific surface ensembles can be obtained by applying in combination high-resolution scanning tunnelling microscopy imaging and area integrating spectroscopic techniques to bimetallic surfaces whose morphology and composition are varied in a systematic and controlled way.

Bimetallic surfaces of alloys often show superior catalytic performance. For bimetallic surfaces, two mechanistic concepts have been introduced to account for the experimentally observed pronounced dependence of reaction rates on surface composition: the so-called ensemble effect and the 'ligand effect'. The former assumes that a minimum of neighbouring surface atoms of one type is required to make possible adsorption or reaction on the surface, which for surfaces consisting of a dispersed mixture of two or more atomic species yields a pronounced concentration dependence. The ligand effect describes the stepwise change in electronic and chemical character of a surface atom A when the neighbouring (surface) atoms are successively replaced by B-type metal atoms.

Experimental results based on photoelectron spectroscopy, HREELS and LEED indicate that a hydrogenated K/Cu(100) interface blocks the adsorption of CO [151]. The catalytic properties of a surface are determined by its composition and structure on the atomic scale. Structural effects are often investigated using well defined single-crystal surfaces (model catalysts) [152]. This approach, however, cannot take into account the characteristic behaviour of supported catalysts such as the influence of dispersion and the role of the substrate (so-called size effects) in catalysis. Size effects in heterogeneous catalysis are generally explained by the proportion of low-coordinated active sites with metal cluster size (the geometrical effect) or by the electronic structure of clusters relative to their size (the electronic effect). A good model of a supported catalyst consists of metal particles deposited on to a non-porous support film or crystal. To date, Pd is probably the metal most investigated in this way. An increase in CO oxidation turn-over rate with decreasing particle size was observed for a Pd/Al_2O_3 catalyst. This behaviour was explained by larger accessibility of the gas-phase molecules for corner and edge sites of the particle surface [153–155]. Later, a new effect was observed, namely a decrease in the CO oxidation turn-over rate on a Pd/mica catalyst with increasing particle density, that could not be explained using the accessibility model. Explanations were proposed on the basis of an increase in the effective CO flux towards the particles by the capture of CO admolecules diffusing over the substrate. Subsequently it was shown that the CO adsorption rate on alumina-supported Pd particles increases with CO diffusion over the support surface. The diffusion of admolecules is interrupted by desorption or by trapping by catalyst particles. The mean diffusion length determines the width of the so-called capture zones around the particle.

Many catalytic reactions are structure sensitive; the rate depends on the detailed geometrical structure of the surface atoms of the catalyst. Structure sensitivity usually manifests itself as a dependence of the rate per surface atom on the average size of the catalyst particles [156]. The understanding is that for particle diameters $d < 100$ the relative number of step and kink sites increases dramatically with decreasing d, and these very under-coordinated surface atoms could have a substantially different ability to interact with molecules from the gas phase. Structure sensitivity may reflect a variation in the intrinsic ability of the surface atoms to participate in surface chemistry (the electronic or ligand effect), or it may be related to the availability of a certain number of surface atoms in special geometrical arrangements of importance for the interaction with the reactants (the ensemble effect).

The structure sensitivity of CO adsorption on different flat, stepped, kinked and reconstructed Pt surfaces has been studied using large-scale DFT calculations which indicated an extremely strong structure sensitivity in the adsorption energy with variations up to 1 eV (or 100%) from one structure to the next. It was concluded that any catalytic reaction (adsorption, dissociation, recombination and desorption) involving TM catalysts will, in general, have contributions from d bands to the binding energy of the atomic and molecular adsorbates, and to the height of the barrier along the reaction pathway. If the contributions are large, the stability of the intermediates and the barrier heights will depend on the local coordination number for the TM atoms in the surface through the d band centre.

Supported-metal catalysts are widely used in industry. Determination of the metal surface area and the degree of dispersion of the metals on oxide supports is essential for both the efficient use of precious metals (group 8) and in understanding these catalytic systems. Many techniques have been used for determining metal surface areas and metal dispersions. Techniques such as X-ray diffraction (XRD), electron microscopy and selective chemisorption have been widely used. The XRD line-broadening technique gives the average size of metal crystallites, but its application is limited to catalysts with relatively high metal loading and relatively large metal crystallites. The accuracy of the determination of metal surface area depends on the knowledge of stoichiometry of the adsorption. This is a major limitation, in particular, if the stoichiometry of adsorption changes significantly with metal crystallite size. Despite its wide use, the selective chemisorption method is not good for the determination of small metal surface areas because a very small difference in the amounts of adsorbate gas between the beginning and end of adsorption must be detected. A series of Ru–Cu bimetallic catalysts on silica were prepared by the co-impregnation method. The amount of Ru was maintained constant and Cu loading was varied. CO adsorption was followed by temperature-programmed surface reaction of the pre-adsorbed CO with H_2 to form mainly methane. CO uptake was observed to increase with Cu addition, which could be attributed to some kind of ligand effect. The peak temperature was observed to shift to higher temperatures with increasing Cu content, indicative of a decline in the rate of the methanation reaction with Cu addition. It is suggested that this could be due to a decrease in the CO dissociation rate on the bimetallic catalysts [157].

Pd and Pt are important components of metallic catalysts. Interestingly, their metallic radii are about 10% larger than those of ferromagnetic TMs Fe, Co and Ni. As a result, uncertainty arises concerning the interface geometry when Pt or Pd is deposited on a densely packed surface of a ferromagnetic crystal [158]. For example, Pt monolayers on Fe(001) and Co(001) yield a 1× 1 structure whereas 1 ML of Pd on Co(0001) yields a 11× 1 superstructure. Pt on Co(0001) forms two domains distinguished by either fcc or hcp stacking. Regarding the electronic structure, the spin-resolved photoemission spectra in the normal direction shows for 1 ML of Pd on Co(0001) an interface state of Pd electron character 1.3 eV below the Fermi level E_F. A remarkable property of this state is the inverted exchange splitting. Other electronic features are close to those of the bulk for Pd (Pt).

Other intensively studied systems are Pt and Pd on Ni(111) which have essentially the same approximately 10% metallic radius mismatch. The growth is layer by layer, but LEED shows a diffuse 1× 1 pattern near 1 ML coverage which leads to the suspicion that the growth is not an ideal pseudomorph. The Pt core level in Pt/Ni(111) displays remarkable catalytic properties. It has been argued that, for fully compressed pseudomorphic Pt monolayers or clusters on Ni(111), the Pt core-level shift (CLS) as well as the Pt d bandwidth would be large, and surface reactivity would drop drastically in contrast with the behaviour of the analogous Pd/Ni(111) surface. Reasons have been given that the effective Pt–Pt separation lies well between the Ni–Ni and the bulk Pt–Pt distances. An extremely interesting analogue is represented by the disordered PtNi alloys at stoichiometry close to 1:1. It is known that the (111) surface is a quasipure Pt segregated layer with strong Ni enrichment in the second layer. The CO binding energy is slightly reduced compared with that on Pt(111) and there is no significant CLS at surface Pt atoms compared with the bulk. Similar remarks apply also to the $Pt_{80}Co_{20}$ (111) face. Hence, there is some similarity between the overlayers and alloy surfaces mentioned. In contrast, the Pt surface is compressed less then 5% (2%) in $Pt_{50}Ni_{50}$ ($Pt_{80}Co_{20}$), which again corroborates the idea that the complete compression of Pd (Pt) overlayers is never reached.

Even if the geometry were known, electronic structure calculations of the alloys discussed above would not be accessible to modern rigorous methods since a huge number of non-equivalent atoms are expected in the overlayer. A semiempirical self-consistent tight-binding recursion scheme method was used for the Pd/Co(0001) system. Ideally pseudomorphic 11×1 and 'non-compressed' Pd overlayers were considered; the latter were treated by a mean-field method. The inverted exchange splitting of interface states is shown to result from hybridization with the substrate bands which is different for different spin orientations. Comparison of Pd/Co(0001) results with those for Pt/Co(001), Pd/Ni(111) and Pt/Ni(111) shows that the best agreement is reached if the Pd–Pd (or Pt–Pt) nearest-neighbour separation lies about half-way between the overlayer and substrate nearest-neighbour distance in the elemental crystals. Such a geometry can be achieved in domains separated by defect walls. Clarification of this question can help in understanding the close analogy with the (111) surface properties of the corresponding TM alloys. In many respects CO chemisorption resembles the thoroughly studied Pd and Pt films on electropositive TM substrates. Both the different nature of the substrate and the overlayer compression contribute and drive the surface reactivity in the same direction [158].

The study of diffusion on metal surfaces has recently drawn considerable attention owing to the realization that the migration of adsorbed species often controls catalytic reactions. Despite many efforts to determine reliably the activation energy for surface diffusion, which is reflected in the variety of techniques that have been applied, there is generally poor agreement among the various experiments. For the most widely studied molecule, CO, the values obtained in different investigations on Pt(111) surfaces, for example, vary by about a factor of three. These irreconcilable differences are probably due to the lateral averaging inherent in most techniques which may mask the effects of surface imperfections. Surface diffusion microscopy of CO on Pd(111) supports the notion that 'macroscopic' measurements of the diffusion coefficient do not, in general, yield values typical of the flat defect-free surface. Although they may be relevant to diffusion processes in catalytic reactions at elevated temperatures, comparison with calculations of activation energies for diffusion processes on the atomic scale, for example, is not possible. This will be particularly true of measurements involving laser-induced desorption processes [159].

It is now well known that alkali metals play the role of promoters in catalysis, improving some catalytic properties and parameters of catalytic reactions. Frequently a promoter is added as a precipitant or in order to poison the support's acidity. The role of alkali promoters can be determined by comparison of the results from a clean single-crystal surface with those obtained from a surface containing controlled submonolayer quantities of alkali adatoms [160]. Improved adsorption characteristics of a K-pre-dosed Cu(110) surface with coverage corresponding to a point below the work-function minimum have been confirmed. Analysis of CO-induced orbitals in the photoelectron spectra of the CO/K/Cu(110) interface for low coverages of CO adsorbed at 118 K showed noticeable changes of orbital parameters with increasing CO coverage. Elongation of the C–O bond without dissociation was deduced from the energy separation of 3.4 eV between the 4σ and the 1π orbitals. Weakening of the CO-interface bond with coverage has been found on the basis of a decreasing 5σ–1π separation with increasing 4σ-to-5σ intensity ratio. Perpendicular orientation of CO molecules to the plane of the substrate surface has been concluded from analysis of the 4σ and 5σ–1π orbitals.

A molecular level description of binary alloys is of primary importance in understanding the chemical implication of TM pairing [161]. The use of single crystals as model catalysts coupled with surface techniques provides a convenient tool for the comprehensive study of these alloy surfaces. For selective catalytic processes such as automobile post-combustion or hydrogenation reactions for which both metals are involved, it is essential to describe well the nature of active sites of the surface. Pd–Cu alloys are catalysts for the CO +NO reaction. Although Cu and Pd present both an activity towards NO reduction and CO oxidation, it turns out that Cu is able to dissociate NO even at low temperatures, this step being crucial in NO reduction. Knowing that Pd is most active for CO oxidation, it seems reasonable to suppose that Pd–Cu alloys could be useful catalysts for the reduction of NO by CO. Moreover, the alloying effect could lead to enhanced catalytic properties with respect to the individual Pd or Cu components. The Pd–Cu system is well known to favour segregation of Cu, as with the $Pd_{15}Cu_{83}$ (110) single crystal in which the very first layer is essentially terminated by Cu atoms. The segregation of Cu was demonstrated to be more moderate for the $Pd_{75}Cu_{25}$ (111) single crystal, leading to $Pd_{70}Cu_{30}$ surface composition, that is slightly different from the bulk. Pd–Cu thin films have also shown moderate Cu segregation over a representative series of alloy compositions. The larger freedom of surface atoms in an open surface, such as the (110) surface, surely has significant weight on the magnitude of the segregation. Bulk ordered structures reported for Pd–Cu alloys have compositions around Cu_3Pd (bcc and tetragonal) and CuPd (bcc). The observation of well ordered Pd–Cu surfaces induced by segregation of Cu appeared not to be strictly dependent on bulk composition. Nevertheless, the main interest in alloys for catalysis remains the effective chemical properties (reactivity and electronic structure) obtained for individual metals in the new material. Adsorption properties of Pd in alloys such as $Pd_{75}Cu_{25}$ or $Pd_{67}Ag_{33}$ are drastically affected by the presence of the second metal. For example, the sticking coefficient and the saturation coverage of CO and H_2 on $Pd_{75}Cu_{25}$ (111) are significantly lower than values measured on pure Pd(111). The chemical properties of the Pd–Cu alloy have been investigated by adsorption of CO, NO and H_2 and also by XPS. The amount of CO adsorbed on the surface at 160 K is at least four times that for NO or H_2. Furthermore, the adsorption energies decrease on Pd and increase significantly on Cu in alloys with respect to adsorption on pure metals. The significant shift of core and valence bands observed by XPS and, moreover, the change in adsorption energies of CO and NO are attributed to a strong electronic interaction between Pd and Cu upon alloying. This Pd–Cu interaction has been interpreted in terms of bond formation between the almost full valence sd band of Pd and the resonant dsp band of Cu near the Fermi level. An explanation using back-donation capabilities of the Pd–Cu alloy surface to CO and NO is also given to support the formation of a hybridized MO [161].

One component at a bimetallic surface can alter the chemistry of the other metal component in two primary ways: firstly electronic effects, in which the electronic structure at an adjacent site is modified, and secondly geometric effects, in which the modifier acts simply as a site blocker to reduce directly the size and number of reactive sites (ensembles) on the surface [161]. Distinguishing experimentally between electronic and geometric effects remains a very difficult but important task. Ordered surface alloys are especially useful systems to study in this regard because of their known and stable composition and structure. Evaporation of Sn onto TMs such as Ni, Pd, Pt, Rh, Ru and Cu and subsequent annealing can produce well ordered surface alloys. These surface alloys are often very stable and consist of a single layer of the alloy on top of the substrate. In several cases it has been found that Sn atoms are almost coplanar with the substrate surface atoms, with some outward buckling of Sn atoms. The magnitude of buckling has been correlated to the lattice mismatch of Sn with the substrate. The buckling for Sn/Pt(111) is about 0.022 nm while the buckling for Sn/Ni(111) is about 0.046 nm. Investigation of chemisorption of CO on Ni–Sn alloys formed on a Ni(111) surface using reflection–absorption infrared spectroscopy (RAIRS) and temperature-programmed desorption (TPD) indicated that formation of the Sn/Ni(111) surface alloy strongly suppresses CO adsorption. Only 0.04 ML of CO can be chemisorbed on this surface at 110 K, exclusively at atop sites. The binding energy of the adsorbed CO is reduced to only about 15 kcal mol^{-1}. Additionally, no significant effect of subsurface Sn on CO chemisorption on this alloy was observed. These results are in sharp contrast with other results for CO chemisorption on a surface alloy where the chemisorbed CO saturation coverage, adsorption site distribution and desorption temperature were quite similar to those properties of the Pt(111) surface. This effect was attributed to the repulsive Sn–CO interactions at the Ni–CO distance required for chemisorption. The differences in the chemisorption properties of these Pt–Sn and Ni–Sn alloys were rationalized by considering the different sizes of the surface unit cells and the location of Sn with respect to the surface plane (the Sn buckling distance). These results have important implications for the determination of ensemble sizes at bimetallic surfaces since the surface chemistry depends strongly on the vertical position of the modifier [161].

When gaseous CO approaches a surface, its interaction is governed by the adsorption potential. The potential depth (adsorption energy E_{ad}) of chemisorbed CO on TM surfaces is typically about 0.5–2 eV. When CO collides with a surface, except for the case of reflection from the surface, kinetic energy is transferred into various kinds of excitation (vibrational, rotational, electronic, phonon, etc.) [162]. Usually the molecule does not stick on the surface in the first collision, and it travels on the surface (mobile precursor states), further dissipating its kinetic energy. Finally it is trapped at a potential minimum (i.e. a certain adsorption site). After an absorbed molecule is thermalized at the surface temperature, thermal motion of the adsorbed molecule can be excited by the substrate. The statistical thermodynamic equilibrium of the total adsorption system may be reached through the surface migration (hopping) of adsorbed molecules. There are several possible adsorption sites for CO on TM surfaces, namely a terminal site, a bridged site and hollow sites. In thermal equilibrium, the occupation probability of each type of site is controlled by the free energy of adsorption (adsorption energy and entropy of the system at the given temperature). If the surface temperature is too low to activate surface migration, non-equilibrium adsorbed states, where molecules are initially trapped at a certain local potential minimum, may be observed. On a low-temperature surface, the adsorption site occupancy is determined by the elementary adsorption dynamics and not by thermodynamic equilibrium. On the other hand, when we observe the adsorption of CO at higher temperatures (e.g. room temperature), thermodynamic equilibrium between the adsorption sites is quickly achieved.

Adsorption of CO on to a cold surface at 20 K has been studied by RAIRS. The occupation ratio of bridged CO to terminal CO species on Ni(100) at 20 K ranges from about 3.1 to 0.8 at total coverages from 0.003 to 0.15 ML. Two adsorption processes are observed: direct adsorption of CO on the bare metal surface and indirect collision site conversion. At zero coverage, CO tends to accommodate on the site with the larger adsorption energy. The strong coverage dependence of the occupation ratio even at small coverages suggests that the interaction between CO molecules operates at relatively long range (greater than 10 Å). The isotope experiments suggest that there is substantial interaction between pre-adsorbed (accommodated) molecules and incoming (mobile) CO molecules [162].

The effective PESs for interactions between pairs of adsorbed molecules govern many properties of chemisorption systems. The difficulties associated with determining these surfaces, both experimentally and theoretically, have led to a large body of data for adsorbed molecules that is only now beginning to be understood collectively. CO adsorption on many TM surfaces, such as CO–Ni(111) has been extensively studied. Despite this archive of information on CO chemisorption, our ability to transfer knowledge learned from one system to another is limited. This is true even for apparently similar systems such CO–Ni(111) and CO–Pt(111). Very little predictive power exists, for example, for interaction energies between adsorbed molecules. This situation is changing as more powerful computers become available to accomplish the complex calculations necessary to model these systems. The PESs obtained from such calculations can then be applied to explain the relationship between various data sets for a given system and to predict other properties of the system. In this complementarity between theory and experiment it is important to develop quality data to be used as checks of the emerging calculations. As an example, measurements of the isothermal desorption rate for the CO–Ni(111) chemisorption system have been reported. Values for microscopic lateral interaction parameters were determined by fitting the isotherms in the coverage regime to a lattice-gas model, making the quasiequilibrium approximation, and using a transfer matrix grand partition function. The parameters determined from this analysis were shown to be compatible with a wide range of experimental data for this system, and describe a system that is weakly interacting outside a short-range hard-wall repulsion. Low-coverage Arrhenius parameters were determined by fitting the desorption waveforms. Comparisons were made with the CO–Pt(111) systems. A simple model for substrate-mediated lateral interactions has been discussed on the basis of the relief of surface tensile stress which can qualitatively explain the differences between the two systems [139].

The adsorption of hydrocarbons and CO over Ni and Pt catalysts is well documented. As expected with such key catalytic metals, adsorption studies have been performed on single-crystal systems under high vacuum as well as on supported systems at atmospheric pressure. In general, the studies have involved only a single gas and, with single crystals, have often concentrated on structural aspects of the adsorption. However, it soon becomes apparent that the main emphasis of the studies is adsorption at or below room temperature. The information available at high temperatures is generated principally from thermal desorption studies. Information generated by this route has significant limitations, which are not always appreciated. Adsorption at room temperature followed by thermal desorption to a given temperature is not the same as adsorption at the given temperature. High-temperature adsorption of gases could yield information on the catalyst and on the dynamic nature of the adsorbent–adsorbate interaction. The high-temperature (573 K) adsorption of CO and the high-temperature coadsorption of hydrocarbon–CO was studied over Pt/alumina and Ni/silica catalysts. The Pt catalyst was found to retain H_2 from the reduction process. In general, it was found that, with the Ni system, regeneration of adsorptive capacity could be achieved to some extent, dependent upon the gas being adsorbed, by treatment with H_2 at 573 K. Similar treatment with a Pt catalyst had no obvious effect. Coadsorption studies revealed that single adsorption behaviour was not reproduced in the presence of a second adsorbing gas [163(a)].

Although the Blyholder model has been widely accepted because of its simple and lucid way of describing the bonding mechanism, several studies, both experimental and theoretical, have pointed out deficiencies in the model [163(b)]. An extended Hückel calculation for CO on Pt(111) has shown that the 4σ MO is also partially empty in the adsorbed state and suggested that this orbital could also contribute to bonding [163(c)]. Recently, an X-ray emission spectroscopy experiment by Nilsson *et al.* [163(d)] for CO on Ni(100) has shown the existence of occupied sites with a symmetry which is localized on one of the atoms of the molecule. Since the CO MOs of this symmetry (1π and 2π) are extended over the molecule in the gas phase, Nilsson *et al.* have claimed that it is inappropriate to describe the electronic structure of the adsorption system in terms of MOs, as in the Blyholder model [163d]. In order to address this possibility Aizawa *et al.* [163(b)] investigated the validity of the Blyholder model via a first-principles study of CO bonding to Pt(111). These workers studied the system using a local density functional (LDF) formalism with a slab model to represent the extended metal surface. They developed a population analysis scheme applicable to calculations with plane wave basis sets. For CO on Pt(111), they found the 4σ and 1π orbitals of CO to be completely filled, showing that these orbitals do not play a role in the bonding of CO to the surface. On the other hand, the calculated populations of the 5σ and 2π orbitals indicate that there is substantial 5σ and 2π back donation, supporting the Blyholder model of CO chemisorption, the validity of which was questioned. These results also suggest that a MO-based picture such as the Blyholder model is appropriate for describing simply the chemisorption bond, in spite of the fact that CO MOs rehybridize upon adsorption as has been shown by X-ray emission spectroscopy [163(b)].

The changes in the adsorption energy for CO adsorbed at different coordination sites are much smaller than the changes in binding energies for adatoms at different coordination sites [3]. The relatively small changes for molecular adsorbates are attributed to a balance between changes in donating and back-donating interactions that occur in these sytems. Moreover, CO often prefers adsorptive coordination atop at onefold sites. On the other hand, adatoms prefer to bind to highfold coordination at low surface coverages. It has been shown experimentally that CO adsorbs onefold on a Co(111) surface. The preference for atop coordination is largely due to a strong low coordination directing effect of the donating interaction of the CO 5σ MO to Co d atomic orbitals. Theoretical results for clusters containing seven to eight Co atoms as well as nine to 11 Co atoms predict a strong Co–Co cluster interaction with a preference for the higher twofold and threefold coordination sites, which does not directly accord with experimental observations attributed to these clusters. CO chemisorbed to a spherical cluster provides a better representation of edge atoms and predicts the onefold coordination site of Co to be the preferred site.

According to bond order conservation and delocalization theory, the adsorbate–Co atom interaction is strongly affected by the metal atom's environment. The adsorbate–metal atom interaction will increase when the metal atom has low coordination. The preference for twofold and threefold coordination over onefold coordination in clusters can be directly related to differences in cluster atom reactivity. Bond order conservation essentially indicates that, the fewer the number of atoms that share a bond with the same atom, the stronger are the corresponding metal–metal bonds. Stronger CO chemisorptive bonds to larger clusters are largely due to weakened Co–Co bonds. In the cluster the lower coordination numbers of edge atoms compared with those at centre atoms lead to electron redistribution in which the centre atoms have lower d-electron atomic orbital occupancy than might be expected at the surface. This situation is different from that on a real metal surface where the narrowed d bandwidth on the surface results in increased d atomic orbital electron occupation on the surface atoms compared with that on bulk atoms [3, 165].

Dissociative adsorption is a prototype surface-chemical reaction which is often a rate-limiting step in various catalytic reaction cycles [3]. The prediction of overall catalytic reaction cycles requires detailed computation of the reaction energies of each elementary step in the cycle. In addition, knowledge of the kinetics of each individual step in the overall cycle is required to make an *ab initio* prediction of the overall rate constant. Using the methanation reaction as an example, it is known that the CO dissociation rate goes through a maximum with CO coverage which indicates that, for surface dissociation to occur, empty surface sites next to the adsorbed molecule are required. In order to postulate a plausible mechanism for this reaction it is necessary first to analyse both the initial and the final states of the reaction, that is the associative molecular state (reactants) and surface adatoms (dissociation products). While molecules adsorbed on a metal surface show only small differences in energy with change in coordination number, atoms, on the other hand, are, in general, more sensitive to adsorption site changes and show a preference for higher coordination sites. This implies that a dissociative molecule requires an ensemble of surface atoms to accommodate both the lower-coordination adsorption site and the higher-coordination adatom sites of the products, that is the ensemble effect in heterogeneous catalysis.

The energy change of a surface dissociation reaction depends on the difference in energy of the adsorbed molecule and the adsorbed atoms generated upon dissociation. Adatoms are much more sensitive to changes in surface topology and changes in the composition of the TM surface than are adsorbed molecules. This sensitivity is directly tied to the greater variance in adsorption energies of adatoms relative to molecules. Calculations have been made of the lowest-energy dissociation path for CO on clusters simulating the Rh(111) and Rh(100) surfaces using the semiempirical ASED method and extended Hückel approach which explicitly includes repulsive potentials between the atoms. The reaction path is not only determined by the energies of the initial and final states; it is also governed by the electronic interactions that weaken the dissociating bond. The CO molecule inclines until a strong enough interaction between the O atom and the surface-metal atoms develops. The C–O bond then begins to stretch. It is weakened by electron back donation into the molecular antibonding orbitals. These are the LUMOs of CO—the 2π* orbitals. Their interaction with the surface requires appropriate symmetry of the surface group orbitals [3].

3. Mechanism of N_2 interaction on transition-metal surfaces

The reactions of N_2 with TM surfaces is of considerable theoretical and technological importance [164–208]. It has practical importance in the preparation of nitride coatings and in the stability of ceramic–metal interfaces, and it also plays an important role in understanding the processes of the heterogeneously catalysed ammonia synthesis. The N_2 molecule is an interesting adsorbate to study because of the many ways that it can bond to a surface. In addition to molecular bonding (chemisorption or physisorption), atomic adsorption can occur through dissociation. From a fundamental viewpoint, a comparison of N_2 chemisorption and dissociation with that of isoelectronic CO should provide useful insights into understanding how the substrate and molecular structures lead to the observed molecule–surface bonding and dissociation energetics. While CO adsorption has been the subject of intense study, N_2 has received relatively little attention. The success of the extrapolation of low-temperature kinetic models to the prediction of the kinetics of N_2 dissociation at elevated temperatures (and even the rate of ammonia formation) has distracted, to some extent, from a careful and detailed investigation of the kinetics of N_2 adsorption, desorption and interstate conversion.

A similar picture to the Blyholder model can be used to describe the bonding of TMs to N_2. In these systems, the σ_g and σ_u (donating orbitals) and the $1\pi_g$ (antibonding orbital) are the orbitals that participate predominantly in bonding to the surface. Both experimental [164, 166, 167] and theoretical studies [158, 165, 167] have shown that N_2 is weakly chemisorbed via one of the N atoms and oriented with its bond axis nearly perpendicular to most TM surfaces, including Ni [157–159, 165], Pd [158], Ru [158], W [162, 163], Re [164] and Ir [166]. This geometry is usually described by the well known σ donation and π weak back-bonding concepts. Like CO, N_2 typically bonds to TM surfaces in an orientation normal to the surface plane, but with substantially weaker bond strength. The adsorption process breaks the symmetry of N_2, producing inequivalent N atoms and leading to qualitative similarities to CO. The stronger TM–CO bond is attributed, in general, to the greater ability of CO to act as a π acceptor. For CO and N_2 chemisorption on model Ni clusters, the weaker CO–TM bonds are attributed to greater CO σ donation and π back donation which is believed to result from both the larger spatial extent of the CO 5σ orbital relative to that of N_2 and the localization of the $2\pi^*$ MO on the C end (towards the surface) of CO. Theoretical models vary as to the relative importance of σ against π back donation in forming the N_2–M and CO–TM bonds.

While similar adsorption mechanisms can rationalize the differing adsorption bond strengths of N_2 and CO, comparisons of other experimental results suggest differences in the electronic and vibrational properties of CO and N_2 adsorption on TM surfaces [169]. CO adsorption is accompanied by pronounced increases in work function, in general; N_2 adsorption results in a decrease in the work function. Intense multielectronic excitations are observed in all UPS and XPS studies on N_2 on TMs; such satellite peaks are weak or non-existent for CO. The C–O stretching frequency substantially increases by 30–60 cm^{-1} as a function of CO coverage while the N–N vibrational frequency remains constant or decreases in most of the systems investigated. In contrast with the adsorption of CO, alkali promotion weakens or inhibits the bonding of N_2 to Ru(001). The ratio of the (N_2–metal)-to-(N–N) dipole intensity is substantially larger than the (CO–TM(1))-to-(C–O) intensity. Noting these contradictory results, alternative and qualitatively different mechanisms have been proposed for the bonding of N_2 to TM surfaces. In addition to these contradictions a series of recent experiments have shown that N_2 is strongly chemisorbed on Fe(111) [170–172], Cr(111) [173] and Cr(110) [174], with its intramolecular axis parallel to the surfaces, that is as π-bonded α-N_2 [170].

Low concentrations of electronegative or electropositive additions can strongly affect N_2 catalytic activity on metal surfaces including the promotion of N_2 dissociation by K, and the reduction in the dissociative activity of iron due to the presence of O_2 or S. In contrast with the adsorption of CO, alkali promotion weakens or inhibits the bonding of N_2 to Ru(001) [161, 175–179]. On the other hand, pre-adsorption of O_2 results in metal–N_2 strengthening. For K-promoted Fe surfaces, it was suggested that adsorbed K atoms exert a short-range electrostatic effect and long-range electronic effect on the molecular precursor for dissociation. Bond dissociation of N_2 is promoted by electropositive elements through their electrostatic potential. The potential aids in the filling of the antibonding MOs. Catalytic activity is affected by the local electrostatic potential and by long-range charge redistribution in the TM. The range of the poisoning or promoting effects of a foreign adatom depends on the height of the atom above the surface plane, that is the closer the adatom is to the surface, the shorter is the range. In the case of foreign atoms embedded into the surface, the effects of the adatom dipole moments on catalysis are reduced and the expected catalytic influence of the foreign atom is essentially site blocking. Examples of this behaviour include the decrease in dissociation probability for N_2 on a polycrystalline iron surface owing to pre-adsorbed O or S.

There has been intense study of the interaction of Fe surfaces with N_2, prompted by the great commercial importance of this reaction in the 80-year-old Bosch Haber process for producing ammonia from N_2 and H_2 gases using Fe as a catalyst. The commercial process uses iron oxides that are reduced to elemental Fe during the reaction at about 80 atm, and at temperatures above about 625 K [180–183]. In order to obtain an understanding of how the catalysis works, many studies have been carried out of Fe surfaces interacting with N_2 whose adsorption and subsequent dissociation is believed to be the rate-limiting step. Normal Fe contains many impurities, particularly S, but also C, Cl and P, among others. Furthermore, it reacts rapidly with CO and is very readily contaminated with O_2 and C. To reduce the complexities, most surface studies have been carried out on cleaned Fe surfaces. These have been typically subjected to an extensive cleaning process, so that the starting surface for reactions is largely free from contaminants detectable by Auger electron spectroscopy. Furthermore, since there is evidence that N atoms enter the bulk, many studies have first saturated the surface region so that reproducible starting conditions for adsorption are achieved. While such procedures are necessary in order to have consistent and simplified starting points for study, no elaborate cleaning procedures are used in the commercial process. In catalyst preparation, K and Al oxides (promoters) are fused with magnetite (Fe_3O_4) at about 1870 K followed by reduction. Industrial catalysts might also use oxides of Ca, Mg and Si in the Fe. After reduction, studies have shown that the reduced magnetite exists as platelets 30–500 nm wide, made up of several to many single crystals of Fe, the platelets being separated by spacers of ternary oxides and covered in part by patches or promoter oxides. Evidence has also been adduced that, at the high pressures and temperatures used in this operation, the Fe, possibly as iron nitride, coats potassium aluminate. Although these conditions are very different from those of cleaned single-crystal surfaces, an understanding of the simplest case must precede understanding of the real case.

Adsorption of N_2 and its subsequent dissociation into atomic nitrogen on Fe(111) has been studied in some detail [177, 179, 184–186]. Surface science studies on N_2 dissociation on Fe single-crystal surfaces revealed that the overall dissociation probability is very low for $T > 300$ K and that the open Fe(111) surface exhibited relatively the highest dissociation. The low dissociation rate observed for $T > 300$ K was explained by Ertl *et al.* [176] in their classic paper by a mechanism in which dissociation proceeds via a molecular precursor state. Among the low-index planes, the Fe(111) surface exhibits the highest activity in high-pressure synthesis as well as N_2 chemisorption. For N_2 adsorption on Fe(111), two weakly chemisorbed N_2 states have been identified. In the so-called γ state, N_2 molecules are terminally bonded to first-layer Fe atoms. The slightly stronger bound α state is the precursor to N_2 dissociation with an adsorption enthalphy of about 0.25 eV; the N_2 molecules are terminally bonded to first-layer Fe atoms. The slightly more strongly bound α state, with an adsorption enthalpy of about 0.32 eV, which is the precursor to N_2 dissociation on the surface, has been attributed to N_2 that is π bonded to the surface. While the γ state has been found to have a stretching frequency of 2100 cm^{-1}, consistent with N_2 molecules oriented perpendicular to the surface, the α state exhibits an unusually low stretching frequency of 1490 cm^{-1} consistent with the N_2 axis inclined from the surface normal. The kinetics of dissociative N_2 chemisorption on both clean and K-promoted Fe(111) surfaces indicated that the adsorption energy increases in the vicinity of the coadsorbed K atom.

On Cr(110) surfaces [174] at 90 K, N_2 adsorbs molecularly via a mobile weakly bound precursor state with an unusual valence electronic structure similar to that of π-bonded N_2 on Fe(111). Adsorption into the π-bonded state occurs with a sticking coefficient near unity. The existence of only a single molecular N species on the surface at 90 K is surprising in view of results for Fe(111) where, besides the π-bonded N precursor state to dissociation, two weakly bonded species are found to be present for $T < 100$ K. At 300 K, only dissociative chemisorption is observed, but with a reduced sticking probability and a lower saturation coverage compared with a thermally dissociated molecular adlayer. Low coverages of chemisorbed O_2 do not inhibit N_2 adsorption, but coadsorption effects are observed when a N_2 saturated surface is exposed to large O_2 doses. A bonding geometry with both N atoms coordinated to Cr atoms has been proposed. Small concentrations of elemental Fe at the surface reduces the probability of dissociative N_2 adsorption by orders of magnitude. This decrease in N_2 dissociation is observed despite the formation of a surface chromium nitride on both Cr-rich and Cr-poor surface regions of the Fe–Cr alloy [187].

Our *ab initio* calculations [8] of a Cr_5N_2 cluster indicated that the adsorption geometry at a fourfold site with the N–N axis nearly parallel to the surface, forming an angle of 14.2° with respect to the surface, was the most stable geometry. It is computed to be about three times more stable than the cluster at the fourfold vertical position. The inclination from the vertical position to an angle of 14.2° with respect to the surface results in increased change transfer (0.47 to 0.79) from the surface of N_2, an increase in *R*(N–N) from 1.34 to 1.43 Å, a reduction of the *R*(surf–N) surface–nitrogen distance from 1.07 to 1.00 Å, and an increase in Mulliken overlap population from 0.244 to 0.299 proceeding from the perpendicular to the nearly parallel configuration. A reduction in the nearest nitrogen (N(1))–surface distance with corresponding increase of N–N bond length indicates that the N(1)–surface bond is strengthened, but the molecular N–N bond is weakened. The stretching frequency of 1220 cm^{-1}, calculated at the fully optimized geometry, is small (estimated 50% reduction) compared with the stretching frequencies corresponding to adsorption of N_2 on Ni(100), Ru(100) and W(100) surfaces, which are of the order of 2200–2330 cm^{-1} (closer to the experimental free N_2 stretching frequency) suggesting, according to our model, a dissociative Cr(110) surface. The small stretching frequency calculated for N_2 adsorption on the Cr surface can be correlated with weakening the N–N bond. The $\pi(p_x)$ and $\pi(p_y)$ orbitals of adsorbed N_2 have 3.93 electrons in the perpendicular and 4.95 electrons in the nearly parallel configurations [13]. The number of π electrons in the perpendicular configuration is closer to the number of electrons in free N_2 and indicates large π donation (about 1 electron) to adsorbed N_2 in the parallel orientation, in these so-called π-bonded systems. The much larger back donation (increase in the π antibonding orbital population) in the nearly parallel configuration would explain the weakening of N–N bonds and the larger binding energy to the surface in this configuration. As the N(2) atom (one furthest from the surface) inclines towards the surface, the strong interaction between this increasingly negatively charged atom and some of the positively charged Cr atoms of the surface favours the parallel configuration, lowering the total energy of the system. The HOMO and LUMO energy levels in the inclined configurations are lower than in the perpendicular configuration. Lowering of the Fermi and LUMO energies in the nearly parallel configuration facilitates the occupation of N_2 antibonding orbitals localized above the Fermi level, occupation of bonding orbitals of the TM surface and weakening of the N–N bond. In the parallel configuration, energy levels are more closely spaced.

Ab initio Hartree–Fock calculations were used to analyse N_2 dissociation on doped (bimetallic) Cr(110) surfaces described by Cr_4MN_2 and $Cr_3M_2N_2$ (M = Sc, Ti, V, Fe, Co, Ni, Zn, Mg or Ca) clusters in both perpendicular and inclined configurations. These results indicate that the inclined arrangement is energetically more favourable than the perpendicular configuration. In comparison with monometallic surfaces, some of the bimetallic systems, such as Cr_4ScN_2, Cr_4TiN_2 and Cr_3V_2N2 are found to have larger N–N distances and surface charge transfers, higher Fermi energies and smaller N–N stretching frequencies, indicating greater efficiency of these alloys for dissociation. Cr surfaces doped with another TM (bimetallic systems) can be more efficient for N_2 dissociation because they raise the Fermi energy and reduce the energy gap which facilitates back donation, inclination and consequently dissociation, and electroneutrality when the electron returns to the surface. The addition of other TMs increases the number of d orbitals for back donation. Some 3d-containing TMs, for example, Ti on a Cr(110) surface, also increase the number of d unoccupied orbitals available for the reception of electrons transferred to the surface. The introduction of other TMs to the lattice can introduce more electrons for donation and more unoccupied orbitals to receive the electron when it returns to the surface. Analogous to familiar stepped and open-surface effects, geometric effects caused by substitution can result in modifications of potentials and overlaps between N_2 and the surface yielding important effects on dissociation of diatomic molecules in bimetallic systems [35].

At 300 K, N_2 does not adsorb on Ni(110) but, for $T < 170$ K, N_2 is adsorbed molecularly, forming strongly bonded N adatoms. At 125 K, N_2 is adsorbed molecularly on the terminal and bridge positions of W(100) whereas, at 300 K, one finds that N_2 adsorption is dissociative. For $T > 150$ K, on Pd(110), N_2 is adsorbed molecularly; however, at 300 K, no adsorption is observed. N_2 is physisorbed on the (111) surface of Ag, Pd and Al [163, 187–191].

The adsorption of N_2 on Nb(110) has been studied by EELs and it has been shown that, at 80 K and low exposures, N_2 is chemisorbed dissociatively [195]; at higher exposures, molecular adsorption was found. At 20 K and low exposures, N_2 is chemisorbed in a terminal position whereas, at higher exposures, it is physisorbed. Recent studies of the kinetics and dynamics of N_2 adsorption on Ru(001) indicated increased chemisorption for an incident angle of 60° and increased incident kinetic energy, yielding evidence for a direct activated mechanism for molecular chemisorption [196].

There is always the question of the effect of impurities in normal Fe. Impurities constantly diffuse to the surface at high temperatures and it is not certain that they do not affect gas adsorption and related processes on the surface. Studies on used catalysts have found significant C as well as promoter materials including O_2. Recent studies of N_2 adsorption and native contamination of Fe(211) surfaces indicated that on clean surfaces there is negligible adsorption at low temperatures or room temperature whereas a contaminated surface showed appreciable adsorption. Heating a clean surface in N_2 resulted in low surface N concentration. Because used catalysts in the ammonia synthesis show the presence of C and O, the structures on Fe(211) formed with internal contaminants S and C and external O were studied and indicated that various ordered structures are formed at fractional monolayer concentrations and cannot be excluded from involvement in the catalytic process [192].

Surface IR vibrational spectroscopy is widely used to investigate substrate morphology of catalysts by observing the IR spectrum of an adsorbed probe molecule. Such work may be done on high-area supported catalysts as well as on model single-crystal catalysts of defined surface structure. CO has often been the probe molecule of choice because of its high IR absorption coefficient and the sensitivity of its vibrational frequency to the local bonding environment. However, the use of CO as a probe molecule is sometimes complicated by CO-induced substrate reconstruction and vibrational coupling between adsorbed CO molecules. Recently IR spectroscopy of adsorbed N_2 was used and shown to be a sensitive probe of defect sites on Pt(111) [193]. This study indicated that N_2 adsorbs at 90 K mainly on monovacancies on Pt by σ donation from N_2 to the base of monovacancy sites which possess a low d-electron density compared with surface Pt atoms.

Angle-resolved photoemission extended fine structure (ARPEFS) is a well established technique for determining the spatial structure of atomic and molecular adsorbates on metal surfaces [197]. One of the advantages of the technique is its elemental selectivity due to the unique binding energies of core electrons. ARPEFS studies of N_2/Ni(100) indicated that N_2 stands upright at an on-top site with a N–Ni bond length of 2.25 Å, a N–N bond length of 1.107 Å, a first layer Ni–Ni spacing of 1.76 Å and inequivalent N atoms. It was concluded that a quantitative theoretical treatment of weakly adsorbed systems must include lateral interactions between adsorbates [202]. Scattering of small molecules with kinetic energies in the range of several hundreds of electronvolts up to several kiloelectronvolts at grazing incidence is an interesting tool for the investigation of basic *electronic* and mechanical interactions.

The importance of the different dissociation mechanisms on molecular survival is still controversial. Generally, N_2 is a very inert molecule. The scattering process appears to be well described in terms of elastic collisions of the molecule with surface atoms; however, some workers found a sizeable influence of electronic excitation of N_2^+ due to violent collisions leading to dissociation and also dissociation due to hot electrons.

On a (100) face of Cu, a c(2× 2)N superstructure is formed in which the preferred sites of N_2 are the fourfold hollow sites [200, 201]. For low coverages the overlayer is organized in square-shaped islands separated by one or two bare Cu rows with the island edges running along the (100) directions. For higher N doses, islands coalesce and a structure appears with narrow trenches running in the (001) direction. The lack of island coalescence at low coverages and the appearance of trench-like structures at higher coverages are interpreted as two different strain-relief mechanisms for an incommensurate structure corresponding to Cu_3N. LEED studies of activated N_2 adsorption on the (100) and (*h*11) faces of Cu indicate the existence of two surface phases with a first-order transition between the phases. On the (100) face, the situation corresponds to the formation of an ordered stepped overlayer composed of alternating square island and bare Cu(100) atomic rows. For the (*h*11) stepped faces, one appears to have an unusual N_2-induced facetting into (100) and (*h*11) structures [205–207].

Adsorption of N_2 on Ni surfaces has been extensively studied as a prototypical example of weak chemisorption [208(a)–(d)]. The electronic structure of the system N_2/Ni(100) was studied by means of angle-resolved X-ray emission spectroscopy and *ab initio* calculations. This research shows that it is necessary to use an atom-specific description rather than one that treats the molecule and the substrate as separate units. The weakening of the internal π bond is seen in the appearance of a non-bonding orbital whose character is essentially Ni 3d with a contribution of N 2p lone pair on the outer N atom. The σ system strongly polarizes in order to minimize Pauli repulsion with Ni 4sp states in the substrate [208(c)]. At low temperatures, N_2 adsorbs non-dissociatively and most studies have concluded that it binds exclusively to on-top sites with the molecular axis perpendicular to the surface. Some more recent studies suggest, however, that bridge bonding may also occur on the Ni(110) surface. Thermodynamic measurements for the three surfaces Ni(100), Ni(110) and Ni(111) indicate that N_2 adsorption energies are similar on the first two surfaces and smaller on the last. Adsorption entropies have also been reported for Ni(100) and Ni(110) surfaces.

In recent years, adsorption of N_2 on TM clusters has also been used to probe cluster surface morphology, which gives valuable information on overall geometrical structure. The structures of most Ni clusters in the size range from three to 28 atoms have been determined by this method (the chemical probe method) and show preference for icosahedral packing. The structures of nickel clusters Ni_n, $n = 40$–200, have also been probed with N_2. These studies reveal icosahedral structure with subtle changes in the cluster growth sequence due to surface strains inherent in this type of packing.

Recently, Ni_{38} has been identified as a truncated octahedron (or a distorted version of this structure) by using N_2, H_2 and CO as chemical probes [203, 204]. For the most part, the binding of N_2 to Ni clusters is consistent with what is observed on bulk Ni surfaces. There is no evidence for N_2 dissociative adsorption at temperatures as high as 373 K, although it is important to note that reaction times in typical cluster experiments are only a few milliseconds at most. Non-dissociative adsorption is consistent with observed N_2 saturation levels as well as with the decrease in the extent of adsorption with increasing temperature up to 373 K. Obviously, longer interaction time might produce different results. On-top adsorption of N_2 in the perpendicular configuration is generally observed under saturated conditions (from the saturation levels and simple geometrical considerations), although sideways adsorption cannot be completely ruled out at low coverages. Recent calculations on the adsorption of N_2 on small Ni clusters (two to four metal atoms) show the greatest stability for on-top absorption in the perpendicular configuration.

Previous experimental studies have demonstrated that the extent of N_2 adsorption depends sensitively on the metal coordination of the surface Ni atoms. Atoms having metal coordination of four (i.e. bound to four other Ni atoms) or less will bind two N_2 molecules at saturation. Those with a coordination of five to eight will bind a single N_2, and Ni atoms with metal coordination of nine or greater bind N_2 more weakly or not at all. Equilibrium constants for chemisorption reactions of N_2 with Ni clusters were determined as a function of temperature for cluster sizes $n = 19$–71. A van't Hoff analysis of the data yielded standard-state changes in reaction enthalpy and entropy. In general, the adsorption energy is highest for the smallest clusters investigated, reaching values twice those for N_2 adsorption on bulk Ni surfaces. In many cases, there is a correlation between enthalpy and entropy; high adsorption energy is accompanied by a large change in entropy, and vice versa. These effects are related to the magnitude of the configurational entropy and the frequencies of the frustrated translational and rotational motions of adsorbed N_2. Since the enthalpies and entropies of N_2 adsorption are determined by the nature of the surface atoms of the cluster, their magnitudes can give important structural information. N_2 adsorption is a short-range phenomenon determined by the immediate environment of the adsorbed N_2, and not by long-range or cluster-wide effects [208(a)–(d)].

We summarize this section by noting that the analogy between the chemistry of organometallic compounds and the processes of chemisorption have been the motivation for considerable study, both experimental and theoretical [208(d)]. It seems easier to consider a small cluster with well defined geometry and ligands than a surface. Experimentally, in spite of progress in techniques, the structure of adsorbed systems is not known with the same accuracy as that of organometallic clusters. Metal–metal bonds appear in the skeleton of large clusters and are supposed to look like the metal–metal bonds in metal crystals. The metal–ligand binding should look like that between a metal surface and an adsorbate. This is the case for CO which is one of the most common ligands. The distances and the stretching frequencies are determined even with a single metal atom; the analogy with organometallics has been extended to even mononuclear coordination. The back-donation model is satisfactory even when charge transfers are shown to be almost negligible. Also CO (N_2) do not always remain perpendicular to the surface but may incline towards the surface owing to lateral interactions. The analogy between clusters and adsorption structures is sometimes striking. However, there may be still many systems which do not conform to this simple picture.

What are the main differences between surfaces and clusters [208(d)]? Cluster chemistry is ruled by electron count. The bonding and structure are, in general, understood with the help of the polyhedral skeletal electron pair theory that relates the geometry of the cluster to the number of valence electrons. A change in the count by two modifies the number of vertices in the compound, breaking or forming metal–metal bonds. Note that the electron count is global and associated with a structure. It does not account for isomerization when ligands reorganize themselves around the same skeleton. The electron count also fails to associate an electron pair with each metal–ligand bond. One of the questions about the adsorbate is the fluxionality of the modes for which the theory has only a limited response. On a surface the position of the adsorbate and the type of adsorption are more important than the count of the ligands; the adsorption mode does not vary when one metal is replaced by another metal close by in the periodic table. The number of adsorbates per unit cell (coverage) increases progressively on a surface up to saturation whereas the number of ligands in a cluster is fixed by the 18-electron rule. When the gap between the bonding or non-bonding and the antibonding MOs becomes small, the electron count may become questionable. It is difficult to attribute a given number of electrons to a metal–metal bond on a metallic surface; there are only modest differences between one metal and another with a different number of valence electrons; the Fermi level E_F acts as a reservoir of electrons.

The cluster approach presents several problems. These include truncation where bonds are broken at the boundary of the cluster, generating unpaired electrons or dangling bonds [208(d)]. Other disadvantages of the cluster approach are due to symmetries. Clusters often have high spin multiplicity because symmetry imposes a large number of degenerate orbitals which do not facilitate calculations. Also, when several desorption modes of different symmetry are to be compared, it is difficult to identify an appropriate model. Among the alternatives to clusters are aggregates, infinite crystals, periodic approaches and finite cubes. Aggregates are sets of metal atoms that have features closer to real catalysts than pure crystal surfaces. However, they are often supported and the support is an additional problem in modelling. They also differ from clean well defined surfaces for small dimensions because the ratio of corner to edge atoms is large with respect to real surfaces within a given crystallographic face.

Regarding the metallic state we note that an aggregate has discrete levels. When its size increases, the energy levels become denser and metallic properties emerge leading to an incipient band. At room temperature, the critical size of a cluster that prevents the consideration of discrete levels (quantum size effect, $E_F/2kT$) is about 100 atoms. For small sizes, orbitals and levels of appropriate symmetry are not close enough to E_F and the situation is not ideal. For large systems, orbitals at the active site may be overly dispersed so that their density at E_F is weak. Few answers have been provided for ascertaining the size where local properties fade and collective properties emerge.

Regarding surface reactivity and coordination, we note that, with few exceptions, sites of small coordination are typically more reactive [208(d)]. A site that already has ligands is stabilized and is less reactive than another site with a lower coordination number. Open surfaces are more reactive than dense surfaces, defect sites are more reactive than regular sites, and small aggregates are more reactive than large aggregates. The higher reactivity at the foot of a terrace may simply result from the possibility of binding simultaneously to two facets; binding at a foot may increase coordination more than binding on an edge atom.

We end this section by noting that, despite the criticisms and limitations of the theoretical, experimental and computational methods at present available to interpret a large, diversified and controversial number of experimental results regarding heterogeneous catalysis of CO and N_2 on TM surfaces, the simple donation and back-donation mechanism of Blyholder (modified with the introduction of the tilted precursor state pioneered by our group) can unify and explain most of the experimental data.

4. Breaking bonds of NO on metallic surfaces

NO is important in catalysis, physiology, immunology, neuroscience, pollution control and organometallics and was selected as *Science*'s 'molecule of the year' in 1994 [209(a)]. NO has one electron more than the two isoelectronic molecules CO and N_2 discussed above. In the isolated molecule this additional electron occupies an antibonding $2\pi^*$ orbital with an energy comparable with that of a TM conduction band. This orbital can play a prominent role in the chemisorption system. NO adsorption has similarities to CO adsorption. In comparison with CO, the extent of back donation for neutral NO is more limited, because the π^* orbital is already partially occupied. When NO is bonded to a TM, the bond angle can be related to the extent of back donation. DFT and *ab initio* calculations indicate that NO binds perpendicular to a threefold coordination surface site in Cu(111) and Ni(111). The general mechanism for adsorption is thought to involve the interaction of the NO π orbital by means of back donation of the surface electron density into singly occupied NO π^*. The back-donating interaction dominates the binding of adatoms such as C, O and N to TM surfaces and drives these species to high coordination sites where the degree of coordinative unsaturation is stabilized by forming bonds to a number of different metal surface atoms [3, 209(b)]. The calculated Ni–NO linear and bent geometries obtained using the CASSCF method followed by a CI consisting of all single and double excitations indicate that the linear geometry involves a 3d–$2\pi^*$ bond and that the bent geometry involves a Ni 4d–N 2p bond [16]. *Ab initio* GVB and correlation-consistent CI methods were used to study the interaction of CO and NO with Pd and Pt atoms and indicated that PdNO and PtNO involve a covalent σ bond between a singly occupied metal d_σ orbital and a singly occupied NO $2\pi^*$ orbital. NO is weakly bound to Pd, while CO is strongly bound to Pt and Pd atoms. Dimerization of NO on TM surfaces has been suggested by various researchers [209(e)] on Pt(111), Nb(110) and Ag surfaces, whereas it has been postulated that adsorbed $(NO)_2$ is a possible intermediate in the reaction pathway for the reduction of NO. DFT studies indicate that (NO) is stabilized on Ni_2 clusters [209(f)].

The use of catalytic converters containing TMs (e.g. Pt, Rh and Pd) for the abatement of NO from automotive and stationary sources has resulted in considerable interest in the catalytic chemistry of NO on the surface of these metals. In particular, the decomposition of NO_x in traditional automotive catalytic converters by means of catalytic reduction is an important industrial problem. For an exhaust catalyst to be effective, it needs to facilitate the decomposition of NO_x to atoms leading to recombination to N_2. At the same time, it should catalyse non-dissociative adsorption of CO and facilitate oxidation of adsorbed CO to CO_2. The dissociation of NO is often the rate-limiting reaction step in this process [209(b)–214]. Practical catalysts incorporate Rh and Pt since their activity can be explained by low barriers to NO dissociation, while the CO barriers are high enough to preclude dissociation. The dissociation of CO is analogous to NO dissociation. NO dissociates at room temperatures on surfaces of Fe, Co and Ru. The dissociative fragment distributions of NO and its positive ion scattered from Cu(111) are sharply peaked at an orientation of NO parallel to the surface [47].

Molecular adsorption [215–236] of NO has been observed on many TMs, for example on Ni(111) [216–219], Ni(100) [220], polycrystalline Ni [221, 222], Ru [223, 224], Cu [225], Ir [226, 227], Re [228, 229], Fe [230], Rh [231], Pd [323, 233], Pt [234, 235] and W [236]. Molecular adsorption can take place at various sites on a substrate surface, for example on Ni(111) and Ru(001) at threefold sites as well as at on-top positions. NO is usually adsorbed in a linear or bent configuration, but dissociative adsorption is observed even at low temperatures.

The sticking of NO on Ni(100), on Pt(111) and on CO/Ni(100) as well as the displacement of oriented pre-adsorbed CO by gas-phase oriented NO indicated pronounced steric asymmetry effects and that, in particular, sticking takes place preferentially for incident NO with the N atom pointing towards the surface [47]. NO is mobile on Pt(100) and desorbs in the surface temperature range (-150 °C $< T <$ 100 °C). NO adsorption proceeds by direct chemisorption as well as by an orientation-dependent trapping into a precursor state for low translational energies. Studies of NO chemisorption on various TM surfaces have demonstrated that there can be a strong orientation dependence of the chemisorption probability and it is very natural to assume that similar effects will also occur for dissociative chemisorption.

On the more open Cu(100) and Cu(110) surfaces, there is a higher probability of NO dissociation than on a close-packed Cu(111) surface. The dissociation barrier for NO is much lower than that for CO; NO tends to adsorb dissociatively, while the barrier for CO precludes dissociative adsorption [237, 238]. Also for Pt, the (100) surface was found to be more active in inducing dissociation of NO compared with the (111) surface. The height of the activation barrier decreases as one proceeds to the left in the first TM row of the periodic table. The transitions from dissociative to associative adsorption are different for CO and NO (as NO dissociation barriers are usually lower) and are also a function of the surface geometry. In general, for a given surface the preferred coordination mode of NO (similar to CO) may depend on coverage [208(a), 239, 240]. In particular, on Pt(111), at low coverages, twofold coordination is preferred but, at higher coverages, on-top coordination becomes preferable [241]. On Rh(111), twofold coordination persists at all coverages [242]. On Ru(001), as NO coverage increases, all three coordination modes, threefold, twofold and on-top, have been suggested [243]. Similarly, on Re(001), a bridge-bonded linear NO species has been identified [244]. Also, with increasing coverage, NO sometimes becomes tilted to the surface [245]. Because N_2 formation barriers rapidly increase in the order Pt $<$ Rh $<$ Ru $<$ Re, Rh and Rh–Pt surfaces are projected [239] to be the most efficient catalysts for NO reduction by CO (to N_2 and CO_2). Similarly, Pt surfaces are projected to be the most efficient catalysts for NO reduction by H_2 (to NH_3 and H_2O).

The interaction of NO with Ni(111) has been studied [246–253] with several techniques and some controversy exists in the literature about the orientation of adsorbed NO molecules. XPS measurements [246] found that adsorption in the 300–400 K temperature range is partially dissociative with perpendicularly oriented molecules up to 330 K. Other workers [247] found perpendicular NO molecules at 85 K, which change into a tilted configuration at 250 K. Synchrotron radiation photoemission [248] indicated that, in a c(4×2) layer at 120 K, NO molecules are perpendicular to the surface. Metastable quenching spectroscopy measurements [249] show no changes for a c(4×2) NO layer between 90 and 300 K. NEXAFS measurements [249] have shown that NO molecules adsorbed in the c(4×2) phase on Ni(111) are within 10° of the surface normal. An X-ray photoelectron diffraction [250] study of CO and NO-saturated Ni(111) did not observe any induced tilt of the molecular axis with respect to the surface normal. However, more recent work [251] indicates a strongly tilted or even horizontal NO species on Ni(111) at a coverage of about 0.2 ML [252, 253]. A LCGTO–LDF cluster model [252] investigation of structural and vibrational properties of Ni(111)/NO adsorption complexes indicated a nitrosyl species bound upright to the threefold hollow sites. Bent and tilted structures of the adsorbate are energetically less favoured. It is conjectured that, on the Ni(111) surface, NO molecules in the on-top coordination are stabilized by electronegative coadsorbed O atoms. These on-top NO species might coexist on O-covered surfaces with NO moieties. In the presence of O_2 on the surface, the N–O modes as a whole possess a stronger dynamic dipole moment than that found on a clean Ni(111) surface. Coadsorption studies with NO and CO on surfaces have significance in surface physics and in technical applications involving corrosion and catalysis. If both CO and NO coexist on a surface, then two processes can occur. Either molecules such as N_2 and CO_2 can be produced via chemical reaction or the NO bond prevails and CO is displaced by NO. Recent work indicates that the latter case prevails for the Ni(100) surface [254(a)].

Adsorption experiments show that NO molecules are very reactive on a Ag(111) surface and, in addition to molecularly adsorbed NO, atomic dissociation products are observed even at low temperatures as are other reaction products including N_2O [255–258]. This complexity of the Ag(111)/NO system renders the task of determining the characteristics of the various molecular forms of adsorbed NO difficult, and so knowledge on the adsorption states is still quite limited. Angle-resolved UPS data at 150 K indicated [258] that NO is molecularly adsorbed on the Ag(111) surface with an upright orientation. However, it is not clear which adsorption states were actually detected because this temperature is well above the desorption threshold. NO peaks in the 1300–2000 cm^{-1} region have been observed, which is the characteristic region for ligand-related vibrations of TM nitrosyl complexes. There are peaks at 1153 and 1282 cm^{-1}. It is difficult to understand why the N–O stretching frequency is so low. It is even smaller, by about 60 cm^{-1} than the vibrational frequency of free NO$^-$. Bagus and Illas [259] investigated the NO/Ag(111) system and showed the following.

(*a*) These vibrational features are consistent with NO adsorbed on Ag(111) in a threefold site, but in an O-down orientation.
(*b*) The bond between NO and Ag(111) is highly ionic regardless of NO orientation.
(*c*) The vibrational frequency of the O-down orientation is consistent with experimental results.
(*d*) The origin of the large shift in vibrational frequency is due to the internal electric field generated by the negatively charged adsorbed NO and the image charge response of the metal surface.

While external electric fields are known to modify strongly the vibrational frequencies of adsorbed species, there is no previous knowledge that the same effect may be produced by an internal electric field which arises as a consequence of ionic bonding.

Coadsorption of NO + CO results in the site conversion of CO on Pd(110) and Ni(111). CO_2 and N_2 are produced on Pt(100), Rh(111) and Rh(110) whereas no reaction takes place on Pt(111) and Ru(001). Surface explosions and kinetic oscillations are observed for NO + CO reactions on Pt(100) and other systems, yielding desorption products of CO_2 and N_2. The NO + CO reaction on the Pd(100) surface also yields explosive production of CO_2 followed by gradual N_2 desorption whereas the formation of mixed NO + CO island patterns were found to be a prerequisite to autocatalytic reaction. The local fractional coverage is estimated to be 0.33. As a result of the competition between NO and CO for surface electrons, the CO–metal bond is weakened by coadsorbed NO. On the other hand, strengthening of the NO–metal bond is observed [254(b)].

The periodic part of a structure can be determined from reflection high-energy electron diffraction with a precision of about 0.1 Å and information regarding the corresponding coverages can be gathered. This has been demonstrated, in particular, with the study of the CO-induced (1 × 2) → (1 × 1) structural transition on Pt(110), a transition which is also induced by the adsorption of NO. On the first Pt layer, NO adsorbs on bridge sites and on hollow sites on the (111) microfacets while, in the case of the (1 × 1) structure, first-layer top sites are also occupied [260–262]. As soon as the transition begins, the rearrangement of the first Pt layer provides for additional vacant bridge and top sites in the second layer [261].

NO pollutants in exhaust emissions are commonly [262(a)] controlled by passing the gas over TM-based catalysts. Recent studies of the effect of initial rotation on the sticking of NO on Pt(110) found that supplying the molecule with a modest amount of rotational energy enhances sticking because it rotates from O end down to N end down and chemisorbs, while those molecules initially N end down remain so because of the depth of the chemisorption well. With greater rotational energy the repulsive O end of the molecule is often nearest the surface, causing NO molecules to scatter from regions higher above the surface with resultant reduction of sticking. Chemisorption of NO on Pt(111) leads to loss of spin identity but induces weak magnetic changes in the slab. The strength of the chemisorption bond is in the order fcc > hcp > bridge ⩾ on-top. The diffusion barriers from hcp to fcc sites are 0.22 and 1.02 eV across the bridge and the on-top sites respectively.

The reactions of NO with TMs are also of interest in biochemical systems, atmospheric chemistry and surface chemistry. Nitric oxide acts as a potent bioregulator in several haem-containing enzymatic cycles. The binding of NO to haem Fe centres in metalloproteins is often a crucial protective step in the enzyme reactions that combat toxins in the body. The chemistry of NO is an environmental concern in both the upper and the lower atmospheres. NO undergoes primarily charge transfer reactions in the ionosphere where it contributes to ozone depletion. In the troposphere, NO is implicated in the photodissociative production of smog, which also contains a number of TMs including Ti, Pb, Z, Fe, V, Mn and Ni, in highly polluted areas. Because NO is also a byproduct in the combustion of fossil fuels by automobiles, reactions involving NO on TM surfaces are important in the development of efficient catalysts for catalytic converters.

In the automotive industry, three-way catalysts involving notably Rh, Pd and Pt are used to reduce the emission of the nitrogen oxides NO_x. While Rh is more efficient in the reduction of NO_x than Pd and Pt are and many experimental investigations of these systems have provided new and interesting information, the key reason for the efficiency of Rh is still not well understood. With ever more stringent air quality regulations being imposed on automobile manufacturers, a detailed understanding of the catalytic reduction of NO becomes even more urgent. The adsorption and chemical reaction of NO on Rh, Pd and Pt show a complicated and complex nature. Depending on the crystal surface of the substrate, dissociative adsorption may be promoted or hindered. Also strong dependence of the adsorption site on temperature and coverage has been reported and some of the experimental results are controversial [262(b)].

A full-potential linearized augmented-plane-wave method for thin films was used to study the dynamical and geometrical aspects of NO chemisorption on the TMs Rh, Pd and Pt, indicating stronger bonding of NO to Pd and Pt than to Rh. The metal surface is strongly affected by NO chemisorption, including a buckling that is about 50% larger on Pd and Pt than on Rh. Lower calculated stretching frequencies confirm the idea that NO bonding on Rh is weaker. The electronic properties of NO chemisorption indicate that the $2\pi^*$ state is broadened because of the interaction with TM states. Also the $2\pi^*$ state hybridizes with the TM d states which produces new states lying just below the Fermi energy. This result is consistent with the frequently discussed picture of σ and π back donation. The relative occupancy of the hybridized $2\pi^*$ state has two effects. On the one hand, the filling of the antibonding orbital should elongate and weaken the NO bond. On the other hand, more charge is transferred into the bonding region between NO and the TM, which strengthens the NO–TM substrate bonding. There is a stronger interaction between NO molecules on a Rh surface which, in addition to the NO–metal interaction reduces the NO bond length. In accordance with the higher filling of the hybridized $2\pi^*$ state, there is a stronger polarization of the electrons towards the metal surface. This modifies the electrostatic potential in the surface region and leads to a dipole layer that raises the electronic levels including the Fermi energy and results in a reduction in the work function. The mobility and chemical reactivity of NO on Pd and Pt surfaces are hindered owing to the stronger bonding to the surface and large buckling of the surface layer. These two findings may possibly distinguish Rh as a more efficient catalyst [262(c)].

In the automotive industry, reactions involving three-way catalysts with Rh, Pd and Pt as active metals, NO (more generally NO_x) is reduced and CO and uncombusted hydrocarbons are oxidized [262(d), (e)]. It has been suggested that the dissociation of adsorbed NO is the rate-determining step for reaction on Pd. NO adsorption is mainly associative even if a small fraction of the molecules dissociate at room temperature and higher, presumably on defect sites. In the dissociation of NO, Rh surfaces are superior to Pd surfaces. Associative chemisorption on Rh surfaces can only be seen at low temperatures; however, if the molecule is adsorbed at room temperature, dissociation occurs and is dependent strongly on NO coverage. If at 80 K the Rh(100) surface is saturated with NO, dissociation is hindered until NO desorption at 250 K creates vacancies. For coverage below 0.3 ML at room temperature the decomposition of NO is complete on Rh(111). At saturation coverage (0.67 ML), only 55% of the adsorbed molecules decompose. Molecular chemisorption on a Pd(100) surface at 0.25 ML coverage yields vertical NO molecules on a bridge site. For Rh(100), horizontal NO was proposed at low coverages that is transformed into bridge-bonded vertical NO at higher coverages. For NO on Pd(111), one observes a disordered structure at 0.3 ML with vertically chemisorbed NO molecules on bridge sites, a c(4×2) at 0.5 ML again with bridge sites, a (2×2) structure corresponding to 0.75 ML coverage, and a mixture of sites. For the latter system, simultaneous population of either top and bridge or top and hollow sites has been proposed. IR reflection absorption spectroscopy studies of CO and NO coadsorption on Pd(111) reported that, at low coverages, NO adsorption occurs at hollow sites. N and O are known to bind at high-coordination sites on Pd and Rh metal surfaces: threefold hollow on (111) and fourfold hollow on (100). Atomic N on Pd(100) can be obtained by reaction of NO with H_2 or with CO. With O_2 exposure, ordered structures have been observed on Pd(111), Pd(100) and Rh(100). On Rh(111), O orders in threefold hollow positions in domains of (2×2) structure (with a coverage of 0.25 ML), or otherwise of (2×1) structure (with a coverage of 0.5 ML).

Studies of the interaction of NO with polycrystalline Rh, Rh(111), Rh(100) and Rh(110) generally indicate that, at low temperatures, NO adsorbs molecularly [262(f)]. At low coverages, NO dissociates completely upon heating as witnessed by the desorption of the dissociation product N_2 between 450 and 700 K and, at much higher temperatures, desorption of O_2. Some NO desorbs molecularly at higher coverages and an additional desorption state of N_2 arises. In order to study the overall kinetics of a complicated reaction mechanism, one should isolate the various elementary reaction steps and study their kinetics over a wide range of experimental conditions. In a mixed adlayer, lateral interactions can be included in the kinetic scheme by investigating well defined coadsorption systems. For Rh(111), efforts in this field have led to studies of the interaction of N with Rh(111), the coadsorption of N and O, NO and O_2, NO and N, NO and CO, and NO and H_2. Determination of the kinetic parameters of elementary reaction steps calls for spectroscopies that are able to monitor the surface reaction in real time. The combination of TPD and temperature-programmed static secondary-ion mass spectrometry (TPSSIMS) have become powerful tools. These methods were used to study the kinetics of adsorption, dissociation and desorption of NO on Rh(111). At 100 K, NO adsorption is molecular and proceeds via mobile precursor state kinetics with a high initial sticking probability. TPSSIMS indicates the presence of two distinct NO adsorption states, indicative of threefold adsorption at low coverages and occupation of bridge sites at higher coverages. NO dissociates completely at temperatures between 275 and 340 K. The N(ads) and O(ads) dissociation products desorb as N_2 and O_2 respectively. At higher coverages, the desorption kinetics of N_2 is strongly influenced by the presence of coadsorbed O_2 and dissociation of NO becomes progressively inhibited because of site blocking. The accumulation of N and O on highly covered surfaces causes destabilization of the N atoms that results in an additional low-temperature desorption state of N_2. For high initial NO coverages, above 0.50 ML, dissociation is completely self-inhibited, indicating that all sites required for dissociation are blocked. The desorption of the more weakly bound, presumably bridged NO does not generated the sites required for dissociation; these become available only after desorption of presumably triply coordinated NO.

The NO energy profile on a Pd surface was studied using photoemission spectra and an effective one-electron Hamiltonian and indicated that multicentred adsorption sites are preferred over on-top positions. Binding energies of 32–33 kcal mol^{-1} are found for the (111) and (100) surfaces respectively. Extended Hückel tight-binding calculations and BOC–MP methods were used to study the adsorption of NO on Rh(100). This work showed trends in the decomposition of NO and its reduction to N_2 and NH_3 by CO and H_2 and indicated the importance of coverage. Periodic DFT calculations were performed for the molecular and dissociative chemisorption of NO on Pd(100), Pd(111), Rh(100) and Rh(111) surfaces with generalized gradient approximation exchange–correlation functionals. The periodic systems were modelled by two-dimensional Pd and Rh slabs with frozen geometries, on which a NO, N, O or N +O adlayer is placed. On Pd(100) and Rh(100), at a coverage of 0.5 ML, the bridge site is the most stable arrangement with binding energies of −1.54 and −2.18 eV, respectively. On the (111) surfaces, at a coverage of 0.33 ML, the threefold hollow sites are favoured with binding energies of −2.0 eV for Pd(111) and −2.18 eV for Rh(111). For the dissociated structures, the mixed coadsorption of N and O is favoured in most cases compared with separated domains. The chemisorption of NO, N and O is stronger on Rh surfaces than on Pd surfaces but stability is greater for atomic chemisorption. The absolute values of binding energies decrease with increasing coverage. The NO dissociation is exothermic only for Rh at low coverages, while it is endothermic on Pd owing to the smaller atomic binding energies [262(3)].

5. Interaction of O_2 with metallic surfaces

Considerable research has been undertaken in order to understand the mechanism of O_2 interaction with TM surfaces [263–284]. Whereas dissociative chemisorption of O_2 by clean metal surfaces might be considered the rule in surface science, molecular chemisorption of O_2 is the exception. It occurs on clean surfaces of Ag, Pt and Cu at temperatures above 80 K under UHV conditions and on Pd in the presence of a passivating layer of adsorbed O [263, 280]. O_2 has been cited as binding perpendicularly, tilted and parallel to TM clusters and surfaces. Through back donation from the surface, the low-energy $2\pi^*$ orbital is easily populated which is relevant in the parallel adsorption mode where there is significant weakening of the O–O bond. This is typified by low stretching frequencies and long bond lengths. The mechanism for the three modes involves donation of electrons from the 2π orbital of O_2 to available surface orbitals along with subsequent back donation from the surface to the O_2 $2\pi^*$ orbital, which is accompanied by charge transfer to the adsorbed O_2. The charge transfer and occupation of the $2\pi^*$ orbitals lead to a weaker O–O bond. Both superoxo and peroxo intermediates have been suggested on different surfaces, based on the degree of charge transfer and weakening of the O–O bond. DFT calculations showed that O_2 adsorbs molecularly on Cu(111) with a small adsorption energy, which is consistent with experiments and indicates that threefold coordination is preferred [3]. The difference between parallel and perpendicular adsorption modes is rather small, with the parallel mode being slightly favoured, which is consistent with the relatively low experimental O–O stretching frequency. Mulliken populations for O_2 parallel to the surface indicate that both O atoms pick up substantial negative charge from the surface and form a peroxo species, resulting in a substantially weaker O–O bond as indicated by an 0.22 Å bond length increase from the gas-phase value of 1.21 Å. The results for binding O_2 perpendicularly differ primarily in the degree of charge transfer and O–O bond weakening [3]. The interaction of O_2 on Ag is weaker than on Pd. The molecule O_2 on Ag(110) prefers to bind as a peroxo surface species, which is confirmed by the significantly longer O–O bond length and very low O_2 stretching frequency found for the system. Both the π^* and the σ^* orbitals are highly populated in the adsorbed surface state. Theoretical and experimental results on Pt(110) and Cr(110) indicate that O_2 binds as a superoxo species. For molecular O_2 adsorption the general bonding characteristics are similar to those for CO, that is there is back donation from the surface into O_2 π^* and donation from the O_2 π^* orbital to the surface. Molecular O_2 surface species were observed on Pt, Ag, Cu and Ni, and with clearly identified bands at 630, 710, 766 and 887 cm^{-1} respectively.

The Ag(110) surface has been the focus of considerable attention owing to the commercial use of Ag catalysts for the partial oxidation of ethylene. O_2 molecule adsorption on single-crystal planes can yield ordered forms of adsorbed O_2 in which the surface structure of the metal planes remains almost unaltered. O atoms are covalently bonded to TM atoms of the surface layer. For most metals, O_2 is bound primarily in its precursor state which later moves along the surface searching for a more stable site. When the TM surfaces Cu(110), Ni(110) and Ag(110) are exposed to O_2, etching at step edges and defects is induced at room temperature and one-dimensional metal–O strings are found to grow on the surface, yielding a precursor species [156]. The O_2 heat of adsorption tends to decrease with increased coverage which can be associated with surface irregularity, interaction with adsorbed atoms, and changes in electronic properties of the metallic surface with degree of coverage.

O_2/Ag(110) manifests three distinct adsorption states: physisorbed O_2 ($T < 40$ K), molecularly chemisorbed O_2 (140 K $< T <$ 180 K) and atomically chemisorbed O ($T >$ 180 K) [47, 278, 279]. The molecularly chemisorbed state is regarded as a precursor to dissociative adsorption and, similarly, the physisorbed state is regarded as a precursor to intact molecular chemisorption. One of the most striking features of the dynamical behaviour of this system is the very low sticking coefficient for O_2 on Ag(110) at liquid-N_2 temperatures (i.e. into the molecularly chemisorbed state, possibly via the physisorbed precursor). By contrast, the sticking coefficient into the physisorbed state at $T \approx 30$ K appears to approach unity. Even more significantly, when the physisorbed layer is warmed, the efficiency of conversion into the molecularly chemisorbed state is high, perhaps 50%. These results present a paradox; two different experiments that seem to measure the probability of sticking in the molecularly chemisorbed state give quite different results. Possible and intriguing resolutions of this paradox are associated with the orientation of the chemisorbed O_2 molecule: does it lie parallel to the surface with its axis along the [1–10] direction or parallel to the surface but pointing along the [001] surface? The optimum orientation of the physisorbed precursor is stabilized by the O_2–O_2 interaction in the physisorbed layer where orientation discriminates against conversion into the chemisorbed state.

These results provide striking evidence of the key role played by molecular orientation in molecule–surface interactions, a role which is likely to extend well beyond the model O_2/Ag(110) system. At low temperatures, Ag(110) is also one of the few known surfaces which chemisorb O_2 without breaking the O—O bond, but only weakening it. It has also been proposed that the molecule should lie parallel to the surface in order to yield efficient overlap of O_2 and Ag orbitals, thereby providing a partial rationalization of the observed low O—O stretching frequency [266, 275]. This extremely low frequency was argued to be an indication that the π^* orbitals of the O_2 species are filled and that the σ^* orbital is possibly partially occupied. The O_2 π orbitals normal to the surface interact strongly with second-layer Ag atoms, while π orbitals parallel to the surface interact with first-layer Ag atoms [263, 284].

The gross features of O_2 chemisorption on Ni are well known from experiments. When the Ni(100) surface is exposed to O_2, the molecules dissociate until a coverage of about 0.25 ML is reached, each O occupying a fourfold hollow site. Chemisorbed O_2 has been observed on polycrystalline Ni, but not on the low-index surface of fcc Ni [264, 273]. As O_2 exposure continues, the hollow sites become occupied and the surface reconstructs. Once O atoms have come to rest at their final chemisorption sites, the barrier for diffusion effectively prevents O transport on the surface at normal temperatures. This barrier can be estimated from comparisons with similar systems, for which the barriers are known, to be about 20% of the atomic chemisorption energy [264]. In the case of O on Ni(100), the barrier estimate of 23–26 kcal mol^{-1} is in agreement with theory. Although O_2 is not observed generally on fcc Ni surfaces, there is ample evidence of molecularly chemisorbed O_2 on other TM surfaces. Molecular O_2 was found on both polycrystalline Ga and Cu surfaces. Chemisorption on the Pt(111) surface indicated three O-associated vibration bands at 870, 710 and 390 cm^{-1} (compared with 1580 cm^{-1} for free O_2); the 870 cm^{-1} peak was assigned to O_2 molecules with only a single O—O bond implying that the antibonding π_g orbital was filled for this species [241]. The photoelectron spectra of O_2 on Cu(100) and Cu(110), which display three broad peaks, suggest that the adsorbed molecule is neutral O_2 in a singlet state. Spitzer and Luth [276] suggested a neutral adsorbed O_2 in a singlet state. It has been further suggested that the dramatically lowered intramolecular bond order, which is associated with the reduced vibrational frequency of chemisorbed O_2 is caused by a π_u-to-surface and a surface-to-π_g electron transfer which is also suggested to be the mechanism by which O_2 dissociates [277].

Panas *et al.* [264] used a cluster model approach to indicate that the dissociation mechanism for O_2 on Ni(100) was very similar for the reaction pathway over an on-top position, over a bridge position and over a fourfold hollow position. In the entrance channel a chemisorbed peroxo form of O_2 is first formed, which is strongly bound to the Ni(100) surface by two polar covalent bonds. The binding energy at the fourfold hollow site is found to be 78 kcal mol^{-1} which is about 20 kcal mol^{-1} larger than that for the other two sites and much larger than the chemisorption energies found experimentally for O_2 on Pt(111) and Ag(110). The dissociation of O_2 proceeds by two stepwise electron transfers from the surface over to the O_2 $3\sigma_u$ orbital, which completes the breaking of the O—O bond.

In spite of their importance in applications, relatively little is known about reactions of gas-phase TM atoms compared with TM cations. The laser-induced fluorescence technique was combined with a dc discharge to produce laser photolytic formation of gas-phase TM atoms and provide useful information on bimolecular reactions of TM atoms. In some cases, such information has been extended to the interaction of electronically excited states as well as the ground state. These studies have shown that ground states, the $3d^{n-2}4s^2$ configuration in most cases, are inert, while the excited states of the $3d^{n-1}4s^1$ configuration correlate to higher electronic energies in Ti and V. It is difficult to distinguish between the effect of electron configuration and the effect of electronic energy. Two explanations have been proposed for reactions of Ti and V with oxidants. One is an electron-transfer mechanism in which the electronic energy is the dominant factor. In reactions of molecules with positive electron affinities, the electron-transfer mechanism can explain relative reaction rates semiquantitatively. The other explanation is based on the orbital correlation between the reactant and the product metal oxide. In this mechanism, the electron configuration is the dominant factor. Studies of the reactions of Mo with O_2 have shown that the $4d^5 5s^1$ configuration is more reactive than the $4d^4 5s^2$ configuration although the latter has a higher electronic energy. Efficient depletion of the atoms of $3d^{n-1}4s^1$ configuration by O_2 was interpreted as an attractive interaction correlated to a stable intermediate. The singly occupied antibonding π^* orbitals of O_2 interact favourable with singly occupied 3d orbitals of Co or Ni.

Among the low-index single-crystal faces, the Pt(100) face exhibits peculiarities that are connected with the reconstruction of the first atom layer into a buckled hexagonal arrangement [281–283]. On a reconstructed surface the rate of O_2 adsorption is very low at ambient temperatures, as are the attainable concentrations. High-density adlayers are formed at elevated temperatures. The initially clean metastable substrate adsorbs O_2 with a high efficiency at ambient temperatures in contrast with the reconstructed surface. Recent studies of adsorption of O_2 on Pt(100) surfaces pre-covered with different amounts of Cl indicated that small concentrations of the latter lower the temperature necessary to accomplish O_2 adsorption. Pre-adsorbed Cl lowers the temperature necessary to obtain high-density O_2 adlayers. Coadsorbed Cl destablizes adsorbed O_2.

Recent studies of reaction pathways by surface femtochemistry of routes to desorption and reaction in $CO/O_2/Pt(111)$ indicate that, if CO oxidizes by an atomic pathway, then O-atom capture by CO is highly efficient; if CO oxidizes by a molecular pathway, then the O atoms in the transition state are inequivalent. Bagus and Illas [271] investigated the bonding of O to Cu(100) with a surface cluster model and showed that the bond is ionic with a net charge on O of about 1.5 electrons and supports the commonly held belief that d electrons participate in the bond.

Alloys and bimetallic metal surfaces present various interesting phenomena which should be understandable at the atomic level. The effects of dopant atoms on the catalysis of metal surfaces are especially interesting. The catalytic activity of an alloy or bimetallic system is strongly influenced by its surface composition and structure. To change the surface composition of an alloy or bimetallic system by annealing in UHV requires a rather high annealing temperature. However, a bimetallic surface exposed to active gases such as O_2 readily changes its surface composition at a far lower temperature. These phenomena are explained well by the concept of chemical reconstruction—a type of reconstruction that involves chemical reaction. If the chemical reconstruction takes place on an A–B alloy or bimetallic surface, then the more reactive metal atoms react with the gas so that the segregation of A metal atoms is established. During catalysis a catalyst surface is necessarily exposed to active gases under flow conditions. The notion of chemical reconstruction is indispensable for alloy or bimetallic catalysts. For example, when a clean Pt-enriched Pt–Rh(100) surface is exposed to O_2 at about 500 K, Rh atoms are easily segregated on the surface [285].

It is well known that O_2 adsorption on TM surfaces occurs more rapidly in the presence of alkali metals than on clean metal surfaces. The presence of alkali metals increases both the adsorptive capacity of the surface and the dissociative adsorption rate. The increase in O_2 uptake rate caused by alkali metals is explained by enhanced electron flow into the antibonding molecular orbital and reduction of the activation barrier for dissociation. The presence of alkali metals on a metal surface decreases the electron work function because of the higher electron density localized in the vicinity of the alkali adspecies. O_2 chemisorption on an Fe surface covered with K occurs after prior adsorption of O atoms under the layer of K atoms. The various atom locations in addition to the electron transfer causing the change of work function could be responsible for the kinetic of oxidation of TM surfaces [286].

Since dissociation is assumed to occur by collision upon impact with the surface, the simplest direct mechanism is surface temperature independent. While the simple direct and trapping-mediated models for dissociative chemisorption describe O_2 adsorption on Cu(110) and W(110), they are insufficient for describing O_2 adsorption on many other surfaces including Ru(001) [287(b)]. Early studies of O_2 adsorption on W surfaces led to the conclusion that adsorption occurred by means of a physically adsorbed precursor at low kinetic energies and by means of a simple direct mechanism at higher kinetic energies. Later studies of O_2 adsorption led to an alternate (direct molecular chemisorption) explanation for high-kinetic-energy adsorption.

One of the early studies of O_2 adsorption on single-crystal TM surfaces was made by Wang and Gomer [287(d)] in which the adsorption probability of O_2 on W(100) and W(110) was measured. They determined that dissociative O_2 adsorption proceeded via a physically adsorbed precursor. Subsequently, Rettner *et al.* [287(e)] used supersonic molecular beams to measure the dissociative chemisorption probability of O_2 on W(110) and concluded that the initial dissociative chemisorption of O_2 on W(110) was dominated by a direct mechanism for incident kinetic energies above 0.1 eV and that the dissociation probability increased dramatically with increasing incident kinetic energy. The initial O_2 adsorption probability was also independent of surface temperature and approached unity at high incident energies, which was consistent with the view at the time of a direct mechanism. Dynamical studies of dissociative O_2 adsorption on Cu(110) also support a trapping-mediated mechanism at the lowest kinetic energies and a surface-temperature-independent direct mechanism at higher incident energies. Recent studies of O_2 adsorption states on W(111) at low temperatures indicate three weakly bound molecular adsorption states corresponding to multilayer condensation, physisorption and weak chemisorption. Molecularly adsorbed O_2 serves as an extrinsic precursor to dissociative adsorption of O_2 on W(111). Comparison of molecular chemisorption states for different W surfaces displays the influence of the substrate surface structure on the binding energy of weakly chemisorbed O_2 [285].

Adsorption and dissociation of O_2 and Pt is a necessary step in the operation of an automobile's catalytic converter and exhaust O_2 sensor. Also, in some fuel cells the dissociation of O_2 at a Pt anode is postulated as a step in O_2 reduction. In such applications, the Pt surfaces are heterogeneous with a high concentration of defects that can strongly affect the surface chemistry. As a consequence, the dissociative sticking probability of O_2 increases exponentially with increasing step concentration while the CO oxidation probability decreases. The optimum configuration for CO oxidation occurs with O_2 at a step edge and CO on a terrace. Studies of adsorption and dissociation of O_2 on Pt(335) indicated five vibrational peaks from atomic O on the terraces, on the steps and under certain conditions, from a distinct molecular step species. Dissociation occurs almost exclusively at the steps [287(a)].

In contrast with O_2 adsorption on W(110) and Cu(110), the initial dissociative adsorption probability of O_2 on Pt(111) is influenced by surface temperature. Adsorption decreases with increasing translational energy and surface temperature at low incident energies which is consistent with a trapping-mediated chemisorption mechanism. The adsorption probability increases with increasing incident energy at higher kinetic energies. However, an inverse dependence on surface temperature is observed which is inconsistent with the picture of the simple direct mechanism [287(f)].

It is necessary to discuss the different states of O_2 that have been identified on the Pt(111) surface in order to understand the unprecedented behaviour observed in this system. On Pt(111), four states of O_2 have been identified: a physically adsorbed molecular state, two molecularly chemisorbed states and an atomic state. The two molecular chemisorbed species are a superoxo-like O_2^- species and a peroxo-like O_2^{2-} species. The physically adsorbed state has been identified as the precursor to molecular chemisorption. It is believed that, for adsorption at low energies, dissociation proceeds from the physically adsorbed state sequentially through the surface intermediates to the atomic state which could explain the kinetic energy and surface temperature dependences of the initial adsorption probability in the low-kinetic-energy regime in terms of a trapping-mediated model involving sequential precursors. However, there was no explanation for the temperature dependence of adsorption at high kinetic energies. Rettner *et al.* [287(e)] expanded the sequential precursor mechanism of Luntz *et al.* [287(f)] by allowing for the possibility that the molecule could directly access the molecularly chemisorbed state at higher kinetic energies. This extension of the mechanism gave an accurate description of the kinetic energy and surface temperature dependences of the dissociation probability for O_2 on Pt(111) over the entire range of energies and temperatures studied.

Supersonic molecular-beam measurements of the initial dissociative chemisorption probability of O_2 on Ru(001) as a function of incident kinetic energy, surface temperature and angle of incidence indicated that adsorption in the low-energy regime can be accurately modelled by a trapping-mediated mechanism with a surface-temperature-independent trapping probability into a physically adsorbed state followed by a temperature-dependent kinetic competition between desorption and dissociation [287(b)]. However, there is an unusual surface temperature dependence of the dissociative chemisorption probability in the high-energy regime that is inconsistent with a simple direct mechanism in which the probability rises as the surface temperature is increased. A mechanism involving electron transfer from the Ru surface was suggested to account for this phenomenon.

The importance of Pt as an oxidation catalyst, for example for ammonia oxidation and in car exhausts, provides the incentive for the study of the interaction of O_2 with Pt and much work has been carried out using Pt single crystals. The Pt(100) surface in its most stable reconstructed form has a contracted rotated hexagonal structure, Pt(100)-hex-R which is akin to that of Pt(111) although it is more densely packed and slightly buckled. Supersonic molecular-beam experiments indicate that adsorption on the Pt{100}-(1 × 1) surface differs from that on the reconstructed Pt{100}-hex-R surface in both magnitude and mechanism. The initial sticking probability on the (1 × 1) surface at first decreases with increasing incident energy and then increases as the incident energy exceeds 0.1 eV, in a manner typical of an adsorption process that is precursor mediated at low incident energies and direct at higher incident energies.

Precursor-mediated adsorption at low energies is also indicated by scattering measurements and by the angular variation in the initial sticking probability. At high incident energies the angular variation in the initial sticking probability indicates that adsorption is an activated process. Repulsive lateral interactions exist between adsorbed O atoms. Thermal energy atom scattering measurements show an absence of island formation upon adsorption, in contrast with adsorption on the hex-R face [287(h)]. Molecular-beam measurements of the sticking coefficient at zero coverage for O_2 on a Pt(111) surface as a function of initial energy, angle of incidence and surface temperature indicate that both precursor-mediated and quasidirect dissociation can be observed, depending upon initial conditions. The quasidirect process is revealed by a step increase in sticking with initial energy. This feature is weakly dependent on the surface temperature. Precursor-mediated sticking is well described by standard precursor kinetic models. At low incident energies and surface temperatures, sticking measures trapping into a molecularly adsorbed state. This tapping decreases more rapidly with increasing incident energy than anticipated from simple models.

6. H_2 on transition-metal surfaces

The chemisorption of H_2 on TMs is a process that has been extensively investigated by surface scientists both owing to its importance in catalysis but also because H_2 is one of the simplest adsorbates [47, 288–318]. From a theoretical point of view, H_2 provides simplifying benefits because of its small mass, weak interaction with substrate vibrations, and large separation between rotational and vibrational energy levels that make possible the separate treatment of these degrees of freedom to lowest order. Both Nb and Pd are well known for their capacity as absorbers of large quantities of H_2, producing in this way a sure and efficient manner of keeping the molecule in stock. Absorption of H_2 in some metals is also known to lead to deterioration of the mechanical properties of those metals.

Water decomposition in electrochemical and photoelectrochemical cells leads to the interesting possibility of storing energy in the form of gaseous or dissolved H_2. In an electrochemical cell with two metallic electrodes, electrical energy is converted into chemical energy by splitting H_2O with formation of gaseous H_2. In photoelectric cells that have one semiconductor and one metal electrode, solar energy can be converted into H_2 gas by water decomposition; H_2 dissociation is poisoned by electronegative adsorbates. In the latter case, however, a molecular precursor has not been observed, but it appears that poisoning is more than simply blocking of sites for H adsorption.

Because H_2 is one of the simplest adsorbates, if not the simplest adsorbate, most theoretical methods have been applied to the development of a description of the chemisorption bond of H_2 on metals [47, 288–314]. Among these studies, Nordlander *et al.* [314] applied an extended effective-medium technique in order to explain, in a very simple way, the trends in the chemisorption energies on the TM 3d, 4d and 5d series from variation in parameters describing the pure metal. The computed chemisorption energies are in good agreement with experiment and the trends along a given row are shown to be dominated by the degree of filling of the d band. In general, the sites of highest coordination are favoured, and the differences between sites are found to be small, indicating large H, mobility. Harris and Anderson [296] observed that H_2 dissociates on TMs without apparent activation because of the mechanism that suppresses Pauli repulsion and for which d electrons serve as sinks for s electrons. Pauli repulsion is reduced because s electrons of a TM can revert to the d band and avoid the energy cost of penetrating the H_2 $1\sigma_g$ core. Chemisorption is accompanied by local filling of d holes which enables metal–H bonds to form with only moderate weakening of metal–metal bonds. The SCF calculations of Niu *et al.* [297] indicated that the interaction of H_2 with a Ni^+ ion is characteristically different from the interaction with neutral Ni. While H_2 chemisorbs dissociatively on a neutral metal, it retains the molecular form on an ion. The former (dissociative) result is a consequence of the Pauli exclusion principle whereas the latter (molecular) finding results from electrostatic interaction.

Saillard and Hoffmann [295] investigated how the H–H bond interacts and eventually breaks in the proximity of one or more TM centres for both discrete complexes and clean metal surfaces by comparing the chemistry that occurs in an inorganic complex with that on a metal surface. Donation and back-donation effects previously discussed for CO are also effective for H_2 interaction with metallic surfaces. The electron transfer of H to the metallic surface decreases H–H bonding and increases metal–H bonding. Electron transfer in the opposite direction, that is from an orbital originally on the metal to H_2 has a consequence of decreased H–H bonding and increased metal–H bonding. These two orbital interactions, which are the most important bonding interactions between a H_2 molecule and a discrete TM complex or surface, lead to H–H bond weakening and metal–H bond formation even though they accomplish these actions by charge transfers in different directions. At a crude level, it is generally accepted that the energy barrier to H_2 dissociation, which is observed for metals such as Mg and Cu, arises from the orthogonalization of the metal states to the H_2 bonding orbital as required by the Pauli exclusion principle. The absence of a dissociation barrier on TMs with a partially filled d band is then a result of orthogonalization which can occur through s–d transfer of the metal electrons at minimal energy cost (owing to the high density of d states at the Fermi level).

On a more detailed level, seeded molecular-beam scattering experiments and state-resolved time-of-flight measurements of desorption make possible the determination of the behaviour of sticking probability as a function of the molecular vibrational state, rotational state and momentum parallel to the surface. These studies show that this behaviour is strongly dependent on both the chemical composition and the orientation (crystallographic index) of the surface. Dynamical simulations, using quantum and classical dynamics, have proved invaluable in understanding the behaviour of more complex systems. As an example, the dependence of sticking probability on vibrational state for the H_2/Cu system has been seen to result from a late barrier in the PES, that is the barrier occurs at an extended bond length. By contrast the sticking probability for the H_2/Ni system, in which the barrier occurs at the molecular bond length, shows no vibrational-state dependence. Another example is the absence of parallel momentum dependence of the sticking probability found for the H_2/Cu(100) system for which it has been proposed not, as one might expect, from the absence of surface corrugation in the PES, but from the cancellation of effects of two types of corrugation, that is the variation in both the position and the magnitude of the barrier on the PES [315(b)].

The reaction of H_2 on low-index Cu surfaces stands as the prime example of activated dissociative chemisorption and these systems have been widely investigated experimentally [315(c)]. The experiments have demonstrated the existence of several trends in the dependence of reactivity on internal molecular motion. Putting energy into H_2 vibration enhances reaction (vibrationally enhanced dissociation). Associative desorption experiments have shown that increasing the H_2 rotational quantum number j first inhibits dissociation at low j and then increases it as higher j. The dissociative chemisorption of H_2 on Cu(100) was recently studied using a six-dimensional wave-packet method. All molecular degrees of freedom were treated quantum-mechanically with no dynamical approximations. The PES used as an analytical fit to DFT energies obtained in the generalized gradient approximation with a slab representation of the metal surface. The dependence of the reaction probability on normal incident energy was compared with experiment, and it was suggested that, on the average, the DFT method overestimates the barrier to dissociation by about 0.15 eV for H_2 +Cu(100). In broad agreement with experiments, the calculations show large vibrational inelasticity.

Studies [47, 316] of dissociative chemisorption of H_2 on Cu(111) indicated that the sticking coefficient at fixed translational energy first decreases and then increases with rotational excitation. This behaviour is attributed to an orientation dependence of the sticking coefficient. The molecular-axis orientation upon approach to a particular surface crystallographic direction determines the probability that either atom or both atoms of the molecule experience close collisions with atoms of the surface. Upon approach to a metal surface, both the ground-state singlet and the first-excited triplet states of H_2 are generally considered to be accessible for charge transfer. Adiabaticity arguments suggest that charge transfer occurs as the molecule approaches the surface. Fast neutral H_2 in its ground electronic state is efficiently dissociated in grazing collisions with TM surfaces. The topography of the adiabatic ground state of the H_2/Cu(111) system is well established. The H–H interaction is by no means purely repulsive in the pre-barrier region of the ground-state PES. A repulsive H–H interaction during the approach of the molecule to the surface is crucial and the dynamics of the interaction of fast neutral H_2 with Cu(111) is influenced by additional (higher-lying) PESs. First-principles calculational results, which conflict with conventional wisdom, showed an orientation dependence of the energy of H_2 a few bohrs above a Rh(001) surface. In geometric configurations near the saddle point where an H–Rh bond begins to form, the favoured molecular axis orientation is along the (100) direction, corresponding to the attraction of each H atom to a twofold bridge site. This occurs even though the final destinations of H atoms are fourfold hollows and even though the (100) orientation corresponds to relatively low symmetry.

Metal surfaces often undergo reconstruction with the adsorption of gases. In some cases, one finds non-traditional adsorption-induced reconstruction, that is reconstruction caused by chemical reaction of TM atoms with molecules [156]. When a Ni(110) surface is exposed to H_2, two reconstructions occur, namely adsorption-induced reconstruction and chemical reconstruction, depending on the temperature. For $T < 220$ K, the Ni(110) surface undergoes (1×2) reconstruction but, when the surface is exposed to H_2 at room temperature, one-dimensional Ni–H grows on the surface in the [110] direction.

Investigations of the properties of Fe monolayers on W(110) indicated that desorption of H_2 from H/Fe/W(110) occurred at substantially lower temperatures than from H/W(110), suggesting lower binding energies on the Fe-covered surface. For H on Fe/W(110) the enthalpy and entropy values at low coverages also behave normally with ΔH substantially less than on clean W(110) and the surface entropy corresponding to an excited two-dimensional gas, unlike the H/W(110) case. Presumably, these findings arise from the lower binding energy of H to this surface and could be attributed to Fe–W interactions that decrease H–Fe binding [316].

Adsorption of H_2 on W surfaces has attracted considerable interest since the early days of surface physics, particularly regarding the role of a precursor in the H_2 chemisorption on W. From the earliest experiments it was apparent that the H_2 accommodation coefficient on a polycrystalline W surface, that is the dissociative sticking probability, exhibited unusual temperature-dependent behaviour. Much effort has been expended to characterize the adsorbed H_2 phase and the kinetics of adsorption on W(100) [315(d)].

The adsorption dynamics of H_2/W on rough (111) and (100) surfaces indicate that H_2 adsorbs at low relative translational energies almost exclusively through a precursor path; at high beam energies a direct activated path is followed. H_2 adsorption on a W(110) surface proceeds via a direct activated path [315(e)]. Direct adsorption typically exhibits a forward distribution for the sticking coefficient; in contrast, at low collision energies, the precursor path shows a minimum in the sticking coefficient in the surface normal direction. It was found that the dissociation sticking probability of H_2 on W(100) is independent of coverage and decreases linearly with increasing collision energy after saturation, thereby providing evidence for a precursor mechanism. Supersonic molecular-beam experiments have also indicated the importance of a precursor in the dissociation dynamics in the low-temperature gas regime which appeared to be absent for H_2 dissociation on W(110). The apparent ambiguity concerning the role of a molecular precursor in this case also extends to H_2 dissociation dynamics on Ni and Pt. It has been suggested that both direct and indirect dissociation channels contribute to sticking at energies below about 150 meV and that the contribution of the indirect channel is via an intrinsic precursor which has a surface-structure-dependent sticking probability.

Classical and quantum calculations of the dissociation dynamics of H_2 on W(100) show conclusively that, at low translational energies, dissociation is dominated by strong steering in an essentially direct process. Starting from near unity, the dissociation probability falls with increasing energy because the steering has less time to operate and is therefore less effective. Some molecular trapping occurs as a result of rotational excitation which gives rise to sharp peaks in the quantum dissociation probability.

The distinctive feature of H_2 interacting with surfaces is that the internal molecular bond and the bonding to the surface are produced by the same electrons. Therefore, bonding to the surface is necessarily accompanied by weakening of the internal bonding of the molecule. If one freezes the H–H separation at the isolated molecule value, H_2 orbitals do not contribute to bonding to the surface and the molecule behaves similar to a He atom as it approaches the surface. The first unoccupied H_2 orbital lies far above the vacuum level so that the molecular charge density remains frozen and the interaction with the surface is repulsive. Bonding to the surface is possible due to the relaxation of the H–H bond distance. The increase in the bond distance lowers the $1\sigma_u$ antibonding orbital, giving rise to charge transfer from the H–H bond to the H_2–surface bond. Bonding to the surface involves also appreciable polarization of TM states which gives rise to charge transfer from the molecule to the metal, that is to a local decrease in the work function. The occupation of d states facilitates the polarization of the TM states. As soon as the molecule begins to dissociate, the charge transfer goes in the reverse direction. When H_2 is near the surface, there is appreciable softening of the molecular bond and electron charge accumulates between the protons and the surface in order to minimize the descreened repulsion between protons and surface, at the expense of H_2 bonding. Even in the absence of dissociation, the weakening of the H–H bond should be quite appreciable as H_2 gets close to a TM surface. Dissociation requires that H_2 lies flat or nearly flat on the surface in order to maximize interaction with the TM as the H atoms move apart. As the molecule tilts away from the horizontal orientation, one of the H atoms feels enhanced repulsion and the other becomes increasingly more weakly bound, so that the potential energy increases. However, at low energies, the molecule will be reflected at most location on the surface [317, 319].

The recombination of two H atoms on a TM surface represents the simplest but most fundamental catalytic reaction. In the past, most experiments determined angular and velocity distributions for various substrates. These quantum-state integral measurements provided information on the energetics of this reaction. In many cases an energy barrier against recombinative desorption or, equivalently, dissociative adsorption was found [320]. These experiments led to the conclusion that simple one-dimensional barrier models could not appropriately describe the desorption mechanism. Quantum-state-resolved experiments for recombinative hydrogen desorption from Cu(110) and Cu(111) substrate surfaces indicated slightly less than thermal energy in the rotational degrees of freedom, but very high vibrational populations, up to 50 times the expected thermal value. A high translational barrier of about 0.7 eV against associative desorption of two H atoms on Cu surfaces was deduced. Subsequently, theoretical models based on a two-dimensional PES were developed to account for the vibrational excitation and the high velocity of the desorbing molecules. In these models recombination takes place at a H–H separation of 1.63–0.23 bohr larger than the equilibrium internuclear distance of gas-phase H_2.

Supported Pt catalysts are of tremendous technological importance in a variety of applications, including petroleum naphtha reforming, automobile exhaust conversion and fine chemicals synthesis [321]. Naphtha-reforming catalysts, in particular, may contain Pt clusters containing only a few atoms on a high-surface-area alumina support. H_2 chemisorption of Pt is central to many catalytic reactions, for example hydrogenation and hydrogenolysis; moreover, volumetric H_2 chemisorption is the standard technique for determining Pt dispersion—the percentage of surface-exposed Pt atoms in supported catalysts. *In-situ* spectroscopic characterization of chemisorbed H_2 on supported Pt catalysts is difficult to achieve by conventional spectroscopic techniques; however, *in-situ* X-ray adsorption spectroscopy studies have identified two effects: a relaxation of Pt–Pt bonds in hydrogen-covered clusters relative to bare clusters as well as Pt–H bonding.

There are contradictory observations regarding contracted nearest-neighbour distances in supported clusters prepared *in vacuo* and bulk-like nearest-neighbour distances in supported clusters prepared by H_2 reduction of Pt ions. H_2 chemisorption on small silica-supported Pt clusters was investigated using *in-situ* extended X-ray absorption fine-structure spectroscopy and NEXAFS and found to exhibit a bulk-like Pt first-nearest-neighbour distance and low disorder. In contrast, bare Pt clusters produced by heating *in vacuo* at 300 °C are characterized by a contracted Pt nearest-neighbour distance and greater disorder. These effects are reversed by re-exposure of bare Pt clusters to H_2 at 25 °C. Electronic transitions from Pt 2p levels to H 1s–Pt 5d antibonding states were observed.

For a variety of reasons, adsorption of H_2 on Pd is interesting for chemical technology as well as for basic surface science. Pd can be used as a catalyst for dehydrogenation and hydrogenation indicating a high rate of permeation of H_2 through Pd samples. H_2 dissociates spontaneously on Pd(100), that is molecules with low kinetic energy dissociatively adsorb on Pd(100) surfaces with a large initial sticking coefficient. The preference of non-activated dissociation pathways for low kinetic energies of H_2 is also consistent with the independence of the initial sticking coefficient on incident angle as well as with the measured Maxwell–Boltzmann velocity distribution of desorbing H_2 molecules, which corresponds to the surface temperature of the Pd substrate. There are, however, clear indications that activated pathways exist as well. State-resolved desorption experiments show that the occupancy of the first vibrational state is significantly higher than that corresponding to H_2 molecules in equilibrium at the surface temperature, that is vibrational heating is found. On the other hand, the rotational degrees of freedom are occupied less than implied by the surface temperature. In order to explain these effects, it has been found necessary in dynamics studies on two-dimensional model PESs to assume the presence of a small (about 0.1 eV) barrier in the exit channel, that is in the region of the reaction pathway where the H–H bond is already significantly stretched. The presence of a weak metastable molecular bound state of H_2 and the presence of a precursor state have also been proposed [322].

Dissociative adsorption of H_2 on Pd(100) has been investigated using *ab initio* quantum dynamics and *ab initio* molecular dynamics calculations [323]. The main assumption of the dissociation dynamics was the Born–Oppenheimer approximation. In this study, adsorption corresponds to a process in which statistically distributed molecules hit the surface from the gas phase. For diatomic molecules this requires the calculation of thousands of trajectories; the adsorption probability is then obtained by averaging over these trajectories. Treating all H_2 degrees of freedom as dynamical coordinates carries very high dimensionality and requires statistical averaging over thousands of trajectories. An efficient and accurate treatment of such extensive statistics was achieved in a three-step approach. In the first step an *ab initio* PES was computed for a number of representative points in configuration space. In the second step an analytical representation was determined which served as an interpolation formula between the calculated points. In the third step, dynamical calculations were performed using the analytical representation of the PES.

The *ab initio* molecular dynamics were compared with detailed quantum-dynamical calculations carried out using the same representation of the PES as in the molecular dynamics simulation. Quantum oscillations in the sticking probability as a function of kinetic energy were found which were very sensitive to initial conditions. At low kinetic energies, sticking is dominated by a steering effect that was illustrated using classical trajectories. The steering effect depends on kinetic energy, but not on the mass of the molecules as long as no energy transfer to substrate atoms is considered. A comparison of quantum and classical calculations of the sticking probability showed the importance of zero-point effects on the H_2 dynamics. The calculations demonstrated that an increase in the sticking probability with increasing incident angle could be caused by the dynamics of dissociative adsorption on a corrugated PES. In an intermediate-energy range between 0.05 and 0.35 eV, even values of parallel momentum were found to enhance the sticking probability. At relatively large distances from the surface, incident molecules are first attracted to the on-top sites, but molecules steered to these sites will eventually encounter a barrier to dissociative adsorption of 0.15 eV. For fixed total kinetic energy, increasing the incident angle means decreasing the kinetic energy component normal to the surface and increasing the component parallel momentum. At low kinetic energies, decreasing the kinetic energy normal to the surface makes steering more effective which promotes dissociation.

The PES for dissociative adsorption of H_2 on Pd(100) was investigated using DFT and the full-potential linear augmented-plane-wave method. These methods yielded several dissociation pathways with vanishing energy barriers. The calculated PES shows no indication of the presence of a precursor state. Both results indicate that steering effects determine the observed decrease of the sticking coefficient at low energies of H_2. The topology of the PES is related to the dependence of the covalent H s–Pd d interaction on the orientation of H_2. Differential sticking coefficients for a single-energy nozzle beam of H_2 on Pd(111) and Pd(110) indicated that adsorption in these systems occurs through a direct path with an activation barrier of perhaps 50 meV or less, and a precursor path. There is relatively little difference in the adsorption properties of the (111) and the (110) planes. The appearance of a molecular precursor on the (111) plane can be related to the electronic structure of Pd and, in particular, to the absence of occupied Shockley surface states compared with Ni(111) and Pt(111). Note that pre-adsorbed K on a (110) plane acts as an inhibitor to adsorption. Different inhibiting mechanisms are observed for the direct adsorption path and the precursor path. At high K coverages the precursor path is completely suppressed.

Although the interaction of H_2 with TM surfaces can be considered a classical field of surface science, a complete and detailed understanding of the processes taking place at and on surfaces is still lacking. This holds, in particular, if one includes the whole surface region (comprising, say, the first ten atomic metal layers) where not only relaxation and reconstruction phenomena can occur, but also H_2 dissolution and absorption processes. Several status reports have reviewed the recent literature and focused mainly on H_2–metal surface equilibrium phenomena (structures, interaction energies, etc.) [315(f)]. Although an increasing number of studies are concerned with H–surface interaction dynamics, there still remain various unresolved problems in the area of standard H adsorption thermodynamics and kinetics, an especially important one being H-induced surface relaxation and reconstruction, as well as the existence of so-called subsurface H. It is generally believed that subsurface H should preferentially form on surfaces with open crystallography (i.e. surfaces with high Miller indices).

Another quite important problem encountered in H_2 adsorption on TM surfaces is the local nature of the adsorption site, that is the question of the energetically most favourable coordination site. H atoms are likely to adsorb on highly coordinated sites, preferably fourfold coordination on squared ((100) orientation) surfaces, threefold sites on trigonal surfaces ((111) orientation) and quasithreefold sites on diagonal surfaces ((100) orientation), while bridge-site occupation has been reported only occasionally (e.g. for the W(100) surface). Combined LEED, TDS and HREELs measurements of the interaction of H_2 and D_2 with Pd(210) in the temperature range 100–500 K indicates that H_2 adsorbs spontaneously with a very high initial sticking probability as atoms in three binding states which can be identified with different geometrical adsorption sites including a subsurface site [324]. Even at the lowest adsorption temperatures, no H-induced LEED superstructure appears, indicating vanishing long-range order between the adsorbed H atoms and the absence of a H-induced surface reconstruction.

The interaction of H_2 with TM surfaces, for example Ni(111), has been investigated extensively by both experimental and theoretical methods, because it is important for applications such as catalytic reaction and H storage and because it has led to fundamentally interesting topics such as H-induced surface reconstruction, two-dimensional phase transitions, indirect interaction between adsorbed H atoms, and quantum delocalization [325]. The presence of H_2 in the near-surface region is important for the reactivity of a TM surface in various catalytic reactions, and it cannot be investigated experimentally in a direct way like other atoms because of the low electron density around H. Consequently, a wide range of different effects such as the existence of different adsorption phases, the principal ability of H_2 to penetrate into the near-surface region, surface relaxations and the coverage dependence of the H-induced work-function changes are of theoretical and experimental interest. We note, for example, that *ab initio* calculations indicate that for Pd the energy gain caused by H_2 absorption in subsurface positions is only about 100 meV lower than for H_2 adsorption at the surface. In contrast, for Rh, significant differences between adsorption and absorption were calculated [325].

We summarize by emphasizing that molecule–surface orientation, donation and back-donation mechanisms as well as possible tilted precursor states are important parameters for monitoring the reactions (adsorption and dissociation) of diatomic molecules (CO, N_2, NO, O_2 and H_2) on TM surfaces. Our recent extensive calculations of these diatomic molecules interacting with first-row TMs (Sc to Cu), focusing on the tilted precursor states, suggests that for these molecules and TM surfaces there is a tilted precursor state in which back-donation effects could effectively lead to dissociation [35]. Our proposed unsynchronized resonance bond dissociation model is shown to provide an illuminating explanation of dissociation processes of simple diatomic molecules on TMs.

Acknowledgments

C.A.T. acknowledges financial assistance from PRONEX/FINEP/CNPQ (Brasil). T.C.G. and A.C.P. acknowledge financial assistance from CNPQ (Brasil). W.A.L. was supported by the Director, Office of Science, Office of Basic Energy Sciences, Chemical Sciences Division of the US Department of Energy under Contract No. DE-AC03-76SF00098.

References

[1] van Santen, R. A., 1991, *Theoretical Heterogeneous Catalysis* (Singapore: World Scientific); Dumesic, J. A., Rudd, D. F., Aparicio, L. M., Rekoske, J. E., and Trevino, A. A., 1993, *The Microkinetics of Heterogeneous Catalysis* (Washington, DC: American Chemical Society); Somorjai, G. A., 1994, *Introduction to Surface Chemistry and Catalysis* (New York: Wiley); Rhodin, T. N., and Ertl, G., 1979, *The Nature of the Surface Chemical Bond* (Amsterdam: North-Holland); Hoffman, R. H., 1988, *Solids and Surfaces* (New York: VCM).

[2] Shustorovich, E. M. (editor), 1991, *Metal–Surface Reaction Energetics: Theory and Applications to Heterogeneous Catalysis, Chemisorption and Surface Diffusion* (New York: VCH); Ruette, F., (editor), 1992, *Quantum Chemistry Approaches to Chemisorption and Heterogeneous Catalysis* (Dordrecht: Kluwer).

[3] Pacchioni, G., Bagus, P. S., and Parmigiani, F. (editors), 1992, *Cluster models for Surface and Bulk Phenomena*, NATO Series, Vol. 283 (New York: Plenum); Pacchioni, G., and Bagus, P. S., 1993, *Elementary Reaction Steps in Heterogeneous in Catalysis*, edited by R. Joyner and R. Van Santen, NATO Advanced Study Institute series C (Dordrecht: Kluwer); van Santen, R. A., and Neurock, M., 1995, *Catal. Rev.—Sci. Engng*, **37**, 557.

[4] Ruette, F. (editor), 1992, *Quantum Chemistry Approaches to Chemisorption and Heterogeneous Catalysis* (Dordrecht: Kluwer) (Boston, Massachusetts: Academic Press); van Santen, R. A., 1991, *Theoretical Heterogeneous Catalysis* (Singapore: World Scientific); Moffat, J. R. (editor), 1994, *Theoretical Aspects of Heterogeneous Catalysis* (New York: Wiley); van Santen, R. A., and Niemantsverdrict, J. W., 1995, *Chemical Kinetics and*

Catalysis (New York: Plenum); Davis, M. F. (editor), 1993, *Selectivity in Catalysis* (Washington, DC: American Chemical Society); White, M. G., 1990, *Heterogeneous Catalysis* (Englewood Cliffs, New Jersey: Prentice-Hall).

[5] Somorjai, G. A., 1994, *Introduction to Surface Chemistry and Catalysis* (New York: Wiley); Yoshida, S., Sakaki, S., and Kobayashi, H., 1994, *Electronic Processes in Catalysis, a Quantum Chemical Approach to Catalysis* (Tokyo: Kodanssha) (New York: VCH); Thomas, J. M., and Thomas, W. J., 1997, *Principles and Practice of Heterogeneous Catalysis* (New York: VCH); Ertl, G., Knozinger, H., and Weitkamp, J. (editors), 1997, *Handbook of Heterogeneous Catalysis* (Weinheim: Wiley–VCH); Augustine, R. L., 1996, *Heterogeneous Catalysis for the Synthetic Chemist* (New York: Marcel Dekker); Moulijn, J. A., van Leewen, P. W. N. M., and van Santen, R. A. (editors), 1993, *An Integrated Approach to Homogeneous, Heterogeneous and Industrial Catalysis* (Amsterdam: Elsevier).

[6] Joyner, R. W., and van Santen, R. A. (editors), 1993, *Elementary Reaction Steps in Heterogeneous Catalysis* (Dordrecht: Kluwer); Ruette, F. (editor), 1992, *Quantum Chemistry Approaches to Chemisorption and Heterogeneous Catalysis* (Dordrecht: Kluwer).

[7] Piet, W. N. M., van Leeuwen, P. W. N. M., Morokuma, K, and van Lenthe, J. H. (editors), 1995, *Theoretical Aspects of Homogeneous Catalysis: Applications Ab Initio Molecular Orbital theory* (Dordrecht: Kluwer); Thomas, J. M., and Thomas, W. J., 1994, *Principles and Practice of Heterogeneous Catalysis* (Weinheim: VCH); Augustine, R. L., 1996, *Heterogeneous Catalysis for the Synthetic Chemist* (New York: Marcel Dekker); Moulijn, J. A., van Leeuwen, P. W. N. M, and van Santen, R. A. (editors), 1993, *An Integrated Approach to Homogeneous, Heterogeneous and Industrial Catalysis* (Amsterdam: Elsevier); Joyner, R. W., and van Santen, R. A. (editors), 1993, *Elementary Reaction Steps in Heterogeneous Catalysis* (Dordrecht: Kluwer); Shustorovich, E. (editor), 1991, *Metal–Surface Reaction Energetics: Theory and Applications to Heterogeneous Catalysis, Chemisorption and Surface Diffusion* (New York: VCH).

[8] Blaster, H. U. (editor), 1996, *Proceedings of the Fourth International Symposium on Heterogeneous Catalysis and Fine Chemicals*, Basel, Switzerland, 8–12 September 1996 (Amsterdam: Elsevier); Froment, G. C., and Waugh, K. C. (editors), 1997, *Proceedings of the International Symposium on Dynamics of Surfaces and Reaction Kinetics in Heterogeneous Catalysis*, 15–17 September 1997 (Amsterdam: Elsevier).

[9] Pavão, A. C., Taft, C. A., Guimarães, T. C., and Lester, W. A. Jr, 1994, *Trends chem. Phys.*, **3**, 109, and references therein; Pavao, A. C., Guimarães, T. C., Taft, C. A., and Lester, W. A., Jr, 1999, *Theochem*, **458**, 99; Almeida, A. L., Martins, J. B. L., Taft, C. A., Longo, E., and Lester, W. A., Jr, 1998, *J. chem. Phys.*, **109**, 3671; 1999, *ibid.*, *Int. J. quant. Chem.*, **71**, 153; Taft, C. A., Longo, E., Andres, J., and Lie, S. K., 1998, *J. molec. Struct.*, **426**, 199.

[10] Norskov, J. K., 1992, *Prog. Surf. Sci.*, **38**, 103; Hoffmann, R., 1988, *Solids and Surfaces* (New York: VCM); Albright, T. A., Burdett, J. K., and Whangbo, M. H., 1985, *Orbital Interactions in Chemistry* (New York: Wiley); Baerends, E. J., 1992, *Cluster Models for Surface and Bulk Phenomena*, NATO Advanced Study Institute Series, Series B, Vol. 283, edited by G. Pacchioni and P. Bagus (New York: Plenum); Norskov, J. K., and Lang, N. D., 1980, *Phys. Rev.* B, **21**, 2136; 1982, *ibid.*, **26**, 2875.

[11] Slater, J. C., 1974, *The Self Consistent Field for Molecules and Solids: Quantum Theory of Molecules and Solids* (New York: McGraw-Hill); 1951, *Phys. Rev.*, **81**, 385; 1972, *Adv. quant. Chem.*, **6**, 1; Johnson, K. H., and Messner, R. P., 1976, *Int. J. quant. Chem. Symp.*, **10**, 47; Johnson, K. H., 1973, *Adv. quant. Chem.*, **7**, 143.

[12] Shustorovich, E. M., 1986, *Surf. Sci. Rep.*, **6**, 1; 1990, *Adv. Catal.*, **37**, 101; Shustorovich, E. M., and Bell, A. T., 1992, *Surf. Sci.*, **268**, 397; Sellers, H., 1994, *Surf. Sci.*, **310**, 281.

[13] Hoffmann, R., 1963, *J. chem. Phys.*, **19**, 1397; 1988, *Rev. mod. Phys.*, **60**, 101; 1987; *Angew. Chem., Int. Edn Engl.*, **26**, 846; Hoffmann, R., and Lipscomb, W. N., 1962, *J. chem. Phys.*, **36**, 2179; 1962, *ibid.*, **37**, 2872; Anderson, A. B., and Hoffmann, R. W., 1974, *J. chem. Phys.*, **60**, 4271; Anderson, A. B., and Nichols, J. A., 1986, *J. Am. chem. Soc.*, **108**, 1385; Anderson, A. B., 1976, *Inorg. Chem.*, **15**, 2598; Anderson, A. B., and Maloney, J. J., 1988; *J. phys. Chem.*, **92**, 809; Kang, D. B., and Anderson, A. B., 1985, *J. Am. chem. Soc.*, **107**, 7858; Anderson, A. B., McDevitt, M. R., and Urbach, F. L., 1984, *Surf. Sci.*, **146**, 80; Anderson, A. B., Grimes, R. W., and Hond, S. Y., 1987, *J. phys. Chem.*, **91**, 4245.

[14] Dewar, M. J. S., and Thiel, W., 1977, *J. Am. chem. Soc.*, **99**, 4899; Dewar, M. J. S., Zoebisch, E. G., Healy, E. F., and Stewart, J. P., 1985, *J. Am. chem. Soc.*, **107**, 3902; Stewart, J. J. P., 1989, *J. comput. Chem.*, **10**, 209; Holder, A. J., 1977, AMPAC, Semichem Company; Lipkowitz, K. B., and Boyd, D. B. (editors), 1992, *Reviews in Computational Chemistry* (New York: VCH); Fraga, F., 1992, *Computational Chemistry: Structure, Interactions and Reactivity* (Amsterdam: Elsevier).

[15] Riddley, J., and Zerner, M., 1973, *Theor. Chim. Acta*, **32**, 111; Bacon, D., and Zerner, M. C., 1979, *Theor. Chim. Acta*, **53**, 21; Zerner, M. C., Loew, G. H., Kirchner, R. F., and Mueller-Westerhoff, U. T., 1989, *J. Am. Chem. Soc.*, **102**, 589; Zerner, M., and Salahub, D. R. (editors), 1989, *The Challenge of d and f Electrons: Computation and Theory*, American Chemical Society Symposium Series, Vol. 394 (New York: American Chemical Society).

[16] Bauschlicher, C. W., Jr, 1974, *J. chem. Phys.*, **101**, 3250; Bauschlicher, C. W., Walch, S. P., and Bauschlicher, C. W., Jr, 1985, *Comparison of Ab Initio Quantum in Chemistry with Experiment*, edited by R. Bartlett (Boston, Massachusetts: Reidel); Langhoff, S. R., and Bauschlicher, C. W., Jr, 1986, *Chem. Phys. Lett.*, **124**, 251; Lawley, P. (editor), 1987, *Ab Initio Methods in Quantum Chemistry* (New York: Wiley); Sellers, H., and Golab, J. T. (editors), 1994, *Theoretical and Computational Approaches to Interface Phenomena*.

[17] Ahlrichs, D. R., Scharf, P., and Ehrhardt, C., 1985, *J. chem. Phys.*, **82**, 890; Chong, D. P., and Langhoff, S. R., 1986, *J. chem. Phys.*, **84**, 5606; Szabo, A., and Ostlund, N. S., 1992, *Modern Quantum Chemistry: an Introduction to Advanced Electronic Structure Theory* (London: Macmillan); Balasubramanian, K., Feng, P. Y., and Liao, M. Z., 1987, *J. chem. Phys.*, **87**, 3981.

[18] Harris, S., 1982, *Chem. Phys.*, **67**, 229; Harris, S., and Chianelli, R. R., 1984, *J. Catal.*, **86**, 400.

[19] Parr, R. G., and Yang, W., 1989, *Density Functional Theory of Atoms and Molecules* (Oxford University Press); Thomas, L. H., 1989, *Proc. Camb. Phil. Soc.*, **26**, 376; Fermi, E., 1926, *Z. Phys.*, **48**, 542; Hohenberg, P., and Kohn, W., 1994, *Phys. Rev.*, **136**, B864; Kohn, W., and Sham, L. J., 1965, *Phys. Rev.*, **140**, A1133; Ziegler, T., 1991, *Chem. Rev.*, **91**, 651; Labanowski, J., and Andzelm, J. (editors), 1991, *Density Functional Methods in Chemistry* (New York: Springer).

[20] Dovesi, R., Pisani, C., Roetti, C., and Silvi, B., 1987, *J. chem. Phys.*, **86**, 6967; Dovesi, R., Pisani, C., Roetti, C., and Saunders, V. R., 1987, *Phys. Rev.* B, **28**, 5781; 1994, Thompson, M. R., Hess, A. C., Nicholas, J. B., White, J. C., Anchell, J., and Ebner, X., in *New Developments in Selective Oxidation* II (Amsterdam: Elsevier) p. 167; Jaffe, J. E., and Hess, A. C., 1993, *Condens. Mater.*, **48**, 7903; Velde, G., and Baerends, E. J., 1993, *Chem. Phys.*, **177**, 399; Feibelman, P. J., 1991, *Phys. Rev. Lett.*, **67**, 461; Boettger, J. C., 1993, *Int. J. quant. Chem., quant. Chem. Symp.*, **27**, 147; Hammer, B., Jacobsen, K. W., and Norskov, J. K., 1992, *Phys. Rev. Lett.*, **69**, 1971; Rovoredo Chacon-Taylor, M., and McCarthy, M. I., 1996, *J. phys. Chem.*, **100**, 7610.

[21] Cox, D. M., Kaldor, A., Fayet, P., Eberhardt, W., Brickman, R., Sherwood, R., Fu, Z., and Sondericher, D., 1990, *Novel Materials in Heterogeneous Catalysis*, American Chemical Society Symposium Series, Vol. 437 (New York: American Chemical Society), p. 172; Kaldor, A., and Cox, D. M., 1990, *Pure appl. Chem.*, **62**, 79; Cox, D. M., Zakin, M. R., and Kaldor, A., 1987, *Physical Chemistry of Small Clusters*, NATO Advanced Study Institute Series, Vol. 158, p. 741; Estiu, G. L., and Zerner, M. C., 1994, *J. phys. Chem.*, **98**, 9972; Russier, V., Salahub, D. R., and Mijoule, C., 1992, *J. phys. Chem.*, **96**, 7579; Madlowen, P., and Whitten, J., 1982, *J. chem. Phys.*, **77**, 2673; Blomberg, M. R., Siegbahn, P. E. M., Nagashima, K., and Wennerberg, J., 1991, *J. Am. chem. Soc.*, **113**, 424; Biemolt, W., Kerkhof, G. J. C. S., Davies, P. R., Jansen, A. P. J., and van Santen, R. A., 1992, *Chem. Phys. Lett.*, **188**, 477.

[22] Siegbahn, P. E. M., and Wahlgren, U., 1992, *Int. J. quant. Chem.*, **42**, 1149; Madlowen, P., and Whitten, J., 1982, *J. chem. Phys.*, **77**, 2673; Blomberg, M. R., Siegbahn, P. E. M., Nagashima, K., and Wennerberg, 1991, *J. Am. chem. Soc.*, **113**, 424.

[23] Upton, T. H., and Goddard, W. A., 1981, *CRC Crit. Rev. Solid St. Mater. Sci.*, **10**, 261.

[24] Bagus, P. S., Nelin, C. J., Bauschlicher, C. W., Jr, 1983, *J. chem. Phys.*, **28**, 5423.

[25] Hermann, K., Bagus, P. S., and Nelin, C. J., 1987, *Phys. Rev.* B, **35**, 9467.

[26] Panas, I., Schule, I., Siebahn, P. E. M., and Whalgren, U., 1988, *Chem. Phys. Lett.*, **149**, 265.

[27] Lester, W. A., 1997, *Recent Advances in Quantum Monte Carlo Methods–Recent Advances in Computational Chemistry*, Vol. 2 (Singapore: World Scientific); Ceperley, D. M., and Mitas, L., 1996, *Adv. chem. Phys.*, **93**,1; Anderson, J. B., 1995, *Int. Rev. Phys. chem.*, **14**, 85; Hammond, B. L., Lester, W. A., Jr, and Reynolds, P. J., 1994, *Monte Carlo Methods in Ab Initio Quantum Chemistry* (Singapore: World Scientific).

[28] Blyholder, G., 1964, *J. phys. Chem.*, **68**, 2772.

[29] Sung, S., and Hoffmann, R., 1985, *J. Am. chem. Soc.*, **107**, 578.

[30] Guimaraes, T. C., Pavão, A. C., Taft, C. A., and Lester, W. A., Jr, 1997, *Phys. Rev.* B, **56**, 7001.

[31] Pavão, A. C., Braga, M., Taft, C. A., Hammond, B. L., and Lester, W. A., Jr, 1991, *Phys. Rev.*, **44**, 1910.

[32] Pavão, A. C., Braga, M., Taft, C. A., Hammond, B. L., and Lester, W. A., Jr, 1991, *Phys. Rev.* B, **43**, 6962.

[33] Pavão, A. C., Soto, M. M., Lester, W. A., Jr, Lie, S. K., Hammond, B. L., and Taft, C. A., 1994, *Phys. Rev.* B, **50**, 1868.

[34] Pavão, A. C., Hammond, B. L., Soto, M. M., Lester, W. A., Jr, and Taft, C. A., 1995, *Surf. Sci.*, **323**, 340.

[35] Guimaraes, T. C., Pavão, A. C., Taft, C. A., and Lester, W. A., Jr, 1999, *Phys. Rev.* B, (in the press).

[36] Heinzmann, U., Holloway, S., Kleyn, A. W., Plamer, R. E., and Snowdon, K. J., 1996, *J. Phys.: condens. Matter*, **8**, 3245, and references therein.

[37] Cotton, F. A., and Kraihanzel, C. S., 1962, *Inorg. Chem.*, **84**, 4432.

[38] Grunze, M., Golze, M., Hirschwald, W., Freund, H. J., and Pulm, H., Seip, U., Tsai, M. C., Ertl, G., and Kuppers, J., 1984, *Phys. Rev. Lett.*, **53**, 850.

[39] Bernasek, S. L., 1993, *A. Rev. phys. Chem.*, **44**, 265.

[40] Bozso, F., Ertl, G., Grunze, M., and Wiss, M., 1977, *J. Catal.*, **49**, 189.

[41] Spencer, N. D., Schoonmaker, R. C., and Somorjai, G. A., 1982, *J. Catal.*, **74**, 129.

[42] Moon, D. W., Dwyer, D. J., and Bernasek, S. L., 1985, *Surf. Sci.*, **163**, 215.

[43] Benziger, J., and Madix, R. J., 1980, *Surf. Sci.*, **94**, 199.

[44] Shinn, N. D., and Madey, T. E., 1985, *J. chem. Phys.*, **83**, 5928.

[45] Shinn, N. D., and Madey, T. E., 1986, *Phys. Rev.* B, **33**, 1464.

[46] Shinn, N. D., 1988, *Phys. Rev.* B, **38**, 12248.

[47] Dowben, P. A., Ruppender, H. J., and Grunze, M., 1991, *Surf. Sci. Lett.*, **254**, L482.

[48] (a) Brodén, G., Rhodin, T. N., Brucker, C., Benbrow, B., and Hurych, Z., 1976, *Surf. Sci.*, **59**, 593; (b) Andreoni, W., and Varma, C. M., 1981, *Phys. Rev.* B, **23**, 4379.

[49] Hoffmann, R., Chen, M. M. L., and Thorn, D. L., 1997, *Inorg. Chem.*, **16**, 503; Huber, R., Epp, O., and Formanek, H., 1970, *J. molec. Biol.*, **52**, 349; Norvell, J. C., Nunes, A. C., and Schoenborn, B. P., 1975, *Science*, **190**, 568.

[50] Pauling, L., 1984, *Solid St. Chem.*, **54**, 297.

[51] Heskett, D., Plummer, E. W., and Messmer, R. P., 1984, *Surf. Sci.*, **139**, 558.

[52] Kishi, K., and Roberts, M. W., 1975, *J. chem. Soc., Faraday Trans. I*, **71**, 1715; Mehandru, S. P., and Anderson, A. B., 1986, *Surf. Sci. Lett.*, **169**, L281.

[53] Yoshida, K., and Somorjai, G. A., 1978, *Surf. Sci.*, **75**, 46; Jensen, E. S., and Rhodin, T. N., 1983, *Phys. Rev.* B, **27**, 3338; Moon, D. W., Dwyer, D. J., and Bernasek, S. L., 1985, *Surf. Sci.*, **163**, 215; Moon, D. W., Bernasek, S. L., Dwyer, D. J., and Gland, J. L., 1985, *J. Am. chem. Soc.*, **107**, 4363; Moon, D. W., Cameron, S., Zaera, F., Eberhardt, W., Carr, R., Bernasek, S. L., Gland, J. L., and Dwyer, D. J., 1987, *Surf. Sci.*, **180**, L123; Moon, D. W., Bernasek, S. L., Lu, J. P., Gland, J. L., and Dwyer, D. J., 1987, *Surf. Sci.*, **184**, 90.

[54] Benziger, J., and Madix, R. J., 1980, *Surf. Sci.*, **94**, 119.

[55] Seip, U., Tsai, M. C., Christmann, K., Kuppers, J., and Ertl, G., 1984, *Surf. Sci.*, **139**, 29.

[56] Gonzalez, L., Miranda, R., and Ferrer, N. D. S., 1982, *Surf. Sci.*, **119**, 61; Erley, W., 1981, *J. vacuum Sci. Technol.*, **18**, 472.

[57] Shinn, N. D., and Madey, T. E., 1985, *J. chem. Phys.*, **83**, 52928.

[58] PASSLER, M., IGNATIEV, A., JONA, F., JEPSEN, D. W., and MARCUS, P. M., 1979, *Phys. Rev. Lett.*, **43**, 360.
[59] HEINZ, K., LANG, E., and MULLER, K., 1979, *Surf. Sci.*, **87**, 5959.
[60] TONG, S. Y., MALDONADO, A., LI, C. H., and VAN HOVE, M. A., 1980, *Surf. Sci.*, **94**, 73.
[61] ANDERSSON, S., and PENDRY, J. B., 1980, *J. Phys.* C, **94**, 3547.
[62] LAUTERBACH, J., WITTMANN, M., and KUPPERS, J., 1992, *Surf. Sci.*, **279**, 287.
[63] STOHR, J., and JAEGER, R., 1982, *Phys. Rev.* B, **26**, 4111.
[64] KEVAN, S. D., DAVIS, R. F., ROSENBLATT, D. H., TOBIN, J. G., and MASON, M. G., SHIRLEY, D. A., LI, C. H., and TONG, S. J., 1981, *Phys. Rev. Lett.*, **46**, 1629; ANDERSSON, S., 1977, *Solid St. Commun.*, **21**, 75.
[65] BERTOLINI, J. C., and TARDY, B., 1981, *Surf. Sci.*, **102**, 12.
[66] BIBERIAN, J. B., and VAN HOVE, M. A., 1982, *Surf. Sci.*, **118**, 443.
[67] KLAUSER, R., SPIESS, W., BRADSHAW, A. M., and HAYDEN, B. E., 1986, *J. Electron Spectrosc. Relat. Phenomena*, **38**, 187.
[68] PETERSSON, L. G., KONO, S., HALL, N. F. T., FADLEY, C. S., and PENDRY, J. B., 1979, *Phys. Rev. Lett.*, **42**, 1545.
[69] CHANG, S., TOBIN, R. G., RICHARDS, P. L., and THIEL, P. A., 1974, *Phys. Rev. Lett.*, **52**, 648.
[70] TANG, S. L., BECKERLE, J. D., LEE, M. B., and CEYER, S. T., 1986, *J. chem. Phys.*, **84**, 6488.
[71] STEINRUCH, H. P., WINKLER, A., and RENDULIC, K. D., 1985, *Surf. Sci.*, **152**, 323.
[72] HINES, M. A., and ZARE, R. N., 1993, *J. chem. Phys.*, **98**, 9134.
[73] MILLER, J. B., SIDDIQUI, H. R., GATES, S. M., RUSSEL, J. N., Jr, YATES, J. T., Jr, TULLY, J. C., and CARDILLO, M. J., 1987, *J. chem. Phys.*, **87**, 6725.
[74] CAPUTI, L. S., AGOSTINO, R. G., AMODDEO, A., and COLAVITA, E., 1993, *Surf. Sci.*, **282**, 62.
[75] WESNER, D. A., COENEN, F. P., and BONZEL, H. P., 1989, *Phys. Rev.* B, **39**, 10770.
[76] SURNEV, L., XU, Z., and YATES, J. T., Jr, 1988, *Surf. Sci.*, **201**, 1.
[77] MARUCA, R., KUSUMA, T., HICKS, V., and COMPANION, A., 1990, *Surf. Sci.*, **236**, 210.
[78] DRAKOVA, D., and DOYEN, G., 1990, *Surf. Sci.*, **226**, 285.
[79] ALLISON, J. N., and GODDAD, W. A., III, 1982, *Surf. Sci.*, **115**, 553.
[80] BAUSCHLICHER, C. W., Jr, BAGUS, P. S., NELIN, C. J., and ROOS, B. O., 1986, *J. chem. Phys.*, **85**, 354.
[81] RAATZ, F., and SALAHUB, D. R., 1985, *Surf. Sci.*, **156**, 982.
[82] ROSEN, A., BAERENDS, E. J., and ELLIS, D. E., 1979, *Surf. Sci.*, **82**, 139.
[83] MELE, F., RUSSO, N., and TOSCANO, M., 1994, *Surf. Sci.*, **307**, 113.
[84] NORSKOV, J. K., HOLLOWAY, S., and LANG, N. D., 1984, *Surf. Sci.*, **137**, 65.
[85] RHODIN, T. N., and BRUCKER, C. F., 1977, *Solid St. Commun.*, **23**, 275.
[86] KISKINOVA, M., and GOODMAN, D. W., 1981, *Surf. Sci.*, **108**, 64.
[87] KO, E. J., and MACIX, R. J., 1981, *Surf. Sci.*, **109**, 221.
[88] PACCHIONI, G., and BAGUS, P. S., 1993, *Chem. Phys.*, **177**, 373.
[89] SCHULTZ, P. A., 1990, *J. vacuum Sci. Technol.* A, **8**, 2525.
[90] ANGEVAARE, P. A. J., HENDRICKS, H. A. C. M., and PONEC, V., 1988, *J. Catal.*, **110**, 11.
[91] PIRUG, G., and BONZEL, H., 1988, *Surf. Sci.*, **199**, 371.
[92] DUBOIS, L. H., ZEGARSKI, B. R., and LUFTMAN, H. S., 1987, *J. chem. Phys.*, **87**, 1367.
[93] GORLING, A., ACKERMANN, L., LAUBER, J., KNAPPE, P., and ROSCH, N., 1993, *Surf. Sci.*, **286**, 26.
[94] ROSCH, N., GORLING, A., KNAPPE, P., and LAUBER, J., 1990, *Vacuum*, **41**, 150.
[95] KATSUKI, S., SAKAI, Y., and MIYOSHI, E., 1989, *Surf. Sci.*, **220**, 181.
[96] RODRIGUEZ, J. A., and CAMPBELL, C. T., 1987, *J. phys. Chem.*, **91**, 2161.
[97] BONZEL, H. P., 1987, *Surf. Sci. Rep.*, **8**, 43.
[98] LUFTMAN, H. S., and WHITE, J. M., 1984, *Surf. Sci.*, **139**, 369.
[99] WEIMER, J. J., UMBACH, E., and MENZEL, D., 1985, *Surf. Sci.*, **155**, 133.
[100] MIYOSHI, E., SAKAI, Y., and KATSUKI, S., 1991, *Surf. Sci.*, **242**, 531.
[101] EBERHARDT, W., HOFFMANN, F. M., DE PAOLA, R., HESKETT, D., STRATHY, I., PLUMMER, E. W. L., and MOSER, H. R., 1985, *Phys. Rev. Lett.*, **54**, 1856.
[102] PACCHIONI, G., and BAGUS, P. S., 1989, *Phys. Rev.* B, **40**, 6003.
[103] PAUL, J., 1986, *Nature*, **323**, 1701.
[104] PACCHIONI, G., and BAGUS, P. S., 1990, *J. chem. Phys.*, **93**, 1209.
[105] RUCKMAN, M. W., and STRONGIN, M., 1994, *Accts Chem. Res.*, **27**, 250.

[106] Romeo, R., Majerus, J., Légaré, P., Castellani, N. J., and Leroy, D. B., 1990, *Surf. Sci.*, **238**, 163.
[107] Pick, S., 1996, *Surf. Sci.*, **352**, 300.
[108] Pangher, N., Wilde, L., and Haase, J., 1996, *Chem. Phys. Lett.*, **255**, 378.
[109] Watanabe, K., Ohnuma, H., Uetsuka, H., and Kunimori, K., 1966, *Surf. Sci.*, **368**, 366.
[110] Kunimori, K., Uetsuka, H., Iwade, T., and Ito, S., 1993, *Surf. Sci.*, **283**, 58.
[111] Ohno, Y., Matsushima, T., and Uetsuka, H., 1994, *J. chem. Phys.*, **101**, 5319.
[112] Gordon, M. H., and Tully, J. C., 1993, *Chem. Phys.*, **175**, 37.
[113] Morin, M., Levinos, N. J., and Harris, A. L., 1992, *J. chem. Phys.*, **96**, 3950.
[114] Sutcu, L. F., White, H. W., and Wragg, J. L., 1991, *Surf. Sci. Lett.*, **249**, L343.
[115] Finlay, R. J., Hua Her, T., Wu, C., and Mazur, E., 1997, *Chem. Phys. Lett.*, **274**, 499.
[116] Tully, J. C., and Gomez, M., 1993, *J. vac. Sci. Technol.* A, **11**, 1914.
[117] Yang, H., Whitten, J. L., Huberty, J. S., and Madix, R. J., 1997, *Surf. Sci.*, **375**, 268.
[118] Bagus, P. S., and Pacchioni, G., 1990, *Surf. Sci.*, **236**, 233.
[119] Holloway, S., and Norskov, J. K., 1984, *J. Electroanal. Chem.*, **161**, 193.
[120] Roy, D., and Furtak, T. E., 1986, *Chem. Phys. Lett.*, **139**, 501.
[121] Lambert, D. K., 1988, *J. chem. Phys.*, **89**, 3847, and references therein.
[122] Korzeniewski, C., Pons, S., Schmidts, P. P., and Severson, W. M., 1986, *J. chem. Phys.*, **85**, 4153.
[123] Sellidj, A., and Koel, B. E., 1994, *Phys. Rev.* B, **49**, 8367.
[124] Rodriguez, J. A., and Goodman, D. W., 1992, *Science*, **257**, 897.
[125] Heitzinger, J. M., Gebhard, S. C., Parker, D. H., and Koel, B. E., 1992, *Surf. Sci.*, **260**, 151.
[126] Zhao, Y. B., and Gomer, R., 1990, *Surf. Sci.*, **239**, 189.
[127] Sandell, A., Libuda, J., Bruhwillelr, P. A., Andersson, S., Maxwell, A. J., Martensson, N., and Freund, H. J., 1997, *Phys. Rev.* B, **55**, 7233.
[128] Matsushima, T., Akiyama, H., Lesar, A., Sugimura, H., Torre, G. E. D., Yamanaka, T., and Ohno, Y., 1997, *Surf. Sci.*, **386**, 24.
[129] Beutler, A., Lundgren, E., Nyholm, R., Andersen, J. N., Setlik, B., and Heskett, D., 1997, *Surf. Sci.*, **371**, 381.
[130] Borup, R. L., Sauer, D. E., and Stuve, E. M., 1997, *Surf. Sci.*, **374**, 152.
[131] Zaera, F., Lui, J., and Xu, M., 1997, *J. chem. Phys.*, **106**, 41 204.
[132] Yoshimi, K., Bong Song, M., and Ito, M., 1996, *Surf. Sci.*, **368**, 389.
[133] Tanaka, K., 1996, *Surf. Sci.*, **357**, 721.
[134] Lu, S. H., Yao, J., Zhu, L., Liu, G. L., Liu, F. Q., and Wu, S. C., 1992, *Phys. Rev.* B, **45**, 6142.
[135] Cook, J. C., and McCash, E. M., 1997, *Surf. Sci.*, **371**, 213.
[136] Illas, F., Rubio, J., Souosa, C., Povill, A., Zurita, S., Fernandez-Garcia, M., Ricart, J. M., Clotet, A., and Casanovas, J., 1996, *J. molec. Struct.* (*Theochem.*), **371**, 257.
[137] Ohnishi, S., and Watasi, N., 1996, *Phys. Rev.* B, **49**, 14 619.
[138] Beutl, M., Rendulic, K. D., and Castro, G. R., 1997, *Surf. Sci.*, **385**, 1106; Zasada, I., Hansali, G., LeBosse, J. C., and Lopez, J., 1997, *Surf. Sci.*, **383**, 241; Illas, F., Zurita, S., Marquez, A. M., and Rubio, J., 1997, *Surf. Sci.*, **376**, 279; Smirnov, K. S., and Raseev, G., 1997, *Surf. Sci.*, **384**, L975.
[139] Skelton, D. C., Wei, D. H., and Kevan, S. D., 1997, *Surf. Sci.*, **370**, 64; Morikawa, Y., Mortensen, J. J., Hjammer, B., and Norskov, J. K., 1997, *Surf. Sci.*, **386**, 67; Bertino, M. F., and Witte, G., 1997, *Surf. Sci.*, **385**, L984; Ramsey, M. G., Leisenberger, F. P., Netzer, F. P., Roberts, A. J., and Raval, R., 1997, *Surf. Sci.*, **385**, 207.
[140] Wei, D. H., Skelton, D. C., and Kevan, S. D., 1997, *Surf. Sci.*, **381**, 49; Snabl, M., Borusik, O., Chab, V., Ondrejcek, M., Stenzel, W., Conrad, H., and Bradshaw, A. M., 1997, *Surf. Sci.*, **385**, 11 016.
[141] Hammer, B., Morikawa, Y., and Norskov, J. K., 1996, *Phys. Rev. Lett.*, **76**, 2141.
[142] Ruban, A., Hammer, B., Stoltze, P., Skriver, H. L., and Norskov, J. K., 1997, *J. molec. Catal.* A, **115**, 421.
[143] Mortensen, J. J., Morikawa, Y., Hammer, B., and Norskov, J. K., 1997, *Z. phys. Chem.*, **198**, 113.
[144] Hammer, B., Nielsen, O. H., and Norskov, J. K., 1997, *Catal. Lett.*, **46**, 31.

[145] Hammer, B., and Norskov, J. K., 1997, NATO Advanced Study Institute Series, Series E, Vol. 331, edited by R. Lambert and G. Pacchioni (Dordrecht: Kluwer).

[146] Harl, H., Mendel, K., Metka, U., Volpp, H. R., Willms, L., and Wolfrum, J., 1997, *Chem. Phys. Lett.*, **279**, 275.

[147] Fichtner-Endruschat, and De Renzi, V., Morgante, A., Schwegmann, S., Bludau, H., Schuster, R., Bottcher, A., and Over, H., 1998, *J. chem. Phys.*, **108**, 774.

[148] Bonicke, I. A., Thieme, F., and Kirstein, W., 1998, *Surf. Sci.*, **395**, 138.

[149] Delbecq, F., Moraweck, B., and Verite, L., 1998, *Surf. Sci.*, **396**, 156.

[150] Behm, R. J., 1997, *Acta Phys. Polonica* A, **93**, 260.

[151] Onsgaard, J., Godowski, P. J., Nerlov, J., Quist, S., and Hoffmann, S. V., 1997, *Surf. Sci.*, **398**, 318.

[152] Matolin, V., and Stará, I., 1998, *Surf. Sci.*, **398**, 117.

[153] Ladas, S., Poppa, H., and Boudart, M., 1981, *Surf. Sci.*, **102**, 151.

[154] Matolin, V., and Gillet, E., 1986, *Surf. Sci.*, **166**, L115.

[155] Rumpf, F., Poppa, H., and Boudart, M., 1988, *Langmuir*, **4**, 722.

[156] Boudart, M., 1996, *Adv. Catal.*, **20**, 153.

[157] Sakakini, B. H., and Verbrugge, A. S., 1997, *J. chem. Soc., Faraday Trans.*, **93**, 1637.

[158] Pick, S., 1998, *Phys. Rev.* B, **57**, 1942; Xu, C., and Koel, B., 1995, *Surf. Sci.*, **327**, 38.

[159] Snabl, Borusik, O., Chab, V., Ondrejcek, M., Stenzel, W., Conrad, H., and Bradshaw, A. M., 1997, *Surf. Sci. Lett.*, **486**, L1016.

[160] Godowski, P. J., Onsgaard, J., Christensen, S. V., and Nerlov, J., 1996, *Acta Phys. Polonica* A, **89**, 657.

[161] Rochefort, A., Abon, M., Delichere, P., and Bertolini, J. C., 1993, *Surf. Sci.*, **294**, 43 and references therein.

[162] Kawai, M., and Yoshinobu, J., 1996, *Surf. Sci.*, **368**, 239.

[163] (a) Jackson, S. D., and Munro, N. H. S., 1998, *J. chem. Soc., Faraday Trans.*, **84**, 955; (b) Aizawa, H., and Tsuneyuki, S., 1998, *Surf. Sci.*, **399**, L364; (c) Wong, Y. T., and Hoffmann, R., 1991, *J. phys. Chem.*, **95**, 859; (d) Nilsson, A., Wassdahl, N., Weinelt, M., Karis, O., Wiell, T., Bennich, P., Hasselstrom, J., Fohlish, A., Stohr, J., and Samant, M., 1997, *Appl. Phys.* A, **65**, 147; (e) Zonneyville, M. C., Goerlings, J. J. C., Geerlings, J. J. C., and van Santen, R. A., 1994, *J. Catal.*, **148**, 417.

[164] Hasse, G., and Asscher, J., 1987, *Surf. Sci.*, **191**, 75.

[165] Wu, Y., and Cao, P.-L., 1987, *Surf. Sci.*, **179**, 26.

[166] Ibbotson, D. E., Wittrig, T. S., and Weiberg, W. H., 1981, *Surf. Sci.*, **110**, 313.

[167] Zhou, R.-H., Shi, D.-H., and Cao, P.-L., 1992, *J. Phys.: condens. Matter*, **4**, 2429.

[168] Heskett, D., Plummer, E. W., and Messmer, R. P., 1984, *Surf. Sci.*, **139**, 558.

[169] de Paola, R. A., Hoffmann, F. M., Heskett, D., and Plummer, E. W., 1987, *Phys. Rev.* B, **35**, 4236.

[170] Grunze, M., Golze, M., and Hirschwald, W., Freund, H. J., Pulm, H. J., Seip, U., Tsai, M., Ertl, G., and Kuppers, J., 1984, *Phys. Rev. Lett.*, **53**, 850.

[171] Tomanek, D., and Bennemann, K., 1988, *Phys. Rev.* B, **31**, 2488.

[172] Freund, H. J., Bartos, B., Messmer, R. P., Grunze, M., Kuhlenbeck, H., and Neumann, M., 1987, *Surf. Sci.*, **185**, 187.

[173] Fukuda, Y., and Nagosgi, M., 1988, *Surf. Sci.*, **203**, L651.

[174] Shinn, N. D., 1990, *Phys. Rev.* B, **41**, 9771.

[175] Dowben, P. A., Miller, A., Ruppender, H. J., and Grunze, M., 1988, *Surf. Sci.*, **193**, 336.

[176] Ertl, G., Lee, S. B., and Weiss, M., 1982, *Surf. Sci.*, **1148**, 527.

[177] Whitman, L. J., Bartosch, C. E., Ho, W., Strasser, G., and Grunze, M., 1986, *Phys. Rev. Lett.*, **56**, 1984.

[178] Whitman, L. J., Bartosch, C. E., and Ho, W., 1986, *J. chem. Phys.* **85**, 3688.

[179] Tsai, M. C., Seip, U., Bassignana, I. C., Kuppers, J., and Ertl, G., 1985, *Surf. Sci.*, **155**, 387.

[180] Haneman, D. H., 1997, *Surf. Sci.*, **375**, 71.

[181] Hooper, C. W., 1991, *Catalytic Ammonia Synthesis* (New York: Plenum), p. 253.

[182] Ertl, G., 1994, *Topics Catal*, **1**, 305.

[183] Spencer, N. D., Schoomaker, R. C., and Somorjai, G. A., 1982, *J. Catal.*, **74**, 129.

[184] Grunze, M., Golze, M., Fuhler, J., Neumann, M., and Schwarz, E., 1984, *Proceedings of the Eighth International Congress on Catalysis*, Vol. IV, Berlin, 1984, p. 133.

[185] Ertl, G., 1982, *CRC Crit. Rev. Solid St. Mater. Sci.*, 349.

[186] Grunze, M., Strasser, G., and Golze, M., 1987, *Appl. Phys.* A, **44**, 19.

[187] Dowben, P. A., Ruppender, H. J., and Grunze, M., 1991, *Surf. Sci. Lett.*, **254**, L482.

[188] Kuwahara, K., Fujisawa, M., Jo, M., Onchi, M., and Nishijima, M., 1988, *Surf. Sci.*, **207**, 17.

[189] Grunze, M., Driscoll, R. K., Burland, G. N., Cornish, J. C. L., and Pritchard, J., 1979, *Surf. Sci.*, **89**, 381.

[190] Ho, W., Willis, R. F., and Plummer, E. W., 1980, *Surf. Sci.*, **95**, 171.

[191] Parks, E. K., and Riley, S. J., 1995, *Z. Phys.* D, **23**, 59.

[192] Bozso, F., Ertl, G., Grunze, M., and Weiss, M., 1977, *J. Catal.*, **43**, 18.

[193] Arumainayagam, C. R., Triupa, C. E., Xu, J., and Yates, J. T., Jr, 1996, *Surf. Sci.*, **360**, 121.

[194] Stohr, J., and Jaeger, G., 1987, *Phys. Rev.* B, **26**, 4111.

[195] Franchy, R., and Bartke, T. U., 1995, *Surf. Sci.*, **322**, 95.

[196] Seets, D. C., Wheeler, M. C., and Mullins, C. B., 1996, *Chem. Phys. Lett.*, **257**, 280.

[197] Moler, E. J., Kellar, S. A., Huff, W. R. A., Hussain, Z., Zheng, Y., Hudson, E. A., Chen, Y., and Shirley, D. A., 1997, *Chem. Phys. Lett.*, **264**, 502.

[198] Schlatholter, T., Schlatholter, T., Vicanek, M., and Heiland, W., 1996, *Surf. Sci.*, **352**, 195.

[199] Sitz, G. O., Andrew, Kummel, C., Zare, R. N., and Tully, J. C., 1988, *J. chem. Phys.*, **89**, 2573.

[200] Sotto, M., Gauthier, S., Pourmir, F., Rousset, S., and Klein, J., 1997, *Surf. Sci.*, **371**, 36.

[201] Leibsle, F. M., Flipse C. F. J., and Robinson, A. W., 1994, *Surf. Sci.*, **317**, 309.

[202] Bertino, M., Steinhogl, W., Range, H., Hofmann, F., Witte, G., Hulpke, E., and Woll, Ch., 1996, *Appl. Phys.* A, **62**, 95; Yoshinobu, J., Zenobi, R., Xu, J., Xu, Z., and Yates, J. T., Jr., 1991, *J. chem. Phys.*, **95**, 9393; Rao, C. N., and Ranga Rao, G., 1991, *Surf. Sci. Rep.*, **13**, 221; Varma, S., and Dowben, P. A., 1990, *J. vac. Sci. Technol.* A, **8**, 2605.

[203] Parks, K., Nieman, G. C.., Kerns, K. P., and Riley, S. J., 1997, *J. chem. Phys.*, **107**, 1861.

[204] Parks, E. K., Zhu, L., Ho, J., and Riley, S. J., 1998, *J. chem. Phys.*, **108**, 7206; *ibid.*, 1995, **102**, 7377.

[205] Sotto, M., Gauthier, S., Pourmir, F., Rousset, S., and Klein, J., 1997, *Surf. Sci.*, **371**, 36.

[206] Leibsle, F. M., and Robinson, A. W., 1993, *Phys. Rev.* B, **47**, 15 865.

[207] Zeng, H. C., Sodhe, R. N. S., and Mitchell, K. A. R., 1987, *Surf. Sci.*, **188**, 599.

[208] (a) Parks, E. K., Nieman, G. C., Kerns, K. P., and Riley, S. J., 1998, *J. chem. Phys.*, **108**, 3731; (b) Parks, E. K., Nieman, G. C., Kerns, K. P., and Riley, S. J., 1997, *J. chem. Phys.*, **1207**, 1861; (c) Bennich, P., Wiell, T., Karis, O., Weinelt, M., Wassdahl, N., Nilsson, A., Nyberg, M., Pettersson, L. G. M., Stohr, J., and Samant, M., 1998, *Phys. Rev.* B, **57**, 9274; (d) Minot, C., and Markovits, A., 1998, *J. molec. Struct.* (*Theochem.*), **424**, 119.

[209] (a) Culotta, E., and Koshland, D. E., Jr, 1992, *Science*, **258**, 1862; (b) van Daelen, M. A., Li, Y. S., Newsam, J. M., and van Santen, R. A., 1996, *J. phys. Chem.*, **100**, 2279; (c) Niewenhuys, B. E., 1983, *Surf. Sci.*, **126**, 307; (d) Smith, G., and Carter, E. A., 1991, *J. phys. Chem.*, **95**, 2327; (e) Ludviksson, A., Huang, C., Jansch, H. J., and Martin, R. M., 1993, *Surf. Sci.*, **284**, 328; (f) Duarte, H. A., and Salahub, D. R., 1997, *J. phys. Chem.* B, **101**, 7474.

[210] Root, T., Schmidt, L. D., and Fisher, G. B., 1983, *Surf. Sci.*, **134**, 30.

[211] Oh, S. H., Fisher, G. B., Carpenter, J. E., and Goodman, D. W., 1986, *J. Catal.*, **100**, 360.

[212] Shelef, M., and Graham, G. W., 1994, *Cal. Rev. Sci. Engng*, **36**, 433.

[213] Blanse, B., Wickham, D. T., and Koel, B. E., 1989, *J. Catal.*, **119**, 238.

[214] Fink, T., Dath, J. P., Basset, M. R., Imbihl, R., and Ertl, G., 1991, *Surf. Sci.*, **245**, 96.

[215] Thomas, J. L. C., Bauschlicher, C. W., Jr., and Hall, M. B., 1979, *J. Phys. Chem.*, **A101**, 8530.
[216] Conrad, H., Ertl, G., Kuppers, J., and Latta, E. E., 1975, *Surf. Sci.*, **50**, 296.
[217] Eastman, D. E., and Demuth, J. E., 1974, *Jap. J. appl. Phys., Suppl. 2, Part 2*, 827.
[218] Netzer, F., and Madey, T., 1981, *Surf. Sci.*, **110**, 251.
[219] Botzo, F., Arias, J., Yates, J. T., Jr, Martin, R. M., and Metiu, H., 1983, *Chem. Phys. Lett.*, **94**, 243.
[220] Price, G. L., and Baker, B. G., 1980, *Surf. Sci.*, **91**, 571.
[221] Brundle, C. R., and Curley, A. F., 1975, *Discuss. Faraday Soc.*, **60**, 51; Batra, I. P., and Brundle, C. R., 1976, *Surf. Sci.*, **57**, 12.
[222] Umbach, E., Kulkarni, S., Feulner, P., and Menzel, D., 1979, *Surf. Sci.*, **88**, 65.
[223] Bonzel, H. P., and Fischer, T. E., 1975, *Surf. Sci.*, **51**, 213.
[224] Johnson, D. W., Matloob, M. H., and Roberts, M. W., 1979, *J. chem. Soc., Faraday Trans. I*, **75**, 2143.
[225] Ibottson, D. E., Wittrig, T. S., and Weinberg, W. H., 1981, *Surf. Sci.*, **110**, 294.
[226] Kanski, J., and Rhodin, T. N., 1977, *Surf. Sci.*, **65**, 63.
[227] Fukuda, Y., Honda, F., and Abalais, J. W., 1980, *Surf. Sci.*, **99**, 289.
[228] Ducros, R., Alnot, M., Ehrardt, J. J., Housley, M., Piquard, G., and Cassuto, A., 1980, *Surf. Sci.*, **94**, 154.
[229] Kishi, K., and Roberts, M. W., 1976, *Proc. R. Soc.* A, **352**, 289.
[230] Fukuda, Y., 1981, *Surf. Sci.*, **104**, L234.
[231] Baird, R. J., Ku, R. C., and Wynblatt, R., 1980, *Surf. Sci.*, **97**, 356.
[232] Matsumoto, Y., Onishi, T., and Tamaru, K., 1980, *J. chem. Soc., Faraday Trans I*, **76**, 1116.
[233] Conrad, H., Ertl, G., Kuppers, J., and Latta, E. E., 1977, *Surf. Sci.*, **65**, 235.
[234] Bonzel, H. P., and Pirug, G., 1977, *Surf. Sci.*, **62**, 45.
[235] Masel, R. I., Umbach, E., Fuggle, J. C., and Menzel, D., 1979, *Surf. Sci.*, **79**, 26.
[236] Schicchl, A., and Rosch, N., 1984, *Surf. Sci.*, **137**, 261.
[237] Balkenende, A. R., Gijzemann, A. L., and Geiu, J. W., 1989, *Appl. Surf. Sci.*, **37**, 189.
[238] Balkenende, A. R., Daas, H., Huisman, M., Gijzeman, A. L., and Geis, J. W., 1991, *Appl. Surf. Sci.*, **47**, 351.
[239] Shustorovich, E., and Bell, A. T., 1993, *Surf. Sci.*, **289**, 127.
[240] Shustorovich, E., 1990, *Adv. Catal.*, **37**, 101.
[241] Gland, J. J., and Sexton, B. A., 1980, *Surf. Sci.*, **94**, 355.
[242] Root, T. W., Fisher, G. B., and Schmidt, L. D., 1986, *J. chem. Phys.*, **85**, 4679.
[243] Conrad, H., Scala, R., Stenzel, W., and Unwin, R., 1984, *Surf. Sci.*, **145**, 1.
[244] Tatarenko, S., Alnot, M., and Ducros, R., 1985, *Surf. Sci.*, **163**, 249.
[245] Sung, S. S., Hoffmann, R., and Thiel, P. A., 1986, *J. phys. Chem.*, **90**, 1380.
[246] Breitschafter, M. J., Umbach, E., and Menzel, D., 1981, *Surf. Sci.*, **109**, 493.
[247] Netzer, F. P., and Madey, T. E., 1981, *Surf. Sci.*, **110**, 251.
[248] Steinruch, H. P., Schneider, C., Heimann, P. A., Pache, T., Umbach, E., and Menzel, D., 1989, *Surf. Sci.*, **208**, 136.
[249] Bozso, F., Arias, J., Hanraham, C. P., Yates, J. T., Jr, Martin, R. M., and Metiu, H., 1984, *Surf. Sci.*, **141**, 591.
[250] Asensio, M. C., Woodruff, D. P., Robinson, A. W., Schindleir, K. M., Gardner, P., Ricken, D., Bradshaw, A. M., Conesa, J. C., and Gonzalez-Elipe, A. R., 1992, *Chem. Phys. Lett.*, **192**, 259.
[251] Caputi, L. S., Agostino, R. G., Amoddeo, A., Colavita, E., and Santaniello, A., 1993, *Surf. Sci.*, **282**, 62.
[252] Neyman, K. M., and Rosch, N., 1994, *Surf. Sci.*, **307**, 1193.
[253] Caputi, L. S., Agostino, R. G., Amoddeo, A., Colavita, E., and Santaniello, A., 1993, *Surf. Sci.*, **289**, L591.
[254] (a) Muller, H., Dierks, B., Hamza, F., Zagatta, G., Fecher, G. H., Bowering, N., and Heinzmann, U., 1992, *Surf. Sci.*, **269**, 207; (b) Fink, Th., Dath, J. P., Bassett, M. R., Imbihl, R., and Ertl, G., 1991, *Surf. Sci.*, **245**, 96.
[255] Neyman, K. M., and Rosch, N., 1993, *Surf. Sci.*, **287**, 64.
[256] Behm, R. J., and Brundel, C. R., 1984, *J. vac. Sci. Technol.* A, **2**, 1040.
[257] So, S. K., Francy, R., and Ho, W., 1989, *J. chem. Phys.*, **91**, 5701.

[258] Edamoto, K., Maehama, S., Miyazaki, E., Miyahara, T., and Kato, H., 1988, *Surf. Sci.*, **204**, L739.
[259] Bagus, P. S., and Illas, F., 1994, *Chem. Phys. Lett.*, **224**, 576.
[260] Jakob, P., Stichler, M., and Menzel, D., 1997, *Surf. Sci.*, **370**, L185.
[261] von Glan, R. E., and Korte, U., 1997, *Surf. Sci.*, **375**, 353.
[262] (a) Kinnersley, A. D., Darling, G. R., and Holloway, S., 1997, *Surf. Sci.*, **377**, 567; (b) Loffreda, D., Simon, D., and Sautel, P., 1998, *J. chem. Phys.*, **108**, 6447; (c) Mannstadt, W., and Freeman, A., 1995, *Phys. Rev.* B, **51**, 14616; (d) Colonell, J. I., Gibson, K. D., and Sibener, S. J., 1996, *J. chem. Phys.*, **104**, 6822; (e) Loffreda, D., Simon, D., and Sautet, P., 1988, *J. chem. Phys.*, **108**, 6447; (f) Borg, J. J., Reijersde, J. F. C. J. M., van Santen, R. A., and Niemantsverdriet, J. W., 1994, *J. chem. Phys.*, **101**, 10052.
[263] (a) Upton, T. H., Stevens, P., and Maddix, R. J., 1988, *J. chem. Phys.*, **88**, 3988; (b) Mannstadt, W. A., and Freeman, A., 1995, *Phys. Rev.* B, **51**, 14616.
[264] Panas, I., Siegbahn, P., and Wahlgren, U., 1989, *J. chem. Phys.*, **90**, 6791.
[265] Hashizume, T., Taniguchi, M., Motai, K., Lu, H., Tanaka, K., and Sakurai, T., 1991, *Jap. J. appl. Phys.*, **30**, L1529.
[266] Selmani, A., Andzelm, J. and Salahub, D. R., 1986, *Int. J. quant. Chem.*, **29**, 829.
[267] Kirchner, E. J. J., Baerends, E. J., van Slooten, U., and Kleyn, A. W., 1992, *J. chem. Phys.*, **97**, 3821.
[268] Bahrim, B., Billy, D. T., and Gauyacq, J. P., 1996, *J. chem. Phys.*, **104**, 10014.
[269] Schennach, R., and Bechtold, E., 1996, *Surf. Sci.*, **369**, 277.
[270] Finlay, R. J., Her, T. H., Wu, C., and Mazur, E., 1997, *Chem. Phys. Lett.*, **274**, 499.
[271] Bagus, P. S., and Illas, F., 1990, *Phys. Rev.* B, **42**, 10852.
[272] Buatier de Mongeot, F., Rocca, M., Cupolillo, A., and Valbusa, U., 1997, *J. chem. Phys.*, **106**, 711.
[273] Kamath, P. V., and Rao, C. N. R., 1984, *J. phys. Chem.*, **88**, 464.
[274] Prince, K. C., Paolucci, G., and Bradshaw, A. M., 1986, *Surf. Sci.*, **175**, 101.
[275] Backx, C., De Groot, C. P. M., and Biloen, P., 1981, *Surf. Sci.*, **104**, 300.
[276] Spitzer, A., and Luth, H., 1982, *Surf. Sci.*, **118**, 121.
[277] Rao, C. N. R., Kamath, P. V., and Yashonath, S., 1982, *Chem. Phys. Lett.*, **88**.
[278] Guest, R. J., Hernnas, B., Bennich, P., Bjorneholm, O., Nilsson, A., Palmer, R. E., and Martensson, N., 1992, *Surf. Sci.*, **278**, 239.
[279] Besenbacher, F., and Norskov, J. K., 1993, *Prof. Surf. Sci.*, **44**, 1.
[280] Campbell, C. T., and Paffett, M. T., 1984, *Surf. Sci.*, **139**, 396.
[281] Schennach, R., and Bechtold, E., 1996, *Surf. Sci.*, **369**, 277.
[282] Borg, A., Hilmen, A. M., and Bergene, E., 1994, *Surf. Sci.*, **306**, 10.
[283] Guo, X., Bradley, J. M., Hopkinson, A., and King, D. A., 1994, *Surf. Sci.*, **310**, 163.
[284] Sexton, B. A., and Madix, R. J., 1980, *Chem. Phys. Lett.*, **76**, 294.
[285] Ososvskii, V. D., Lptushinskii, Y. G., Sukretnyi, V. G., Chuikov, B. A., Medvedev, V. K., and Suchorski, Y., 1977, *Surf. Sci.*, **377**, 1664; Matsumoto, Y., Aibara, Y., Mukai, K., Moriwaki, K., Okawa, Y., Nieuwenhuys, B. E., and Tanaka, K., 1997, *Surf. Sci.*, **377**, 32.
[286] Arabczyk, W., and Narkiewicz, U., 1997, *Surf. Sci.*, **377**, 578.
[287] (a) Kundrotas, P. J., Lapinskas, S., and Rosengren, A., 1997, *Surf. Sci.*, **377**, 7; (b) Wheller, M. C., Seets, D. C., and Mullins, C. B., 1996, *J. chem. Phys.*, **105**, 1572; (c) Wang, C., Tobin, R. G., Lambert, D. K., DiMaggio, C. L., and Fisher, G. B., 1997, *Surf. Sci.*, **327**, 267; (d) Wang, C., and Gomer, R., 1979, *Surf. Sci.*, **84**, 329; (e) Rettner, C. T., De Louise, L. A., and Auterbach, D. J., 1986, *J. chem. Phys.*, **85**, 1131; (f) Luntz, A. C., Williams, M. D. and Bethume, D. S., 1988, *J. chem. Phys.*, **89**, 4381; (g) Fisher, G. B., 1997, *Surf. Sci.*, **372**, 267; (h) Bradley, J. M., Guo, X. C., Hopkinson, A., and King, D. A., 1998, *J. chem. Phys.*, **104**, 4283.
[288] Blyholder, G., 1975, *J. chem. Phys.*, **62**, 3193.
[289] Ying, S. C., Smith, J. R., and Kohn, W., 1975, *Phys. Rev.* B, **11**, 1483.
[290] Resch, C., Zhukov, V., Lugstein, A., Berger, H. F., Winkler, A., and Rendulic, K. D., 1993, *Chem. Phys.*, **117**, 421.
[291] Bertolini, J. C., and Tardy, B., 1981, *Surf. Sci.*, **102**, 131.
[292] Williams, A. K., and Lang, N. D., 1977, *Surf. Sci.*, **68**, 136.

[293] ITOH, H., 1976, *Jap. J. appl. Phys.*, **15**, 2311.
[294] TSANG, Y. W., and FALICOV, L. M., 1976, *J. Phys.* C, **9**, 71.
[295] SAILLARD, J. Y., and HOFFMANN, R., 1984, *J. Am. chem. Soc.*, **106**, 2006.
[296] HARRIS, J., and ANDERSON, S., 1985, *Phys. Rev. Lett.*, **55**, 1583.
[297] NIU, J., RAO, B. K., and JENA, P., 1992, *Phys. Rev. Lett.*, **68**, 2277.
[298] KUNZ, A. B., MICKISTH, D. J., and DEUTSCH, P. W., 1973, *Solid St. Commun.*, **13**, 35.
[299] BOLAND, J. J., 1991, *Phys. Rev. Lett.*, **64**, 1539.
[300] SZYMERSKA, I., and LIPSKI, M., 1976, *J. Catal.*, **41**, 197.
[301] THOMAS, S., 1974, *Appl. Phys. Lett.*, **24**, 1.
[302] TAKASU, Y., and SHIMIZU, H., 1973, *J. Catal.*, **29**, 479.
[303] WILLIAMS, F. L., and BOUDART, M., 1973, *J. Catal.* **30**, 438.
[304] BOWMAN, R., TONEMAN, L. H., and HOLSCHER, A. A., 1973, *Surf. Sci.*, **35**, 8.
[305] VAN SANTEN, R. A., and SCAHTLER, W. M., 1974, *J. Catal.*, **33**, 202.
[306] WILLIAMS, F. L., and NASON, D., 1974, *Surf. Sci.*, **45**, 377; GHIOTTI, G., CHIORINO, A., and BOCCUZZI, F., 1993, *Surf. Sci.*, **287**, 228.
[307] BIRD, D. M., CLARKE, L. J., PAYNE, M. C., and STICH, I., 1993, *Chem. Phys. Lett.*, **212**, 518.
[308] NORSKOV, J. K., and HOUMOLLER, A., 1981, *Phys. Rev. Lett.*, **46**, 257.
[309] MUSCAT, J. P., and NEWNS, D. M., 1980, *Surf. Sci.*, **99**, 609.
[310] RAY, A. K., and HIRA, A. S., 1987, *Phys. Rev.* B, **37**, 9943.
[311] MUSCAT, J. P., 1981, *Surf. Sci.*, **110**, 389.
[312] VARMA, C. M., and WILSON, A. J., 1980, *Phys. Rev.* B, **22**, 3795.
[313] BAETZOLD, R. C., 1982, *Solid St. Commun.*, **44**, 781.
[314] NORDLANDER, P., HOLLOWAY, S., and NORSKOV, J. K., 1984, *Surf. Sci.*, **136**, 59.
[315] (a) FEIBELMAN, P. J., 1991, *Phys. Rev. Lett.*, **67**, 461; (b) HAYDEN, B. E., and LAMONT, C. G., 1991, *Surf. Sci.*, **243**, 31; (c) KROES, G. J., BAERENDS, E. J., and MOWREY, R. C., 1997, *J. chem. Phys.*, **107**, 3309; (d) BUTLER, D. A., HAYDEN, B. E., and JONES, J. D., 1994, *Chem. Phys. Lett.*, **217**, 423; (e) BERGER, H. F., RESCH, CH., GROSSLINGER, E., EILMSTEINER, G., WINKLER, A., and RENDULIC, K. D., 1992, *Surf. Sci. Lett.*, **275**, L627; (f) MUSCHIOL, U., SCHMIDT, P. K., and CHRISTMANN, K., 1998, *Surf. Sci.*, **395**, 182; (g) WHITE, J. A., BIRD, D. M., and PAYNE, M. C., 1996, *Phys. Rev.* B, **53**, 1667.
[316] HARDER, R., NESBITT, A., GOLICHOWSKI, A., HERRMANN, and SNOWDON, K. J., 1994, *Surf. Sci.*, **316**, 478; NAHM, T. U., and GOMER, R., 1997, *Surf. Sci.*, **375**, 281.
[317] MULLER, J. E. 1992, *Surf. Sci.*, **272**, 45.
[318] COLONEL, J. I., GIBSON, K. D., and SIBENER, S. J., 1996, *J. chem. Phys.*, **104**, 6822.
[319] KARIKORPI, M., HOLLOWAY, S., HENRIKSEN, N., and NORSKOV, J. K., 1987, *Surf. Sci.*, **179**, L41; FEIBELMAN, P. J., 1991, *Phys. Rev. Lett.* **67**, 461.
[320] SCHROTER, L., KUHENHOFF, S., DAVID, R., BRENIG, W., and ZACHARIAS, H., 1992, *Surf. Sci.*, **261**, 243.
[321] REIFSNYDER, S. N., OTTERN, M. M., SAYERS, D. E., and LAMB, H. H., 1997, *J. phys. Chem.* B, **101**, 4972.
[322] WILKE, S., and SCHEFFER, M., 1996, *J. Am. chem. Soc.*, **53**, 4926.
[323] GROSS, A., and SCHEFFLER, M., 1998, *Phys. Rev.* B, **57**, 2493.
[324] MUSCHIOL, U., SCHMIDT, P. K., and CHRISTMANN, K., 1998, *Surf. Sci.*, **395,** 182.
[325] YANAGITA, H., SAKAI, J., ARUGA, T., TAKAGI, N., and NISHIJIMA, M., 1997, *Phys. Rev.* B, **56**, 14 952.